**US Army Corps
of Engineers**
Construction Engineering
Research Laboratories

The CERL Equipment Fragility and Protection Procedure (CEFAPP)

Experimental Definition of Equipment Vulnerability to Transient Support Motions

by
James Wilcoski, James B. Gambill, and Steven J. Smith

19980428 131

This report documents a new test procedure for defining the vulnerability of critical equipment to earthquake and other transient support motions. The CERL Equipment Fragility and Protection Procedure (CEFAPP) defines the capacity of equipment to withstand transient support motion in terms of amplitude versus frequency. The amplitude is the support motion or response spectrum amplitude at which failure occurs. Failure may comprise actual mechanical damage, temporary loss of function, acceleration or strain levels at critical locations, or any other user defined criteria. The frequency content of support motion is critical as it determines the manner (modes) in which equipment responds and fails. CEFAPP requires narrow-band random sweep tests. These tests consist of random motions concentrated within a narrow frequency range; that sweep across a wide frequency range over time. Test amplitudes are increased and tests repeated until the equipment fails. The amplitude, frequency, and mode of failure are recorded as single data points for each failure. All failure data are plotted, and confidence bands may be plotted across the spectrum if enough failure data is gathered. CEFAPP was validated through time history, site specific and design spectra testing of equipment, demonstrating that the procedure reasonably defines the vulnerability of the selected equipment.

Design engineers evaluating the installation of equipment can define predicted motions at equipment installation locations in terms of response spectrum. These response spectra, defining the demand, are overlaid against the experimentally defined equipment capacity plots to evaluate the adequacy of equipment. Any number of demand environments may be compared against the experimentally defined capacity without need for further expensive—and often over-conservative—qualification testing.

Equipment manufacturers can test their equipment according to CEFAPP as a design aid, because the test results define improvements needed to withstand potential demands. Currently, manufacturers primary goal is to pass a qualification test envelope—often expressed as a design response spectrum. If their equipment fails when testing to such an envelop, CEFAPP can be used as a diagnostic tool to characterize the failure and guide equipment improvements, ensuring passage of qualification tests.

DTIC QUALITY INSPECTED 3

USER EVALUATION OF REPORT

REFERENCE: USACERL Technical Report 97/58, *The CERL Equipment Fragility and Protection Procedure (CEFAPP)*

Please take a few minutes to answer the questions below, tear out this sheet, and return it to USACERL. As user of this report, your customer comments will provide USACERL with information essential for improving future reports.

1.   Does this report satisfy a need? (Comment on purpose, related project, or other area of interest for which report will be used.)

_____

_____

_____

2.   How, specifically, is the report being used? (Information source, design data or procedure, management procedure, source of ideas, etc.)

_____

_____

3.   Has the information in this report led to any quantitative savings as far as manhours/contract dollars saved, operating costs avoided, efficiencies achieved, etc.? If so, please elaborate.

_____

_____

4.   What is your evaluation of this report in the following areas?

   a. Presentation: _____

   b. Completeness: _____

   c. Easy to Understand: _____

   d. Easy to Implement: _____

   e. Adequate Reference Material: _____

   f. Relates to Area of Interest: _____

   g. Did the report meet your expectations? _____

   h. Does the report raise unanswered questions? _____

i. General Comments. (Indicate what you think should be changed to make this report and future reports of this type more responsive to your needs, more usable, improve readability, etc.)

_____

_____

_____

_____

_____

_____

5. If you would like to be contacted by the personnel who prepared this report to raise specific questions or discuss the topic, please fill in the following information.

Name: _____

Telephone Number: _____

Organization Address: _____

_____

_____

6. Please mail the completed form to:

    Department of the Army
    CONSTRUCTION ENGINEERING RESEARCH LABORATORIES
    ATTN: CECER-TR-I
    P.O. Box 9005
    Champaign, IL 61826-9005

REPORT DOCUMENTATION PAGE

Public reporting burden for this collection of information is estimated to average 1 hour per response, including the time for reviewing instructions, searching existing data sources, gathering and maintaining the data needed, and completing and reviewing the collection of information. Send comments regarding this burden estimate or any other aspect of this collection of information, including suggestions for reducing this burden, to Washington Headquarters Services, Directorate for information Operations and Reports, 1215 Jefferson Davis Highway, Suite 1204, Arlington, VA 22202-4302, and to the Office of Management and Budget, Paperwork Reduction Project (0704-0188), Washington, DC 20503.

1. AGENCY USE ONLY *(Leave Blank)*	2. REPORT DATE March 1997	3. REPORT TYPE AND DATES COVERED Final

4. TITLE AND SUBTITLE The CERL Equipment Fragility and Protection Procedure (CEFAPP)	5. FUNDING NUMBERS 4A162784 AT41 CA7
6. AUTHOR(S) James Wilcoski, James B. Gambill, and Steven J. Smith	

7. PERFORMING ORGANIZATION NAME(S) AND ADDRESS(ES) U.S. Army Construction Engineering Research Laboratories (USACERL) P.O. Box 9005 Champaign, IL 61826-9005	8. PERFORMING ORGANIZATION REPORT NUMBER TR 97/58

9. SPONSORING / MONITORING AGENCY NAME(S) AND ADDRESS(ES) Headquarters, U.S. Army Corps of Engineers ATTN: CEMP-ET 20 Massachusetts Ave. NW Washington, DC 20314-1000	10. SPONSORING / MONITORING AGENCY REPORT NUMBER

11. SUPPLEMENTARY NOTES
Copies are available from the National Technical Information Service, 5285 Port Royal Road, Springfield, VA 22161.

12a. DISTRIBUTION / AVAILABILITY STATEMENT Approved for public release; distribution is unlimited.	12b. DISTRIBUTION CODE

13. ABSTRACT (Maximum 200 words)

The CERL Equipment Fragility and Protection Procedure (CEFAPP) is a new testing protocol that defines the capacity of equipment to withstand seismic and other transient support motion in terms of amplitude versus frequency. The amplitude is the support motion or response spectrum amplitude at which failure occurs. Failure may comprise actual mechanical damage, temporary loss of function, acceleration or strain levels at critical locations, or any other user-defined criteria. The frequency content of support motion is critical as it determines the manner (modes) in which equipment responds and fails. CEFAPP uses narrow-band random sweep tests to determine the amplitude, frequency, and mode of failure, and records these as single data points for each failure. All failure data are plotted, and confidence bands may be plotted across the spectrum if enough failure data are gathered. CEFAPP was validated through time history, site-specific spectra, and design spectra testing of equipment.

Design engineers can define predicted motions at equipment installation locations and overlay these data onto the experimentally defined equipment capacity plots to evaluate the adequacy of equipment. Equipment manufacturers can test their equipment according to CEFAPP as a design aid, because the test results define improvements needed to withstand potential demands.

14. SUBJECT TERMS Equipment evaluation Seismic vulnerability CEFAPP Vibration analysis			15. NUMBER OF PAGES 160
			16. PRICE CODE

17. SECURITY CLASSIFICATION OF REPORT Unclassified	18. SECURITY CLASSIFICATION OF THIS PAGE Unclassified	19. SECURITY CLASSIFICATION OF ABSTRACT Unclassified	20. LIMITATION OF ABSTRACT SAR

Foreword

Contents

Distribution

List of Tables and Figures

1 Introduction

Background

Earthquakes often cause more costly damage to building contents than to the buildings themselves (FEMA 1994). Much of this damage can be reduced by anchoring or bracing equipment to the structure. Some kinds of equipment may be protected by allowing sufficient "rattle space" between the equipment and other surfaces. However, sensitive equipment with this problem has been damaged by even moderate earthquakes because the equipment itself lacks sufficient strength.* Other building motions, created either by accidental or hostile explosions, can create building vibration that will damage equipment.

Critical equipment must remain operable following either earthquake or explosive shock induced vibration. Emergency response equipment such as communication systems, computers, power supplies, and critical medical components must continue to function. Other critical equipment includes items that support hazardous material handling or storage operations at facilities such as nuclear power plants. Some critical systems may include components whose loss would result in significant financial losses, such as computers and communication equipment that control large corporate financial and inventory data management systems.

Critical equipment for facilities such as military command centers and nuclear power plants often is experimentally qualified on a shake table using motions that define the worst-case demand. However, existing qualification methods are often based on either response spectra or acceleration power spectral density (APSD) testing that does not provide information on the specific frequency of motions that caused failures. Other current qualification test methods are based on overconservative sine-sweep or sine-beat testing that produces unrealistic response at the equipment resonance frequency. Furthermore, these kinds of qualification tests must be repeated for new demand requirements—for example, when one type of equipment is to be used at muliple locations that have different vibration

---

* For example, high-voltage (230 kV and larger) porcelain power transformer bushings have experienced numerous failures in recent earthquakes (1994 Northridge, in particular). Another example is damage to a well anchored gamma camera at the Sepulvada Veterans Administration Medical Center in the 1994 Northridge earthquake.

environments. Repetition of qualification tests is expensive, and the data they produce do not provide a complete profile of equipment fragility.

As an alternative to blanket qualification of critical equipment against a worst-case demand, it is proposed that equipment capacity be defined experimentally as an envelope of support motion or response spectra amplitude at failure across a frequency spectrum. Then the ability of the equipment to withstand differing support motions or design response spectra (i.e., vulnerability) at proposed installation locations and against various dynamic motion hazards may be analyzed without additional shake table tests. A single CEFAPP test series will provide all data necessary to evaluate the equipment against any number of specific demands. This new approach should yield significant cost savings for vulnerability testing, provide more reliable information for equipment procurement, and enable owners to optimize equipment protection.

As an alternative to equipment qualification testing, the U.S. Army Construction Engineering Research Laboratories (USACERL) has developed and tested an alternative procedure called CEFAPP—the CERL Equipment Fragility and Protection Procedure.

Objective

This report documents the development and validation of an equipment-fragility test procedure that may be used as an alternative to conventional equipment qualification methods, or for diagnostic testing in support of qualification testing.

Approach

Defining equipment fragility using the CERL Equipment Fragility and Protection Procedure (CEFAPP) requires the following steps:

- development of narrow-band random records
- preparation for fragility testing
- failure definition
- conducting and documenting fragility tests
- development of equipment fragility test envelopes.

Chapter 2 illustrates the procedure based on the test record generated from analog random signal and sweeping filters. The fragility amplitude was defined by support motion spectral velocity.

Chapter 3 presents seismic and shock validation tests that evaluate the example presented in Chapter 2.

Chapter 4 presents an example of an actual CEFAPP test based on digital records generated by a Matlab routine. In this example the fragility amplitude was defined by response spectrum acceleration. (It is recommended that users of CEFAPP use the Matlab routine, which is shown in Appendix A.) Chapter 4 includes a section on evaluating the quality of the generated signals and also illustrates the use of the fragility data by comparing fragility-based capacity against various seismic design response spectrum demands.

Chapter 5 provides a more generalized discussion of defining seismic or shock demand in terms of a spectrum and comparing these with equipment capacity (from Chapter 2) to evaluate the equipment vulnerability and guide protective systems.

Mode of Technology Transfer

CEFAPP will be disseminiated through the Army Corps of Engineers in an Engineer Technical Letter. CEFAPP will impact future revisions of Army Technical Manual (TM) 5-809-10-1, *Seismic Design Guidelines for Essential Buildings*, and/or TM 5-809-10-2, *Seismic Design Guidelines for Upgrading Existing Buildings*. The contents of ESL-TR-87-57, *Protective Constructive Design Manual*, also will be impacted. USACERL will also work with appropriate technical committees to seek adoption of CEFAPP in industry standards.

2 The CEFAPP Experimental Procedure

USACERL developed CEFAPP for defining the vulnerability of equipment by physical testing on a shake table. Throughout this report the reader is referred to plots produced from tests on the USACERL shake table[*]. These plots and related figures are presented immediately before Appendix A.

Development of Narrow-Band Random Records

CEFAPP tests equipment using progressively greater narrow-band random sweep motions. Figure 1 is an example of such test motions. These motions may be in any direction, but normally testing will be uniaxial to minimize confusion over the cause of failure. The swept random signal is scaled such that it follows some predetermined spectrum envelope, such as a design response spectrum. Figure 2 shows the vertical motion envelope of USACERL shake table capacity (prior to its triaxial upgrade), which was used in the development of this procedure rather than a design spectrum. Thus the initial shape of the random signal will depend on this design spectrum. The initial shape of the random signal should not have an impact on the eventual shape of the fragility envelope for a given equipment item unless the shake-table motion limits are encountered prior to creating failures within a particular frequency range. The narrow-band random signal is created by sweeping the random signal through high- and low-pass filters. This process creates a random signal with the energy of motion concentrated within prescribed frequency limits, and the center frequency moves at a defined rate with respect to time. The record shown in Figure 1 was created by sweeping filters across the random signal at a rate of 12 octaves/minute. Each octave is a doubling in frequency, so the center frequency of the record doubles every 5 seconds. Table 1 defines the relationship between time and center frequency. Figure 1 shows this relationship between center frequency of the record and time, which are both plotted on the abscissa axis. The energy of the signal at any given time is concentrated within 1/3 octave by offsetting the high- and low-pass filters 1/6 octave from the center frequency throughout the record. Multiple narrow-band

---

[*] All tests were conducted on the USACERL biaxial shake table, which has since been upgraded to a triaxial system with fully controlled translations and rotations in six directions. The upgrade includes new control and data-acquisition systems.

random records of this type should be generated. An infinite number of records could be generated, and they should all have the same general characteristics of amplitude and frequency. The frequency range of generated records will differ depending on the predetermined spectrum envelope or the frequency capability of the shake table being used. The record shown in Figure 1 has a frequency range of 2 – 512 Hz, which equates to 8 octaves and a test duration of 40 seconds (i.e., sweeping 1 octave every 5 seconds). The signal shown in Figure 1 was created by generating an analog random signal and sweeping analog filters across the signal.

Appendix A presents a Matlab routine for digitally generating narrow-band random sweep signals (RANSWP.M). This routine allows more options in signal generation and does not require the hardware needed for analog signal generation. RANSWP.M can generate a signal with a much lower starting center frequency and a linear varying sweep rate.

Chapter 4 presents a detailed example to illustrate the development of narrow-band random sweep records and failure documentation. These examples are strictly for earthquake applications, as evidenced by the low frequency ranges and slow sweep range. The first has a frequency range of 0.5 – 64 Hz, which covers 7 octaves and has a sweep rate of 6 octaves/minute, giving a test duration of 70 seconds. The second has a frequency range of 0.2 – 51.2 Hz, covers 8 octaves with a sweep rate of 6 octaves/minute and a test duration of 80 seconds. This same routine could be used to generate signals more appropriate for a shock-induced vibration environment, with a higher frequency range and faster sweep range.

Table 1. Time vs center frequency of narrow-band random sweep motions.

Log(f)	Frequency f (Hz)	Time t (sec)	Octave
0.301	2	-0.833	
0.3512	2.245	0.000	
0.4014	2.52	0.833	1/3 rd Oct
0.4515	2.828	1.667	
0.5017	3.175	2.500	1/3 rd Oct
0.5519	3.564	3.333	
0.6021	4	4.167	Full Oct
0.6522	4.49	5.000	
0.7024	5.04	5.833	1/3 rd Oct
0.7526	5.657	6.667	
0.8027	6.35	7.500	1/3 rd Oct
0.8529	7.127	8.333	
0.9031	8	9.167	Full Oct
0.9533	8.98	10.000	
1.0034	10.08	10.833	1/3 rd Oct
1.0536	11.31	11.667	
1.1038	12.7	12.500	1/3 rd Oct
1.1539	14.25	13.333	
1.2041	16	14.167	Full Oct
1.2543	17.96	15.000	
1.3045	20.16	15.833	1/3 rd Oct
1.3546	22.63	16.667	
1.4048	25.4	17.500	1/3 rd Oct
1.455	28.51	18.333	
1.5051	32	19.167	Full Oct
1.5553	35.92	20.000	
1.6055	40.32	20.833	1/3 rd Oct
1.6557	45.25	21.667	
1.7058	50.8	22.500	1/3 rd Oct
1.756	57.02	23.333	
1.8062	64	24.167	Full Oct
1.8564	71.84	25.000	
1.9065	80.63	25.833	1/3 rd Oct
1.9567	90.51	26.667	
2.0069	101.6	27.500	1/3 rd Oct
2.057	114	28.333	
2.1072	128	29.167	Full Oct
2.1574	143.7	30.000	
2.2076	161.3	30.833	1/3 rd Oct
2.2577	181	31.667	
2.3079	203.2	32.500	1/3 rd Oct
2.3581	228.1	33.333	
2.4082	256	34.167	Full Oct
2.4584	287.4	35.000	
2.5086	322.5	35.833	1/3 rd Oct
2.5588	362	36.667	
2.6089	406.4	37.500	1/3 rd Oct
2.6591	456.1	38.333	
2.7093	512	39.167	Full Oct
2.7594	574.7	40.000	
2.8096	645.1	40.833	1/3 rd Oct
2.8598	724.1	41.667	
2.91	812.7	42.500	1/3 rd Oct
2.9601	912.3	43.333	
3.0103	1024	44.167	Full Oct

A band width of only 1/3 octave was considered as this is a reasonable balance of concentrating the energy of the signal within a band narrow enough to identify the frequency of failure and wide enough to preserve some random character to the signal (i.e., not so narrow as to unrealistically excite the equipment as would be the case with a sine-sweep signal). The 1/3 octave is also a standard frequency increment for random experimental testing.

For the analog generated records presented in this chapter, a sweep rate of 12 octaves per minute was chosen based on the numerical analysis of several single degree of freedom (SDOF) oscillators subjected to various seismic time histories and narrow-band random records with different sweep rates. A strong-motion cycle (SMC) was defined as any response in an oscillator that exceeds 50% of the Maximum oscillator cycle between positive and negative peaks. SDOF oscillators, at 2 Hz increments (i.e., at 2, 4, 6, 8, 10 and 12.2 Hz) and at 2 and 5% critical damping, were excited by the seismic time histories. These time histories were recorded in the El Centro, Park, Taft, and Melendy earthquakes, which contain a wide range of frequency content and duration of strong-motion shaking. Figure 3a shows the 12.2 Hz, 2% damped SDOF oscillator response to the El Centro time history. Figure 3b shows the same oscillator response in the strong motion region, with each SMC labeled (total of 14 SMCs). Table B (in Appendix B) summarizes the results of this SDOF oscillator for each of the 14 SMCs. Table B1 shows the cycle time, positive peak, negative peak, difference, and percent of the maximum for each SMC identified in Figure 3b.

The sweep rate (SR) that would excite an equivalent number of cycles is calculated for each frequency (f_n). This rate can be expressed by the following equation[*]:

$$SR = \frac{BandWidth}{SMC} \; f_n = \frac{(1/3\,octave)}{(SMC)}(f_n)(60sec/min) \qquad \text{[Eq 1]}$$

Table 2 presents the number of SMCs and SRs for the El Centro, Park, Taft, and Melendy earthquakes for 2 and 5% damped oscillators. The results in Table 2 show that the SR needed to give an equivalent number of SMCs generally increases as frequency increases. A slow SR, such as those shown in Table 2 at the lower frequencies, is more conservative as it will excite the equipment more severely. However, the tests presented in this chapter (using surplus desktop computers) showed that the equipment was most vulnerable to failure at frequencies above 15 Hz. Table 2 indicates that 6 octaves/minute would be a conservative and yet reasonable SR assuming equipment vulnerability at the higher frequencies of 8 to 12.2 Hz. Earlier SR calculation methods led to a less

---

[*] See Appendix B.

Table 2. Calculated strong motion cycles (SMC) and sweep rate (SR) for SDOF oscillators.

Oscilla-tor Frequen-cy (Hz)	El Centro				Park				Taft				Melendy			
	2%		5%		2%		5%		2%		5%		2%		5%	
	SMC	SR	SMC	SR	SMC	SR	SMC	SR	SMC	SR	SMC	SR	SMC	SR	SMC	SR
2	9	4.4	5	8	7	5.7	4	10	25	1.6	12	3.3	8	5	5	8
4	8	10	4	20	9	8.8	7	11.4	28	2.8	22	3.6	10	8	5	16
6	24	5	17	7.1	7	17	6	20	23	5.2	14	8.6	10	12	7	17.1
8	24	6.7	14	11	10	16	9	18	35	4.6	24	6.7	16	10	12	13
10	17	12	18	11	11	18	10	20	48	4.2	37	5.4	9	22	6	33
12.2	14	17	8	31	29	8.4	19	13	31	79	17	14	10	24	9	27

conservative SR of 12 octaves/minute, upon which testing reported here is based. Details on the numerical analysis of SDOF oscillators subjected to time history and narrow-band random base motion are provided in Appendix B.

The testing reported in this chapter and in Chapter 4 was based on waveforms with constant sweep rates, of 12 and 6 octaves/minute, respectively. Table 2 indicates that the ideal waveform would begin at a slower sweep rate and end at a greater rate. The revised Matlab routine RANSWP.M, shown in Appendix A, satisfies this need with the capability to generate records with linear varying sweep rates.

A more rigorous method for calculating sweep rate to produce equivalent numbers of SMCs is needed. The narrow-band random signal produces a Rayleigh distribution for the absolute value of its peaks (Thomson 1981). Future research will investigate defining SR based on an improved numerical analysis of narrow-band random signals.

Preparation for Fragility Testing

The equipment is fastened to the shake table in the configuration for which the vulnerability must be defined. A test fixture is often used to accommodate the normal anchorage configuration of the equipment and the attachment points of the shake table. This fixture must be very stiff to eliminate any fixture motion relative to the shake table. This fixture is instrumented with accelerometers near the attachment points to the equipment. A single accelerometer can be used if it can be assured that all attachment points move together as a unit. The stiffness of the test fixture and possible need for multiple accelerometers to record support

motion should be evaluated in light of the maximum frequency at which fragility data are to be gathered. For example, if fragility data are to be gathered up to 100 Hz, then the test fixture and fastening system must not be excited by motions at or below 100 Hz. For large equipment with multiple attachment points, the motions near each attachment should be measured and they should be plotted relative to each other to ensure that they are of equivalent magnitude and frequency. The equipment fragility data are obtained by processing this support motion data (from a single accelerometer), as described later in this report.

The equipment may also be instrumented with accelerometers or displacement gages at other locations if equipment response is desired. Equipment response may be needed for measuring failures, as discussed below under "Failure Definition," but these data are not required for fragility definition. Modes of failure can be understood by measuring the amplitude and frequency of motions at critical locations on the equipment. Low-level modal analysis tests are recommended to define the natural frequencies and mode shapes of the equipment. The equipment will be most severely excited at its natural frequencies, which can lead to failure at relatively low support motions. The modal analysis results can aid in understanding the fragility test results and can help guide any required upgrading of the equipment itself or its support conditions. It is recommended that low-level random or sine-sweep tests be done to define the natural frequencies and mode shapes both before and after equipment-fragility testing. Damping should also be measured for each mode both before and after testing using white noise random or sine decay tests. Modal testing after the fragility testing is used to determine if the modal characteristics changed due to yielding or other damage. Changes in modal characteristics are significant because they change frequency-dependent equipment fragility.

All tests presented in this chapter were conducted in the vertical direction because of the suspected vulnerability of the equipment being tested, but the identical procedure could be repeated along either horizontal axis.

Failure Definition

Methods of defining failure must be established. Failure may be loss of function, actual physical damage, or some measured response that is determined to be unacceptable. Examples of loss of function include memory loss in a computer system or a temporary short-circuit in electronic equipment. Actual physical damage is permanent damage to some portion of the equipment. Measured response that is unacceptable might include strains in a material at a particular

location that exceed acceptable limits, or accelerations at a location that may damage an attached subcomponent. Failures also may occur when rattle space is inadequate and impact or contact occurs between two components. Measured response would require the installation of sensors at the critical locations. After the test, the response data are inspected and, if the limits are exceeded, the time at which the failure occurs is documented for later recording on fragility envelopes. An example of measured response that defines failure is strains in the porcelain at critical measured locations in power transmission components such as live tank breakers. Currently strain values at critical locations are the pass/fail criteria for qualification tests of these components. The method for defining failure in equipment qualification tests could also be used for defining failure in this test procedure. The time at which failure occurs during the test must be determined in order to document the corresponding frequency of the motions that caused failure.

Original development of this procedure was done by testing old IBM[*] XT personal computers. Figures 4a and 4b show one of these computers on the USACERL shake table. The commercial computer diagnostic software package Norton Utilities (Symantec Corp., 10201 Torre Ave., Cupertino, CA 95014) was used to detect read/write errors to the hard disk. This software was running throughout testing, and each failure of this type was caused by physical damage to the hard drive. The head impacted the disk, causing permanent damage to the hard drive media. The software indicated the time at which this error occurred. The time of each error was recorded by a hand-held "switch" with its own data channel.

Conducting and Documenting the Fragility Tests

The narrow-band random tests begin at very low amplitudes, with amplitude gradually increasing for subsequent tests.

Documenting Frequency and Amplitude of Failure

The "switch" data channel recorded the time that failures occurred. The frequency/time relationship shown in Table 1 and Figure 1 was used to determine the frequency of failure. The support motion accelerometer record was used to determine the amplitude of failure. As the amplitude is increased, the equipment begins to fail. Each failure is documented as a data pair of support-motion amplitude versus center frequency of the narrow-band motion at the time of

---

[*] IBM Corp., Old Orchard Rd., Armok, NY 10504.

failure. When possible the mode of each failure should be recorded. After an initial failure is produced, the test should be repeated at the same amplitude and then at slightly lower amplitude if failures continue. If no other failures occur, the tests should be repeated at slightly greater amplitude. The purpose of this is to begin to populate a failure envelope with data from several failures.

Notching the Support Motion

If multiple failures occur within a fairly narrow frequency range, then the support motion must be modified to cause failures outside this range. This can be done by "notching" the support motion frequency spectrum. The notched record is constructed by multiplying the narrow-band random signal with an attenuation function that has the same number of data points as the random signal. The magnitude of the attenuation function varies from 0 to 1.0 to give the desired notch shape. The notches used in the USACERL tests included flat and sloped straight line segments. The amplitude is significantly reduced within the notch range. Then the scale of the notched signal is increased so that failures are created outside the notched frequency range. Figures 5a through 5c show the attenuation function for Fragility Test 67 at USACERL—the scaled envelope for this test in terms of velocity and the actual narrow-band test record that fits this envelope.

Data Filtering and Integration

Support motion acceleration motions were filtered and integrated as described in Appendix C to yield the velocity versus frequency records such as those shown in Figure 1. Support motion and fragility data also may be plotted in terms of spectral acceleration versus frequency.

Failure Amplitude Based on SDOF Response

The failure amplitude is further refined by defining for each record an envelope that is intended to approximate the amplitude of the support motion across the frequency spectra. This is achieved by calculating the maximum response of SDOF oscillators with 50% damping subjected to the measured support motions. For each octave of support motion data the response of 10 SDOF oscillators, spaced equally across this frequency range (at 1/10 octave increments) are calculated. Figure 5c shows both the support motion time history and the envelope approximating the support motion for Fragility Test 67. This envelope for the actual random support motion in Test 67, may be compared to the ideal envelope in Figure 5b, from which the random signal was generated. The dots

shown on Figure 5c mark failure points, which are placed on these envelopes at the frequency causing failure. These failure points are in a format that can be compared, for validation purposes, with the amplitude generated in a similar manner from actual earthquake records. This amplitude is also a more accurate measure of the support motions at that frequency than the ideal envelope used to generate the random signal. The fragility data are hereinafter referred to as the amplitude on these SDOF oscillator envelopes at the frequencies where failures occurred. Appendix D gives the details for the development of these SDOF oscillator envelopes.

Fragility data presented in Chapter 4 use the recommended and much simpler method of defining fragility data in terms of response spectra amplitude at the frequency of failure.

Fragility Data for Tests Conducted at USACERL

Figures 6a through 6n plot all the test data that caused failures in the testing conducted at USACERL. Each plot includes the support motion records, SDOF oscillator envelopes approximating amplitude and actual failure data. Figures 6a and 6h repeat the test records shown in Figure 1 and Figure 5c. Gradually increasing the width of the notch and the amplitude of the remaining signal allows the creation of failures across the frequency range being tested, up to the operating limits of the shake table.

Development of Equipment Fragility Test Envelopes

The amplitude and frequency for each failure described above are plotted together. Figure 7 shows the SDOF envelopes of support motion and failure data for tests conducted at USACERL. Figure 8 shows the same failure points plotted without the support motion envelopes. An equipment fragility test envelope is created when all failure points from a particular test configuration are plotted together, as illustrated in Figure 8. The amplitude may be plotted in terms of spectral velocity or acceleration. For equipment particularly vulnerable at lower frequencies, spectral displacement could be plotted, because displacement may be a critical concern due to limitations such as slack in cables or rattle space between components. When sufficient failure points are generated across the frequency range, confidence bands could be developed. These bands may indicate for example, that if predicted support motions fall below the band, the equipment has a 95% chance of survival. Multiple bands could be generated to represent various percentage levels for probability of survival.

3 Seismic and Shock Validation Testing

Validation tests were conducted using seismic and shock waveforms. The seismic waveform was recorded in the Lucerne earthquake. The seismic record was amplified to 251% of the recorded motions (LUC3D5), as this was the minimum level needed to fail the equipment tested at USACERL. This record and its corresponding spectrum are plotted in Figures 9a and 9b, respectively. The seismic spectrum was generated from the time history in the same manner as from the fragility records, so a valid comparison of amplitude and frequency of failure could be made. The seismic time history and spectrum, shown in Figures 9a and 9b show the amplitude and time of failure and predominant frequency that caused failure.

The shock record used was generated as a predicted motion for naval applications. This shock record was amplified to 102% of the recorded motions (A12D12), as this was the minimum level to cause failure. This record and its corresponding spectrum are plotted in Figures 10a and 10b. The shock spectrum was generated from the entire shock record. The peak amplitude and corresponding frequency were chosen as the failure point, as this peak dominates the spectrum. The short duration of the test did not allow identification of the portion of the signal that caused the failure.

The modified response spectra are also applied to the seismic and shock records. This is done without the octave marching as it would not have any meaning in the context of an arbitrary site record. The spectra for the seismic and shock records are finally compared to the envelope of the failure ordinates from the fragility data to determine the suitability of the equipment to the environment.

Figure 11 shows all the failure points plotted on the equipment fragility envelope shown in Figure 8 plus the seismic and shock validation points shown in Figures 9b and 10b. Figure 11 illustrates that the equipment-fragility test procedure reasonably predicts the amplitude at which either the seismic or shock records would produce failure. This figure suggests that a slower sweep rate may have more conservatively predicted the equipment failure because the seismic record actually produces failure at a lower level. The earlier discussion on selecting a sweep rate, based on the calculations summarized in Table 2, indicates that a

sweep rate of 6 rather than 12 octaves/minute should have been used. This is consistent with the results of the validation tests.

The numerical analysis of SDOF oscillators was repeated for the Lucerne seismic and shock records used here to determine what sweep rates should be used based on the procedure presented previously for defining an appropriate sweep rate. Similar to Table 2, Table 3 presents the number of SMCs and SR for the Lucerne seismic record with 2% damping. This table also gives the SR for Lucerne at 5% damping and for the shock record at 2 and 5% damping. The results in Table 3 show that the sweep rate needed to give an equivalent number of SMCs generally increases as frequency increases. This table also indicates that a sweep rate of 6 rather than 12 octaves/minute would have better excited an equivalent number of strong motion cycles. This is particularly true for the 16 Hz oscillator excited by the Lucerne seismic record, which yielded equivalent SRs of 8.6 and 5.6 octaves/minute, for 2 and 5% critical damping, respectively. The equipment failures caused by the Lucerne record were at a frequency close to 16 Hz (12.5 Hz), which suggests the equipment was vulnerable to support motion in this frequency range. Had a slower sweep rate been used in the fragility tests, the equipment response would experience greater amplification such that smaller support

Table 3. Calculated SR for SDOF oscillators for the Lucerne seismic and shock records.

Oscillator Frequency (fn)	Lucerne Seismic Record				Shock Record			
	2%		5%		2%		5%	
	SMC	SR	SMC	SR	SMC	SR	SMC	SR
2	15	2.7	10	4.0	0*	—	0*	—
4	40	2.0	30	2.7	0*	—	0*	—
6	14	8.6	13	9.2	4	30.0	2	60.0
8	15	10.7	16	10.0	8	20.0	5	32.0
10	24	8.3	25	8.0	7	28.6	5	40.0
12.2	19	12.8	16	15.3	8	30.5	4	61.0
16**	37	8.6	57	5.6	5	64.0	3	106.7
21	24	17.5	25	16.8	6	70.0	4	105.0
32	55	11.6	30	21.3	10	64.0	6	106.7
40	***	—	***	—	4	200.0	3	266.7

* The 2 and 4 Hz SDOF oscillator acted as an isolator in responding to the high—frequency shock record, such that the response is essentially zero.

** The Lucerne seismic and shock records have a smaller time step than those records in Table 2, allowing the computation of the response of SDOF oscillators at higher frequencies.

*** The Lucerne record produces very little response in the 40 Hz oscillator because this record has almost no energy at 40 Hz, causing the oscillator to move as a rigid body.

motions would cause failure. This would have brought the fragility data shown in Figure 11 into closer agreement with the seismic validation failure. The calculations summarized in Table 3 indicate that a sweep rate of 12 octaves/minute does reasonably produce an equivalent number of SMCs as the shock record. Chapter 4 presents further development and validation of CEFAPP, confirming its potential for defining equipment capacity to withstand support motions.

4 Example Fragility Testing of a Power Transformer Bushing

This chapter presents the development of digital test records and their use in fragility testing of a power transformer bushing. The Tennessee Valley Authority (TVA) conducted seismic qualification tests on a 500 kV power transformer bushing using TESS, the Triaxial Earthquake and Shock Simulator at USACERL. The bushing sustained no permanent damage in these qualification tests, and TVA subsequently donated the bushing to USACERL for fragility testing. The use of this bushing provided an opportunity to demonstrate CEFAPP on critical equipment that may be vulnerable to seismic motions. Figure 12 shows the TVA bushing mounted on the TESS.

CEFAPP is illustrated by developing records based on seismic design spectra. The early records were used for fragility testing of the bushing. The starting point for defining support motions can be based on design response spectra or some other predetermined spectrum envelope. The examples presented in this chapter are based on design response spectra. The selected spectrum defines the initial shape of random signal but should not have an impact on the eventual shape of the equipment fragility envelope.

All spectrum plots in this chapter are based on response spectra of SDOF oscillators to the generated support motions. This allows direct comparison of equipment response spectra capacity with design response spectra demand. Alternatively, all spectrum plots in Chapter 2 are based on equipment support motion spectra that are equated to the building response spectra; in that case equipment support motion spectra capacity would be compared with the building response spectra demand.

This chapter presents both the development of test waveforms and a method of documenting failures in order to illustrate the vulnerability evaluation based on response spectra capacity and demand. The specific example presented here uses the seismic design spectra from IEEE 693[*] as the basis for its narrow-band

---

[*] Institute of Electrical and Electronics Engineers 693, *Recommended Practices for Seismic Design of Substations*, Draft 6 (IEEE, 1997).

random sweep motions. The bushing fragility test records that follow were
generated by an early version of the Matlab routine RANSWP.M that is now used
in CEFAPP. However, the current version of this routine generates higher-quality
records. This quality difference is central to the section entitled "Evaluating the
Quality of Generated Signals," in which examples of the improved waveforms are
presented. It is appropriate at this point to alert the reader that these improved
waveforms were based not on the IEEE 693 spectra (which were the basis for the
USACERL bushing fragility test data) but on a different seismic design response
spectrum (see Bellcore GR-63-CORE, October 1995). Therefore, the reader should
use the improved waveforms to compare quality only—not the specific data values.

Seismic Design Response Spectra

Widely accepted design spectra should be used when available for the equipment
being tested. The first set of spectra used in this example (Figure 13) are from
Figure 3 in IEEE 693, which defines the high seismic performance level (PL) with
2% of critical damping. According to section 9.3.1 IEEE 693, "Equipment that is
shown by this practice to perform acceptably in ground shaking up to the High
Seismic Performance Level is said to be seismically qualified to the High Level."
Thus, these spectra provide an industry-recognized starting point for defining the
test motions for electrical power substation equipment. The leakage criteria for
bushings (IEEE 693, sec D.5.1.d) require that the bushing gasket not leak when
subjected to the PL shake table testing that has been adjusted for the influence
of the transformer and local flexibility at the bushing mounting. Section D.4.3 of
IEEE 693 states that the acceleration levels at the bushing flange can be doubled
to account for this amplification of the transformer. Such modification was not
applied to the "starting point" spectra as the fragility data generated could be used
for bushings attached to a variety of transformers. The fragility data generated
from this test procedure will later be compared with design spectra that should
be modified to reflect amplification from the transformer. Testing at the high
seismic PLs allows direct comparison with ultimate strength of porcelain or other
components. Figure 13 shows the spectra for both the horizontal direction and
vertical, where the vertical is simply 80% of horizontal values (IEEE 693, A.1.1.1).

Later waveform development was based on seismic design spectra from the
Bellcore, Network Equipment–Building System (NEBS) Requirement: Physical
Protection, GR-63-CORE, Issue 1, October 1995. The required response spectrum
for Zone 4, shown in Figure 5-15 of the Bellcore report, serves as the "starting
point" for the later waveform development.

Generating Narrow-Band Random Records

The next step is to generate random motions that span the full frequency range. An earlier version of the Matlab routine, "RANSWP.M" (shown in Appendix A), generated a random signal between 0 and Nyquist frequency (½ sample rate), exceeding the entire range of the spectra shown in Figure 13.

This same routine is used to sweep high- and low-pass filters across this random signal at a user-defined rate. Figures 14a through 14j are examples of records (Ran1 through Ran10) generated using RANSWP.M. The variables used to generate these records are defined below. These are the same variables used in the improved version of RANSWP.M that also allow a linear varying sweep rate. The terms in parethese are the variable names that RANSWP.M assigns to each of the input requests.

Initialization Time (kern). The waveform created by RANSWP.M is based on pseudo-random numbers generated by Matlab. A default value of zero is used for the random number generator at the beginning of new Matlab sessions. Using this default value would lead to the generation of exactly the same signal for each new session in Matlab. Therefore, the user is prompted to enter the current time, which is used as the starting point of the random number generation, formatted as hour.minute (e.g., 11.21 for 11:21 AM).

Sample Rate (aqrate). This is the frequency at which data points are generated (inverse of time step) in the digitized record. Experience (see Otnes and Enachson 1972) indicates that 2.5 samples per cycle, or a sample rate of at least 2.5 times the ending frequency, is needed. For the records in Figures 14a through 14j, this becomes (64 Hz + 1/6th octave) x 2.5 = 180 Hz.

Beginning Sweep Rate (swratelow). This is the rate at which the high- and low- pass filters sweep across the random record at the beginning of the record. The basis for defining this rate is presented in Chapter 2 under "Development of Narrow-Band Random Records," and in Appendix B.

Ending Sweep Rate (swratehigh). This is the rate at which the high- and low-pass filters sweep across the random record at the end of the record. The sweep rate varies linearly with time (and logarithmically with frequency) between the beginning and ending sweep rates.

Beginning Center Frequency (centerlow). This defines the lower frequency of interest for which the fragility tests are to be conducted, normally based on the

lower frequency limit of the design response spectra. This frequency should be chosen at a conservatively low point recognizing that data may later be needed at frequencies lower than anticipated in the original test program. Additionally, this value should not be greater than ½ the lowest natural frequency of the equipment being tested, recognizing that response amplification will occur near the natural frequencies.

Ending Center Frequency (centerhigh). This similarly defines the upper frequency of interest, and also should be chosen at a conservatively high point.

Filter Bandwidth (band). This is the difference in frequency between the high-pass and low-pass filter at any point in time during the sweep. This variable is defined in terms of octaves (doubling of frequency) and remains constant throughout the record. This variable is held constant at 1/3 octave for all tests using this procedure, as this width is narrow enough to define the frequency at which failure occurs, yet wide enough that the signal remains somewhat random (i.e., not a sine sweep).

Filter Error (error). This quantifies the allowable filter error as defined in Appendix A.

Table 4 gives the values for these parameters used to generate the records. The second column gives the values used to generate the record shown in Figure 2, which was the intial record for all the fragility data presented in Chapter 2. This record was generated electronically as an analog record and then digitized at the sample rate shown in Table 4. The third column gives the values used to generate all the records shown in Figures 14a through 14j.

Table 4. Narrow-band random signal generation Matlab program parameters.

Parameter	Figure 2 Values	Figure 14a - 14j Values	Figure 23a* Values
Sample Rate (Hz)	2000	200	200
Beginning Sweep Rate (octaves/min)	12	6	6
Ending Sweep Rate (octaves/min)	12	6	6
Beginning Center Frequency (Hz)	2	0.5	0.2
Ending Center Frequency (Hz)	512	64	51.2
Filter Bandwidth (octaves)	0.333	0.333	0.333
Filter Error (octaves)			0.2

*The last column of the table gives the values used to generate the record shown in Figure 23a. This record has already been scaled in the manner described in the following paragraphs. These values were used in the most recent version of the Matlab routine, which gives the best quality waveforms.

Scaling the Narrow-Band Random Records

The amplitude of the records shown in Figures 14a through 14j are unitless. They are scaled across their frequency range to produce levels consistent with the baseline design response spectra. This scaling can be illustrated by scaling the records shown in Figures 14a through 14j to produce response spectrum levels consistent with Figure 13. This is done by generating a response spectrum for each record using the same percentage of critical damping used to generate the baseline design response spectra (e.g., 2% for Figure 13). The response spectra are plots of the maximum response of SDOF oscillators subjected to support motions across a frequency range. Response spectra are generated from the unitless records shown in Figures 14a through 14j using the shake table software. Input parameters for generating the response spectra include the following:

- **Minimum Frequency**, which is normally the same as the Beginning Center Frequency defined above.
- **Maximum Frequency**, which is normally the same as the Ending Center Frequency defined above.
- **Number of Frequency Points per Octave**, which defines the increment in frequency for the response spectrum calculations, which for the spectra shown in Figures 15, 17, and 20 is 24, yielding 168 points (SDOF oscillators) across the 7 octave record.
- **Percentage of Critical Damping**, which is the same value used for defining the design response spectra—2% for this example.

Figure 15 shows the unitless response spectrum plots for each of the narrow-band random records in Figures 14a through 14j plus the IEEE 693 design spectra from Figure 13. Next, the narrow-band records are scaled so their response spectra become equivalent to the amplitude shown in the design spectra. Figure 15 shows where and to what degree the unitless spectra need to be scaled to produce response spectra equivalent to the design spectra. Table 5 shows frequency ranges and expressions (linear in this example) used to scale the unitless spectra. Figure 16 graphically shows the expressions for scaling the horizontal (lateral and longitudinal) and vertical narrow-band random records. Figure 16 also includes the information from Table 5 to provide direct comparison with the plots of Figure 16. Time for the narrow-band random records is directly related to the center frequency as defined by the sweep rate, with their ranges shown in Table 5. The dual frequency/time axis for Figure 16 illustrates the center frequency and time correspondence.

Table 5. Scaling relationship for narrow-band random records.

Frequency Range, $f_{n-1} - f_n$ (Hz)	Time Range $t_{n-1} - t_n$ (seconds)	Scale Number & Amplitude,		Horizontal Scaling, $S_H(g)$	Vertical Scaling, S_V (g)
		n	A_n (g)		
		0	12		
0.5 - 1.122	0 - 11.67	1	8	$\dfrac{A_1 - A_0}{t_1 - t_0}(t - t_0) + A_0$	0.8 S_H
1.122 - 8	11.67 - 40	2	2	$\dfrac{A_2 - A_1}{t_2 - t_1}(t - t_1) + A_1$	0.8 S_H
8 - 33.903	40 - 60.833	3	0.25	$\dfrac{A_3 - A_2}{t_3 - t_2}(t - t_2) + A_2$	0.8 S_H
33.903 - 64	60.833 - 70	4	0.2	$\dfrac{A_4 - A_3}{t_4 - t_3}(t - t_3) + A_3$	0.8 S_H

Figure 17a shows the scaled response spectra after multiplying the spectra in Figure 15 by the expressions shown in both Table 5 and Figure 16. The amplitudes of the response spectra in Figure 17a vary greatly from the ideal IEEE 693 envelopes. From these records, three are selected that have the smallest variation from the design spectrum, and these are used for shake table motions. Each of these records has significant energy across the frequency range of interest. Ran8, Ran3, and Ran9 are used for lateral, longitudinal, and vertical motions, respectively. These selected spectra are plotted in Figure 17b. Ran9 was selected for the vertical record because of its relatively small amplitude at the lower frequencies, so as to avoid the large displacements at low frequencies that would quickly exceed the vertical displacement capacity of the TESS. Also, vertical motions at lower frequencies are less important than horizontal because buildings that house critical equipment will amplify low frequency horizontal motions at the natural frequencies of the building. The primary modes of a building will almost always be at lower frequencies in the horizontal directions than the vertical. Therefore, most equipment will experience greater motions at the lower frequencies in the horizontal directions than vertical because of the building amplification. Earlier modal testing of the bushing revealed a dominant first mode at 6 Hz, particularly in the longitudinal direction. Therefore, Ran3 was selected for the longitudinal direction as it has a somewhat more uniform distribution of energy in this frequency range. Ran8 had a similar response spectrum as Ran3, and was selected for the lateral signal.

The expressions in Table 5 are next used to scale the unitless narrow-band time histories — Ran8, Ran3, and Ran9 in Figures 14h, 14c, and 14i, respectively — to give those shown in Figures 18a – 18c. The records shown in Figures 18a – 18c are plotted with respect to both time and frequency again to illustrate the time/center frequency correspondence. Finally, these records are used in actual tests on the shake table, beginning at very low levels. Table 6 shows the percent amplitude of Figure 18 motions used in preliminary tests on the TESS. Figures 19a – 19c show the achieved TESS motions in the lateral (Y), longitudinal (X), and vertical (Z) directions at 29% of the input motions (Test File Frag9) shown in Figures 18a – 18c. The amplitude of these records is great enough so that the achieved motions are much greater than the noise level measured at the TESS, but still below levels that could cause failure. From these records, test response spectra (TRS*) are generated for each of the three directions. Figure 20 shows the TRS plotted relative to 29% of the IEEE 693 design response spectra to guide further revision of the scaling expressions. The expressions shown in Table 5 may be revised based on the achieved motions so future tests will more closely follow the ideal design spectra. Then the input motions of Figures 18a – 18c are adjusted by the revised expressions. In this example these expressions were not revised because the TRS matched the design response spectra (see Figure 20).

Evaluating the Quality of the Generated Signals

The frequency content of the record shown in Figure 18b was examined further to evaluate the effectiveness of the signal generating routine. Three time/center frequency regions of this record were selected. Figures 21a through 21d show the orginal record (Figure 18b) and the three selected regions. Each of these regions contains a 5 second portion (plus 0.42 second ramp up and ramp down) of the original record, which equates to a 1/2 octave change in center frequency. These regions of the record were created by multiplying the original time record by an attenuation function that has values of zero before the region of interest, ramps up to 100% in 1/24 of an octave, remains constant at 100% for 1/2 octave, ramps down to zero over 1/24 of an octave, and finally is zero for the remainder of the record. The quality of the filters may be evaluated by creating approximate attenuation functions (with respect to frequency) and comparing these with the response spectrum of each region. These approximate attenuation functions account for the sweeping of the center frequency across 1/2 octave and the band

---

* The TRS are the calculated response spectra that are developed from actual time history motion of the shake table for the particular test conducted and value of damping. These do not need to envelop the design spectra from IEEE 693, as would be the case for IEEE 693 qualification tests. Still, the eventual maximum TRS from fragility tests will exceed the design spectra, unless early failures cause notching of the test records, resulting in reduced TRS in the notch region.

Table 6. Amplitude of tests conducted on CERL TESS (percent of Figure 18 records).

Date of Test	Test File Name	Test Level, % Fig 18	High-Pass (HP) Filter or Notch	Failure or Other Observations
10/11/96	Frag9	29%	-	None
10/17/96	Frag10	50%	1.2 Hz HP- Long only	
10/23/96	Frag11	50%	1.2 Hz HP- Long only	Fluid leaked from the Bushing South Side at 36 seconds (6.1 Hz) - documented w/dsl LVDT =0.015"
10/23/96	Frag12 Frag13	60%	1.2 Hz HP Long & Vert	Fluid leaked from both North & South side at 35 sec (5.7 Hz) - 36.8 sec (6.3 Hz), Porcelain Slippage at 35 sec (5.7 Hz) (dst).
10/28/96	Frag14	60%	1.2 Hz HP - all 3 axes, Notch1	None
10/28/96	Frag15	80%	1.2 Hz HP - all 3 axes, Notch1	Fluid leaked from South side at 32.5 seconds (4.8 Hz)
10/28/96	Frag16	80%	1.2 Hz HP - all 3 axes, Notch2	None
10/28/96	Frag17	100%	1.2 Hz HP - all 3 axes, Notch2	None
10/28/96	Frag18	120%	HP 1.2 Hz Lat. & Long., 1.8 Hz Vert., Notch2	None
10/29/96	Frag19	140%	HP 1.2 Hz Lat. & Long., 1.8 Hz Vert., Notch2	None
10/29/96	Frag20	160%	HP 1.2 Hz Lat. & Long., 1.8 Hz Vert., Notch2	Fluid leaked at 39 seconds (7.55 Hz)
10/29/96	Frag21	180%	HP 1.2 Hz Lat. & Long., 1.8 Hz Vert., Notch2	Fluid leaked at 30 seconds (4.0 Hz) and 39 seconds (7.55 Hz)
10/30/96	Frag22	200%	HP 1.2 Hz Lat. & Long., 1.8 Hz Vert., Notch3	None
10/30/96	Frag23	220%	HP 1.2 Hz Lat., 1.5 Hz Long. & 1.8 Hz Vert., Notch3	Fluid leaked at 22 seconds (2.3 Hz), dsl & dtx show that 2.3 Hz table motion excites the 6 Hz bushing rocking mode.
10/30/96	Frag24	80%	1.2 Hz HP 3 axes	Greater leaks at 32.5 seconds (2.3 Hz)
10/30/96	Frag25	100%	1.2 Hz HP 3 axes	Major leaking and dst = 0.018" slip at 35 seconds (5.6 Hz)
10/31/96	Frag26	120%	HP 1.2 Hz Lat& Long, 1.8 Hz Vert	Major leaking and dst = 0.015" slip at 35 seconds (5.6 Hz) and 0.03" slip at 37.5 seconds (6.7 Hz).
10/31/96	Frag27	140%	HP 1.2 Hz Lat& Long, 1.8 Hz Vert	Major leaking
10/31/96	Frag28	160%	HP 1.2 Hz Lat& Long, 1.8 Hz Vert	Major leaking and det = 0.03" slip at 33 sec (4.9 Hz), dst = 0.01" slip at 35.8 sec (6.0 Hz) and 0.015" at 37.5 sec. (6.7 Hz).

NOTES: dsl = displacement at the south side of bushing along the longitudinal direction; dst = displacement at south side of the bushing along the transverse direction; dtx = TESS longitudinal displacement; det = displacement at the east side of bushing along the transverse direction; LVDT = linear variable differential transformer sensor.

width of 1/3 octave. The 1/3 octave width means the lower frequency limit (high-pass filter) will be 1/6 octave below the center frequency at the begining of the region and the higher frequency limit (low-pass filter) will be 1/6 octave above the center frequency at the end of the region. This results in a total width of each region being 11/12 of an octave (1/6 + 1/24 + 1/2 + 1/24 + 1/6 octave), if the sweeping filters are perfect. These approximate attenuation functions with respect to frequency for the three regions are shown in Figure 22a. Response sprecta were generated for the three regions shown in Figure 21b through 21d, and are shown in Figure 22b.

The response spectrum for each region (Ran31, Ran32, and Ran33) shown in Figure 22b should be close to the amplitude of the overall response spectrum (Ran3 longitudinal) within the frequency regions shown in Figure 22a. Figure 22b shows excellent agreement in frequency content and response spectrum amplitude for both the 2nd and 3rd regions (Ran32 and Ran33). However the first region (Ran31) shows the Ran 31 response spectra shifts to lower frequencies relative to the attenuation function shown in Figure 22a and overall response spectra (Ran3 longitudinal in Figure 22b). Also, the amplitude of the regional response spectrum has dropped relative to the overall response spectrum. The amplitude in individual region spectra are less than the overall spectrum because the overall spectrum includes response to motions at the oscillator frequencies that had been set to zero with the attenuation for the regional records but still contained energy at the oscillator frequency due to imperfections in the filters. Furthermore as damping increases, the response of oscillators (which makes up the response spectrum) to support motions away from the oscillator frequency increases. Figure 22b indicates that the first region amplitude falls below the overall spectrum by about 33%. Another issue to evaluate is how quickly the response spectrum for each region drops off outiside the frequency ranges defined in Figure 22a. Filter imperfections lead to response spectra for each region that are wider than the 11/12 octave defined above.

As noted previously, the routine for generating records was improved. The new records were scaled to the Bellcore Required Response Spectrum for Zone 4, in the same manner as the Ran 3 record presented earlier. Figure 23a shows one of the scaled records (Bel2). The parameters for creating this record are shown in Table 4. This record begins at a lower center frequency of 0.2 Hz and sweeps up to 51.2 Hz. The new routine adds a filter error variable (error), which is defined in Appendix A. Five regions of this record were selected to evaluate the quality of this revised routine. Figures 23b – 23f show the five selected regions. This signal can be evaluated using the same attenuation function as Ran3 because the sweep rate, band width, and sampling rate are the same. This also allows a direct

comparison of the quality of the signal. The approximate attenuation functions for this signal are shown in Figure 24a. Response spectra were generated for the original record (Figure 23a) and the five regions shown in Figure 23b through 23f, and they are shown in Figure 24b.

The response spectrum for each region (Bel21, Bel22, Bel23, Bel24, and Bel25) shown in Figure 24b should be close to the amplitude of the overall response spectrum (Bel2) within the frequency regions shown in Figure 24a. Figure 24b shows excellent agreement in frequency content and response spectrum amplitude for all but the first region. The frequency of the first region (Bel21) is much less than that of the first region using the earlier routine (Ran31). The lower frequency regions are more challanging for the routine. The second region using the revised routine (Bel22) is still at a lower frequency than the first with the old routine (Ran31), and it produces a better agreement with the overall signal response spectrum (Bel2). The response spectrum for Bel22 is less than Bel2 because the region of the signal selected by the attenuation function is slightly greater in frequency (Figure 24a) than the peak in the overall response spectrum (Bel2). The response spectra for the regions shown in Figure 24b "dropoff" faster than those based on the earlier routine (Figure 22b). This dropoff reflects the improved performance of the filters in removing energy outside the desired frequency range. The new routine also reduces the high-frequency noise seen in the early portions of the record. This can be seen by comparing the early portions of the records shown in Figure 21a and 23a.

Increasing Test Levels and Notching the Records

All remaining presentation and discussion of test waveforms are illustrated using the old matlab routine that resulted in the scaled signals shown in Figures 18a – 18c. These records are gradually increased from the levels shown in Figures 19a – 19c until failures occur. Then the input signals are notched using revisions of the scaling expressions shown in Table 5, and the amplitudes of subsequent tests are increased to cause failures at other frequencies. In a similar manner the signals and expressions in Table 5 may be revised to avoid exceeding the shake table motion limits. Alternatively, the driving signals in Figure 18 may be reduced by filtering these records. Table 6 (Test File Name Frag10) shows that the longitudinal motion in Figure 18b was filtered with a 1.2 Hz high-pass (HP) filter to avoid exceeding the longitudinal displacement limits of the TESS. An HP filter removes energy in the signal below the chosen frequency. The resulting decrease in achieved acceleration is reflected in a reduction of the TRS. Figures

25a – 25c show the achieved TESS motions at 50% of Figures 18a - 18c, but with the longitudinal motion of Figure 18b filtered at 1.2 Hz.

Figure 26a shows the scale and notch (Notch 2) for Fragility Test Frag17, which used 100% of the Figure 18 motions. To scale the record, Notch 2 slopes down from 100% of the original levels at 4.49 Hz to 1% at 4.62 Hz, remains constant at 1% to 6.92 Hz and slopes back up to 100% at 7.13 Hz. Figures 26b – 26d shows the achieved TESS acceleration in the lateral, longitudinal, and vertical directions, illustrating the effect of the notch in the time domain. Figure 26e shows the TRS generated from these motions. The TRS show the effectiveness of the notch in reducing shake table motions within the desired frequency range by scaling the time history input motions. Note that further improvements would be seen if the new Matlab rountine had been used for signal generation. Figure 26e also includes IEEE 693 spectra for comparison with the TRS. Figures 27a – 27c are Notches 1 through 3, which were used in the fragility tests as indicated in Table 6.

Documenting Failures Based on Response Spectra Amplitude

The modal frequency and equivalent viscous damping should be measured for each significant equipment mode of vibration. This basic information is needed to understand the response of the equipment to support motions. The primary transformer bushing modes of vibration (lateral and longitudinal) and associated damping are given in Table 7. The damping values were calculated from the half-power band-width of the acceleration transfer functions between the TESS and top of the bushing, based on low-level sine-sweep tests. The second modes of the bushing are near 30 Hz and are much less significant than the primary modes shown in Table 7. However, other types of equipment may have higher modes that do contribute significantly to the dynamic response of equipment.

For each failure, the time of failure is recorded and the center frequency of motion at that time is determined. The maximum response of an SDOF oscillator at that

Table 7. Bushing primary modes of vibration and associated damping.

Mode of Vibration	Natural Frequency (Hz)	Equivalent Viscous Damping (% Critical)
1st Longitudinal	5.66 Hz	2.5 %
1st Lateral	6.35 Hz	3.0 %

frequency is calculated, which is the amplitude of the TRS (e.g., Figure 20) at the frequency of failure. This value of response spectrum amplitude together with the frequency of failure becomes a failure data point. These same values for each failure are plotted to produce a failure envelope. This failure envelope can now be compared directly with site-specific spectra or design spectra, as they represent the response of SDOF oscillators across a spectrum with the same damping (e.g., 2% of critical damping in this example).

Normally fragility tests will be uniaxial, and the same tests may be repeated in all three axes. However, for the IEEE 693 guidelines, tests are to be triaxial, with the horizontal design response spectrum shown in Figure 13 applied both in the lateral and longitudinal direction, plus the vertical design spectrum applied vertically. When triaxial tests are conducted, three independent random signals are needed for the tests to be truly triaxial. Because the test motions in each of the three directions are unique, the TRS will also differ, and the test engineer must determine which amplitude from the three TRS is the dominant cause of failure. Normally this will be the direction of motion that causes amplified equipment response at the frequency of failure.

Figure 28a shows the maximum achieved response spectra for all fragility tests up through Frag23, along with the IEEE 693 design spectra. The amplitude of these tests went as high as 220% of Figure 18, but with a large notch around the natural frequency of the bushing. Figure 28b shows all the failure points, the same maximum achieved TRS, and the IEEE 693 design spectra. The failures are summarized in Table 6. Each failure comprises either visible fluid leakage or slippage at the porcelain/flange connection, as defined in IEEE 693, sec D.5.1.[*] Note the V-shaped plot of the failures, with the amplitude of motions that cause failure increasing with distance away from the bushing natural frequency. This V-shape will be steeper for equipment with low damping due to the sharpness of resonance. After pushing the test levels very high outside the notch region (i.e., 220% of Figure 18 motions), further tests were conducted with the notch removed. The tests without notches caused increased leakage and slippage, but no additional failure modes were observed. The notch-less tests were conducted up to 160% of Figure 18 (Frag 24 – Frag 28). The maximum achieved TRS for these tests can be seen in Figure 28c along with the IEEE 693 design spectra.

---

[*] These qualification acceptance criteria state that there shall be no evidence of damage, such as broken, shifted, or dislodged insulators, visible leakage of oil, or broken support flanges. The visible fluid leaks and shifting seen at the bushing porcelain/flange connection therefore constitute a type of failure even though the leaks or minor slippage themselves will not impair bushing performance in the field. The bushing tested at USACERL was filled with 75 gallons of water to represent the weight of oil. Had it been filled with oil the leakage would have lubricated the connection and the slippage may have been much worse, leading to gasket or porcelain failure.

The fragility data presented in Figure 28b can be compared with design response spectra or site-specific spectra to evaluate the equipment's (i.e., bushing's) vulnerability to other support motion. This use of the fragility data was evaluated by testing the bushing according to the IEEE 693 high performance level spectra and particular site-specific spectra. Figure 29a shows the maximum achieved TRS for IEEE 693 random tests. The TESS motions were generated by the shake table software to fit the high performance level spectra, with 20 seconds of strong motion and 5 seconds of ramp-up and ramp-down. The TRS shown in Figure 29a are based on 50% of the generated test motions and the IEEE 693 spectra envelopes are plotted at the same 50%. The test levels were reduced to 32%, at which level leaking was first observed. The TRS amplitude at the 6 Hz natural frequency of the bushing (i.e., response of an SDOF oscillator at 6 Hz) was 1.28 g. This data point is shown in Figure 29a. Table 8 summarizes these tests.

The IEEE 693 tests require random motions with energy across a broad frequency range (see Figure 29a). Random motion tests such as these are necessary in conjuction with fragility tests to confirm that high- and low-frequency modes do not couple to produce a mode of failure that would not be seen in the sweeping narrow-band random fragility tests. Thus these tests validate that coupled modes have not been overlooked in the fragility test procedure.

In a similar manner, the bushing was tested against time histories generated to fit TVA site-specific spectra. Leaking was first initiated at 200% of these motions and the resulting TRS are plotted in Figure 29a. The amplitude of the TRS at 6 Hz for the site-specific-spectrum-based test was slightly greater at 1.61 g. This is because the dominant energy for the site-specific waveform peaks at slightly

Table 8. Qualification tests conducted on CERL TESS (percent IEEE 693 HP level and TVA site-specific).

Date of Test	Test File Name	Test Level, % Fig13	High-Pass (HP) Filter	Failure or Other Observations
10/29/96	IEEE2	20%	None	None
10/29/96	IEEE3	30%	1.0 Hz HP- Long only	None
10/29/96	IEEE4	50%	1.0 Hz HP all 3 axes	Major fluid leaks
10/29/96	IEEE5	40%	1.0 Hz HP all 3 axes	Moderate fluid leaks
10/30/96	IEEE6	35%	1.0 Hz HP all 3 axes	Small leaks
10/30/96	IEEE7	32%	HP 1.0 Hz Long & Vert	Small leak
10/29/96	EQTST31	200%*	None	Site-Specific Spectra, Small Leak

* The test level of EQTST31 was 200% of the time-histories generated to fit the TVA site-specific spectra.

greater frequencies than the 6 Hz bushing frequency, whereas IEEE 693 specifies a broad distribution of energy across the spectrum. Table 8 also summarizes the site-specific test.

The magnitude of the TRS at failure and at 6 Hz, from both the IEEE 693 and site-specific tests, agree well with the magnitude of failure in the fragility tests at 6 Hz. Figure 29b shows the failure points from the fragility, IEEE 693, and site-specific tests. However, the fragility tests reveal more information in terms of the equipment's vulnerability to motions away from its own natural frequency — the sharpness of the V, for example, in Figure 28b. Test data from Frag 23 suggest that 2.3 Hz motions excited a 6 Hz (first mode) response in the bushing. This observation is based on comparing the TESS-achieved acceleration and longitudinal (axis of bushing) displacement from a linear variable differential transformer (LVDT) around 22 seconds.

All observations made here are based on TESS motions, TESS motion TRS and limited strain, and LVDT measurements near the bushing flange. Test data could be analyzed further to evaluate the response of the bushing, but these few observations are sufficient to illustrate the application of CEFAPP.

There also are other potential modes of failure that may not even be associated with the equipment's first mode of vibration. Many additional observations can be made about modes of failure from fragility test data, revealing additional information about the nature of equipment response and vulnerability. Fragility testing may also be used to evaluate methods of upgrading vulnerable equipment.

Probability Considerations for Fragility Data

It should be noted that the fragility data shown in Figure 28b are failure points for only one narrow-band random sweep record (Ran3, which has been scaled, HP filtered and notched). Other narrow-band random sweep records would create somewhat different failure data. However, failure is primarily due to a resonant response of some portion of the equipment, and equipment response is similar to that of the response of an SDOF oscillator, of which response spectra are made up. A single failure point on the TRS is the response of an SDOF oscillator, with the center frequency attributed to failure and the damping for which the response is calculated. Therefore, a different narrow-band random signal, scaled to produce the same equipment failure/response would generate a response similar to an SDOF oscillator at the frequency of failure, resulting in a failure point of essentially the same magnitude and frequency as that from the original record.

Real-world equipment response will differ somewhat from that of an SDOF oscillator, especially for equipment modes of vibration with large damping. The response of equipment will also be somewhat load-path dependent, especially if the equipment responds in a nonlinear manner. If the equipment failure causes significant material or geometric nonlinear response, the modes of vibration and therefore frequency of failure will shift (normally decreasing because of the reduced stiffness that damage causes). Such nonlinear response will make the equipment response and fragility data path dependent. Modal testing should be conducted both before and after fragility testing to determine if there was a frequency shift at the modes of vibration responsible for failure. In the case of the bushing, the frequencies shown in Table 7 did not shift, which confirms that the bushing failures did not cause permanent mechanical damage and that the bushing response was not path dependent. Because the primary bushing modes of vibration have very low damping (2.5 % in the longitudinal direction, as indicated in Table 7), the bushing failure data from only one record is reasonable. If other equipment being tested had greater damping, or the failure modes included significant nonlinear response, testing with multiple narrow-band random sweep records may be necessary. In the case of significant nonlinear response, a new undamaged equipment specimen (or the original one with the damaged components replaced) would have to be tested with the new narrow-band random sweep record.

Variations in equipment construction may lead to variation in the fragility data if the modes of failure are influenced by properties of the equipment that vary. For example, if a failure mode is very dependent on a particular welded connection, then a large tolerance in weld construction or variations in the quality of the weld will lead to large variation on the resulting fragility. This condition would require the testing of several specimens in order to build a statistically significant fragility data set. From these data, confidence bands or probability of failure lines (drawn across the response spectra data envelope) would be added to the fragility data. The bushing failure leakage and slippage is dependent on the flange detailing, porcelain details at this connection, gasket construction, and tension in the spring-loaded center tension rod. It is assumed that all of these are standard for this model and manufacturer of bushing, with possible exception in the prestress of the tension rod. Therefore, it must be understood that the fragility data presented here are only applicable for the particular bushing tested; the users of such data would need to investigate whether their bushing varies (in the construction related to the failure modes) from the one tested here. Again, it must be emphasized that this fragility test is only intended as a demonstration of CEFAPP and such details on bushing construction had not been gathered.

Using the Fragility Data

The fragility data collected in the narrow-band random sweep tests define the capacity of the equipment tested. Site-specific or IEEE 693 design spectra define the demand. Equipment vulnerability is determined by comparing the capacity and demand. For example, Figure 30 shows the bushing fragility data (capacity) together with site-specific and IEEE 693 spectra (two cases of demand). The fragility data plot above the site-specific spectrum, indicating that the bushing is not vulnerable to this seismic demand. However, the fragility data plot below the IEEE 693 spectrum (between 4 and 7 Hz), indicating a predicted failure to this seismic demand. In a similar manner the bushing capacity may be compared with other site-specific or design spectra. As noted previously, the IEEE 693 spectrum in Figure 30 should be modified to reflect transformer amplification. If the demand spectra plots above the fragility data (capacity), then the equipment is vulnerable to the type of failure that the fragility data represents (i.e., bushing fluid leaking and slippage in this example).

Equipment vulnerability is defined as that region on the spectrum plot where the demand exceeds the capacity. Multiple regions may define more than one mode of failure, induced either by different failure mechanisms (e.g., leaking, slippage or porcelain fracture) or different modes of vibration (e.g., first or second lateral). Defining this vulnerability will guide equipment retrofit approaches.

If equipment fails qualification tests, CEFAPP also can be used as a diagnostic procedure to define the mode or modes of failure that prevented passing the qualification tests. The information gathered on mode of failure and amplitude and frequency of failure can be used to design a retrofit that will ensure the equipment passes the qualification test requirements.

Quantifying equipment dynamic characteristics and modes of failure is essential to developing equipment protection. Analytical models can be developed, based on the vulnerability data gathered, that allow the generalization of the vulnerability data to equipment with similar dynamic characteristics and modes of failure. Vulnerability of equipment not tested could be defined based on such models.

5 How to Use the Test Results

Chapter 4 presented a specific example of the use of CEFAPP in the vulnerability evaluation of a power transformer bushing. This chapter more generally presents the definition of equipment demand and shows how that demand is compared with the capacity as defined in Chapter 2 and illustrated in Chapter 4.

Defining Predicted Equipment Support Motions

These motions may result from vibration of the supporting structure caused by earthquakes, explosions from accidents or terrorist attack, or heavy vehicle traffic near the building. The predicted motions will normally be expressed in terms of design response spectra. Development of site-specific response spectra based on site conditions and ground motion potential will form the most accurate basis for defining equipment support motion. In the absence of these data, earthquake response spectra can be developed following two methods. The first is using the current guidance in the 1994 *NEHRP*[*] *Recommended Provisions for Seismic Regulations for New Buildings* (comprising FEMA[**] 222A, Part 1 – Provisions, and FEMA 223A, Part 2 – Commentary). The second and preferred method will be to use the 1997 NEHRP *Recommended Provisions* which according to 1994 NEHRP FEMA 222A (Appendix to chap 1, p 19) will provide "a new, more rational seismic design procedure." This document states that:

> unlike the current design procedure, which uses the relatively dated USGS (U.S. Geological Survey) peak velocity and peak acceleration ground motion maps, the revised procedure will be based on the USGS spectral response maps, which are being revised.

Final maps are already available from USGS and preliminary guidance on their use is available in the *1991 NEHRP Recommended Provisions for the Development of Seismic Regulations for New Buildings* (FEMA 222, Part 1 Provisions), Appendix to Chapter 1, "Preliminary Spectral Response Maps and Method for Establishing Design Ground Motions."

---

[*] NEHRP: National Earthquake Hazards Reduction Program.
[**] FEMA: Federal Emergency Management Agency.

The example seismic design spectra developed in this chapter are based only on the first mode response of the equipment-supporting structure. These design spectra provide simple response-spectra-based demand that can be used to illustrate the demand versus equipment fragility comparison that establishes equipment vulnerability. However, a more rigorous definition of design response spectra based on multi-mode dynamics of the structure is recommended. A modal analysis approach that parallels the modal analysis procedure in Section 2.4 of NEHRP 1994 is given in Singh, Suarez, Matheu, and Maldonado (1993, hereinafter referred to as "NCEER-93-0013").

Shock design response spectra are commonly used, based on code guidance or time history analysis. At this time only brief comments are made on defining predicted motions based on shock response spectra. However the procedures laid out in detail for seismic spectra also apply to shock-induced vibration response spectra.

Site-Specific Response Spectra

When sufficient information can be obtained on seismic or shock motion potential, site-specific response spectra may be developed. This will allow more precise definition of predicted motions, which will result in potential savings due to less severe demand on the equipment. Site-specific response spectra will require detailed knowledge about fault characteristics near the site, geological data, building construction type, and specific location of equipment to be installed. Figure 31 is an example of a site-specific response spectrum.

Current Guidance from 1994 NEHRP Recommended Provisions

The seismic response spectrum is developed from FEMA 222A. These provisions serve as a broadly accepted source document for building design codes. The response spectrum is developed from these provisions for the building site under consideration by determining the variables shown below:

1. Effective peak acceleration, A_a from Map 1 and Table 1.4.1.1 or Map 3
2. Effective peak velocity-related acceleration, A_v from Map 2 and Table 1.4.1.1 or Map 4
3. Soil profile type A through F as defined in Section 1.4.2
4. Seismic coefficient, C_a, from soil profile type and A_a from Table 1.4.2.4a
5. Seismic coefficient, C_v, from soil profile type and A_v from Table 1.4.2.4b
6. Response modification coefficient, R, from Table 2.2.2, based on the structural system and seismic force resisting system of the building
7. Modal period of vibration (in seconds) of the mth mode of the building, T_m

8.   Modal seismic response coefficient, C_{sm}, is determined by (Equation 2.4.5-3):

$$C_{sm} = \frac{1.2 C_v}{R T_m^{2/3}}$$ [Eq 2]

9.   maximum modal seismic response coefficient, C_{smMAX}, is (Section 2.4.5):

$$C_{smMAX} = \frac{2.5 C_a}{R}$$ [Eq 3]

Equations 2 and 3 (for C_{sm} and C_{smMax}) are plotted to give the seismic response spectrum. The seismic response spectrum is replotted in terms of spectral acceleration (C_{sm} and C_{smmax}) versus frequency (Hz); or spectral velocity, V (inches/second), versus frequency. The spectral velocity and frequency are calculated from the modal seismic response coefficient, C_{sm}, and modal period, T_m, as follows:

$$f_m = \frac{1}{T_m} \qquad and \qquad V = \frac{a}{\omega} = \frac{386\, in/sec^2/g\ C_{sm}}{2\pi f_m}$$ [Eq 4]

Example Response Spectrum Based on 1994 NEHRP Recommended Provisions

To illustrate this procedure a response spectrum is developed for San Francisco, CA, soil profile type D (stiff soil) and an ordinary moment frame building of reinforced concrete:

1.   Effective peak acceleration, A_a, from Map 1 is 0.4g
2.   Effective peak velocity-related acceleration, A_v, from Map 2 is 0.4g
3.   Soil profile type D, based on section 1.4.2.
4.   Seismic coefficient, C_a, from Table 1.4.2.4a for soil profile type D and A_a = 0.4g is 0.44g.
5.   Seismic coefficient, C_v, from Table 1.4.2.4b, for soil profile type D and A_v = 0.4g is 0.64g.
6.   Response modification coefficient, R ,from Table 2.2.2, for an ordinary moment frame building of reinforced concrete is 3.
7.   Modal period of vibration (in seconds) of the mth mode of the building is T_m.
8.   Modal seismic response coefficient, C_{sm}, is determined by (Equation 2.4.5-3):

$$C_{sm} = \frac{1.2\,C_v}{R\,T_m^{2/3}} = \frac{(1.2)(0.64g)}{3\,T_m^{2/3}} = \frac{0.256g}{T_m^{2/3}} \qquad \text{[Eq 5]}$$

9. Maximum modal seismic response coefficient, C_{smMAX}, is (Section 2.4.5):

$$C_{smMAX} = \frac{2.5\,C_a}{R} = \frac{(2.5)(0.44g)}{3} = 0.367g \qquad \text{[Eq 6]}$$

Figure 32a shows the expressions above for C_{sm} and C_{smMax} plotted with respect to period (T_m), giving the seismic response spectrum. Figure 32b re-plots the seismic response spectrum in terms of spectral acceleration (C_{sm} and C_{smMax}) versus frequency.

Future Guidance from 1997 NEHRP Recommended Provisions

The more rational design procedure to be made available in the 1997 NEHRP Recommended Provisions will use USGS Spectral Acceleration maps. Draft versions (intended for trial design) of these maps are available in the 1994 NEHRP Recommended Provisions, Maps 5 through 13. Final versions of the USGS Spectral Acceleration maps are now available from USGS on the Internet at http://wwwneic.cr.usgs.gov/eq/finmaps.shtml. Table 9 summarizes spectral maps from both sources that are available as of this writing. Figures 33a, 33b and 33c show these maps for California/Nevada for 2% probability of exceedence (PE) in 50 years for spectral acceleration periods of 0.2 seconds, 0.3 seconds, and 1.0 seconds, respectively. Figures 34a, 34b, and 34c show similiar maps for the 2% PE for the Central and Eastern United States.

Defining the seismic threat for such low probabilites is appropriate for critical facilites and equipment. The 2% PE in 50 years is equivalent to a return period of 2500 years (i.e., estimate these levels of seismic motions every 2500 years). The 5% PE and 10% PE in 50 years equate to return periods of 1000 and 500 years, respectively. For the low probablities of 2% PE, the greatest spectral accelerations for the New Madrid area in the Central United States are almost as great as those in California. However, for the higher probabilities (5% and 10% PE) the seismic threat for the West coast is much greater, because severe motions are expected much more frequently.

Table 9. Seismic spectral response maps from NEHRP 1994 and USGS Internet home page.

Region	Spectral Acceleration Period	Probability of Exceedance in 50 years	Spectral Acceleration Value	Draft 1994 NEHRP Map No.	Final USGS Map No. by Region
National	0.2 sec	10%	$S_{A(0.2)}$		4
National	0.2 sec	5%	$S_{A(0.2)}$		5
National	0.2 sec	2%	$S_{A(0.2)}$		6
National	0.3 sec	10%	$S_{A(0.3)}$	5	7
National	0.3 sec	5%	$S_{A(0.3)}$		8
National	0.3 sec	2%	$S_{A(0.3)}$	9	9
National	1.0 sec	10%	$S_{A(1.0)}$	7	10
National	1.0 sec	5%	$S_{A(1.0)}$		11
National	1.0 sec	2%	$S_{A(1.0)}$	11	12
California/Nevada	0.2 sec	10%	$S_{A(0.2)}$		4
California/Nevada	0.2 sec	5%	$S_{A(0.2)}$		5
California/Nevada	0.2 sec	2%	$S_{A(0.2)}$		6
California/Nevada	0.3 sec	10%	$S_{A(0.3)}$	6	7
California/Nevada	0.3 sec	5%	$S_{A(0.3)}$		8
California/Nevada	0.3 sec	2%	$S_{A(0.3)}$	10	9
California/Nevada	1.0 sec	10%	$S_{A(1.0)}$	8	10
California/Nevada	1.0 sec	5%	$S_{A(1.0)}$		11
California/Nevada	1.0 sec	2%	$S_{A(1.0)}$	12	12
Central/Eastern U.S.	0.2 sec	10%	$S_{A(0.2)}$		4
Central/Eastern U.S.	0.2 sec	5%	$S_{A(0.2)}$		5
Central/Eastern U.S.	0.2 sec	2%	$S_{A(0.2)}$		6
Central/Eastern U.S.	0.3 sec	10%	$S_{A(0.3)}$		7
Central/Eastern U.S.	0.3 sec	5%	$S_{A(0.3)}$		8
Central/Eastern U.S.	0.3 sec	2%	$S_{A(0.3)}$		9
Central/Eastern U.S.	1.0 sec	10%	$S_{A(1.0)}$		10
Central/Eastern U.S.	1.0 sec	5%	$S_{A(1.0)}$		11
Central/Eastern U.S.	1.0 sec	2%	$S_{A(1.0)}$		12

Preliminary guidance on developing spectral response maps, using the data provided in the draft maps from 1994 NEHRP and the USGS Internet site, is given in the *1991 NEHRP Recommended Provisions* (FEMA 222, Part 1, Appendix to Chapter 1). The method presented in that appendix is modified slightly to incorporate the new spectral acceleration values for the 0.2 second period available on the USGS Internet site. Since the USGS Internet maps are final, all spectral acceleration values will be taken from these maps. The following variables are determined from these maps, together with 1991 NEHRP and 1994 NEHRP, and are defined below:

1. Spectral acceleration (0.2), $S_{A(0.2)}$, is the spectral response acceleration coefficient, at a period of 0.2 second, expressed as a fraction of gravity, from the USGS locations shown in Table 9.

2. Spectral acceleration (0.3), $S_{A(0.3)}$, is the spectral response acceleration coefficient, at a period of 0.3 second, expressed as a fraction of gravity, from the USGS locations shown in Table 9.

3. Spectral acceleration (1.0), $S_{A(1.0)}$, is the spectral response acceleration coefficient, at a period of 1.0 second, expressed as a fraction of gravity, from the USGS locations shown in Table 9.

4. Soil coefficient, S, is based on the soil profile types defied in Table 3.2 (Appendix to Chapter 1, 1991 NEHRP).

5. Response modification coefficient R, from Table 3.3, is based on the structural system and seismic force resisting system of the building.

6. Modal period of vibration (in seconds) of the mth mode of the building is T_m.

7. n = 1 for $T_m \leq 1.0$ second; or 2/3 for $T_m > 1.0$ seconds.

8. Modal seismic design coefficient, C_{sm}, is determined by (Equation 5-3):

$$C_{sm} = \frac{S_{A(1.0)}S}{RT_m^n} \qquad\qquad \text{[Eq 7]}$$

9. Maximum modal seismic design coefficient, C_{smMAX}, is (Section 2.4.5):

$$C_{smMAX} = \frac{S_{A(0.2)}}{R} \qquad and \qquad C_{smMAX} = \frac{S_{A(0.3)}}{R} \qquad \text{[Eq 8]}$$

The equations above for C_{sm} and C_{smMAX}, are plotted with respect to period (T_m) to give the seismic response spectrum. If $S_{A(0.2)}$ and $S_{A(0.3)}$ differ, interpolate the values for C_{smMAX} between the periods of 0.2 and 0.3 seconds. The seismic response spectrum is replotted in terms of spectral acceleration versus frequency.

Example Response Spectrum Based on 1997 NEHRP Recommended Provisions

To illustrate this procedure a response spectrum is developed for San Francisco, CA, soil profile type S_2 (stiff clay) and an ordinary moment frame building of reinforced concrete. Critical emergency response equipment is located in the building and it is determined that the most conservative 2% PE in 50 years should be used for defining the seismic demand.

1. Spectral acceleration (0.2), $S_{A(0.2)}$, from USGS California/Nevada Region Map 6 (see Figure 33a) is 3.2 g.
2. Spectral acceleration (0.3), $S_{A(0.3)}$, from USGS California/Nevada Region Map 9 (see Figure 33b) is 3.2 g.
3. Spectral acceleration (1.0), $S_{A(1.0)}$, from USGS California/Nevada Region Map 12 (see Figure 33c) is 3.0 g.
4. Soil coefficient, S, for soil profile type S_2, is 1.0.
5. Response modification coefficient, R, for an ordinary moment frame building of reinforced concrete is 2.
6. Modal period of vibration (in seconds) of the mth mode of the building is T_m.
7. n = 1 for $T_m \leq 1.0$ second; or 2/3 for $T_m > 1.0$ seconds.
8. Modal seismic design coefficient, C_{sm}, determined by (Equation 5-3):

$$C_{sm} = \frac{S_{A(1.0)}S}{RT_m^n} = \frac{(3.0g)(1.0)}{2T_m^n} = \frac{1.5g}{T_m^n} \qquad \text{[Eq 9]}$$

9. Maximum modal seismic design coefficient, C_{smMAX} is (Section 5.5):

$$C_{smMAX} = \frac{S_{A(0.3)}}{R} = \frac{3.2g}{2} = 1.6g \qquad \text{[Eq 10]}$$

$$C_{smMAX} = \frac{S_{A(0.2)}}{R} = \frac{3.2g}{2} = 1.6g \qquad \text{[Eq 11]}$$

Figure 35a shows the expressions above for C_{sm} and C_{smMax} plotted with respect to period (T_m), giving the seismic response spectrum. Figure 35b replots the seismic response spectrum in terms of spectral acceleration versus frequency.

Shock Motions

A significant threat to equipment is shock-induced building vibration caused by either accidental or hostile explosions. Shock motions at locations where equipment is to be installed are commonly defined in terms of a shock response spectra. Figure 36 is an example of a shock response spectrum for a floor slab in a building based on a finite element analysis of the building. This spectrum defines the support motion demand that equipment installed at this location must withstand.

Comparing Equipment Capacity and Demand

The equipment fragility (capacity) as defined by this test procedure is next compared to the predicted support motions (demand). This is illustrated using the CERL fragility data and the predicted support motions defined by response spectra whose development was described above. Figure 37 shows the fragility data (from Figure 8), site-specific response spectrum (from Figure 31), 1994 NEHRP-based earthquake spectrum for San Francisco (from Figure 32b), 1997 NEHRP-based earthquake spectrum for San Francisco (from Figure 35b), 1997 NEHRP-based earthquake spectrum for Memphis, (2%PE) and shock response spectrum (from Figure 36). The 1997 NEHRP-based spectrum for San Francisco is much greater than the 1994 NEHRP spectrum; in fact the 1997 spectrum with 10% PE is much greater than the 1994 spectrum. This is because the new USGS maps provide a degree of micro-zonation. Not only the USGS spectral acceleration but also peak acceleration maps now provide this micro-zonation such that the San Francisco location has peak acceleration values for 10% PE of 1.0 g. For the same location the 1994 NEHRP maps give a 0.4 g effective peak acceleration value for the same 10% PE in 50 years, based on the broader boundaries of this most severe seismic zone. All earthquake spectra shown in Figure 37 are based on soil profile type S_2 (stiff clay) and an ordinary moment frame building of reinforced concrete.

If the predicted motions, represented by the design response spectra (demand), fall below the fragility data throughout the frequency range, the equipment is adequate as long as it is anchored in the same manner as it was during the shake table testing. The equipment is vulnerable if the response spectra exceed the fragility data along any portion of the frequency range. This indicates that the equipment must either be strengthened or protected against the design-spectra-based predicted motions within that frequency range. The earthquake design spectra shown in Figure 37 fall below the equipment fragility data all across the frequency range, except for the 1997 NEHRP-based San Francisco spectrum at 2% PE, which falls slightly above in the 4 to 17 Hz range. Had the slower sweep rate of 6 octaves/minute been used in the fragility testing, as defined based on later sweep-rate calculations and the validation test results, the equipment would have failed at lower levels, resulting in greater vulnerability relative to the spectra shown in Figure 37. All fragility data presented in Chapter 2 and this chapter are based on vertical support motions only, to which the tested equipment was particularly vulnerable. While Figure 37 illustrates the use of these data, actual comparison must be based on support motion demand and capacity in the same direction.

The predicted shock spectra shown in Figure 37 exceed the equipment fragility data for the entire frequency range above 6 Hz; thus the equipment is vulnerable to the shock motions above 6 Hz.

If a building is analyzed using a time-history analysis rather than a response spectrum approach, response spectra could be generated from the time histories. Generated time histories taken from locations where the equipment is to be installed can be used to generate response spectra using the method explained in Appendix D for the development of SDOF oscillator envelopes with 50% damping. Alternatively, response spectra can be generated from the design ground motion and anticipated damping of the building. From either approach the generated response spectra can be laid over the equipment fragility data to evaluate the vulnerability of equipment.

Guidance for Developing Equipment Protection Systems

Appropriate equipment strengthening or stiffening will raise the failure points above the predicted support motions. Alternatively, if the equipment is vulnerable to support motions at relatively high frequencies, the equipment may be protected by mounting the equipment on isolators. In general, the frequency of the equipment/isolator system should be no greater than the minimal vulnerable frequency of the unisolated frequency divided by $\sqrt{2}$. This will reduce the motions affecting the equipment at any isolator damping. Details on shock isolation design are provided in the *Shock and Vibration Handbook* (Harris 1988). The isolation however, could produce significant amplification of motions (especially for lightly damped isolators), and thus increase the response spectra demand near the natural frequency of the isolated system. For the predicted shock spectra shown in Figure 18, the equipment may be protected by mounting it on isolators that will result in an isolated system natural frequency at or below 4.2 Hz (6 Hz/$\sqrt{2}$).

As was discussed earlier, equipment may be instrumented at key locations to evaluate the modes of failure. In the testing of desktop computers done at USACERL, the predominant failure was read-write errors caused by the read-write head impacting and damaging the hard disk surface. An accelerometer was attached to the hard disk case to measure the vertical vibration of the hard disk. Figure 38a shows the response of the hard disk during Fragility Test 72, and Figure 38b shows the support motion at the base of the computer during the same test. Comparing the two shows significant amplified motion at the hard disk relative to the support locations. This amplification occurs between 32 and 90 Hz.

The computer frame appears to have provided significant attenuation of the support motion below 32 Hz and isolation above 90 Hz. The amplification is caused by resonance response in the computer frame and/or hard disk within the frequency range of amplification. This helps to explain why the computer failed at relatively low support motions within this range. Methods of protecting this equipment would naturally focus on this vulnerability.

Quantifying equipment dynamic characteristics and modes of failure is essential to developing equipment protection. Analytical models can be developed, based on the vulnerability data gathered, that allow the generalization of the vulnerability data to equipment with similar dynamic characteristics and modes of failure. Vulnerability of equipment not tested could be defined based on these models.

6 Conclusions

The CERL Equipment Fragility and Protection Procedure (CEFAPP) was developed to determine if equipment is vulnerable to predicted support motions.CEFAPP defines the frequency range at which the equipment is vulnerable and the mode or modes of failure created. The data generated by CEFAPP can be used to develop methods of protecting equipment, either by strengthening or isolation of the equipment.

The use of CEFAPP to test a power transformer bushing was presented in Chapter 4. Validation tests support the accuracy of this procedure for defining the capacity of equipment. The failure envelopes developed here can effectively be compared with seismic demand, thereby reducing the need for additional testing for other seismic hazards (e.g., using the same equipment at other locations). This is especially true if demand is defined by site-specific spectra, because earthquake potential is then expressed with respect to its frequency content. Equipment vulnerability for various locations may be evaluated by comparing various site-specific spectra with the capacity spectrum defined by the original fragility testing, thus eliminating need for further testing to accommodate new or unanticipated demands.

The characterization of equipment vulnerability may also be used to develop analytical models that would allow generalization to equipment with similar dynamic characteristics and modes of failure. With such models, the vulnerability of equipment not tested could be defined.

CEFAPP can be used to evaluate the effectiveness of prototype equipment protection design. Strengthening methods, isolation techniques, and combinations of the two may be evaluated by conducting fragility tests on protected equipment. CEFAPP could be used by equipment manufacturers to define the capability of their equipment to withstand a variety of dynamic support motions. Manufacturers could publish such information in their product literature, and the information could be used by equipment procurement personnel to assess the adequacy of the equipment for their installation, or to determine what protection may be needed. CEFAPP could significantly increase reliability and decrease the cost of critical equipment by reducing or eliminating the need for expensive qualification testing.

A more rigorous method for calculating sweep rate to produce equivalent numbers of strong motion cycles is needed. Future work in this area will investigate how to define sweep rate based on an improved numerical analysis of narrow-band random signals.

References

Bellcore, Network Equpiment-Building System (NEBS) Requirements: Physical Protection, Bell Communications Research, GR-63-CORE, Issue 1, October 1995.

Drake, J.L, et al., Protective Construction Design Manual, ESL-TR-87-57 (Air Force Engineering and Service Laboratory, November 1989).

FEMA, NEHRP Recommended Provisions for Seismic Regulations for New Buildings 1994 Edition, Part 1 Provisions, FEMA 222A, May 1995.

FEMA, NEHRP Recommended Provisions for Seismic Regulations for New Buildings 1994 Edition, Part 2 Commentary, FEMA 223A, May 1995.

FEMA, NEHRP Recommended Provisions for the Development of Seismic Regulations for New Buildings 1991 Edition, Part 1 Provisions, FEMA 222, January 1992.

FEMA, NEHRP Recommended Provisions for the Development of Seismic Regulations for New Buildings 1991 Edition, Part 2 Commentary, FEMA 223, January 1992.

FEMA 74, Reducing the Risks of Nonstructural Earthquake Damage – A Pictoral Guide (Federal Emergency Management Agency, September 1994), pp 7–12.

Harris, C.M., Shock and Vibration Handbook, 3d ed. (McGraw-Hill, 1988), chap 30–34.

IEEE 693, Recommended Practices for Seismic Design of Substations, draft 6 (Institute of Electrical and Electronics Engineers, 1997).

Otnes, R.K., and L. Enachson, Digital Time Series Analysis (John Wiley & Sons, 1972).

Rabiner, Lawrence R., and Bernard Gold, AT&T Theory and Practice of Digital Signal Processing, (Prentice-Hall, Englewood Cliffs, NJ).

Singh, M.P., L.E. Suarez, E.E. Matheu, and G.O. Maldonado, Simplified Procedures for Seismic Design of Nonstructural Components and Assessment of Current Code Provisions, NCEER-93-01 (National Center for Earthquake Engineering Research, August 1993).

Sues, R.H., C.E. Murphy, and R.A. Frank, Protective Constrution Design Manual Change 5, Expedient Hardening Methods for Structures Subjected to the Effects of Non-Nuclear Munitions (Air Force Engineering and Services Laboratory, ESL-TR-87-57, June 1991).

Thomson, W.T., Theory of Vibration With Applications (Prentice-Hall, 1981), pp 404–420.

Figures Referenced in Main Body of Report
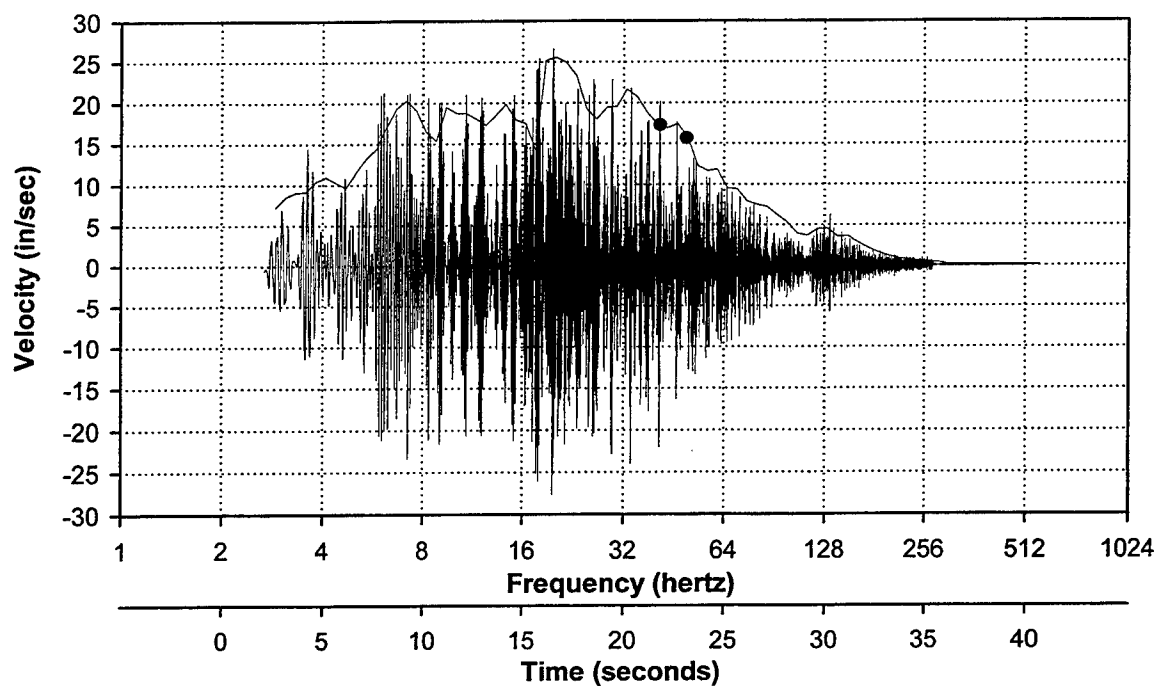
Figure 1. Example of narrow-band random sweep motions, Test 72.
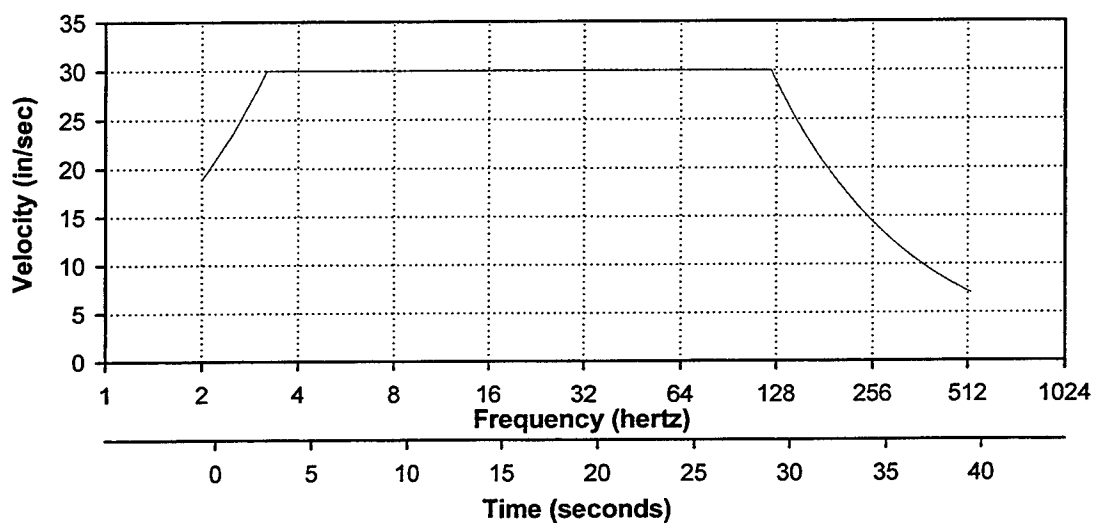
The upgrade of the USACERL shake table, which is now triaxial, included an increase in velocity capacity to 50 inches/second in the longitudinal and new lateral axes.

Figure 2. Envelope of the USACERL shake table vertical capacity.
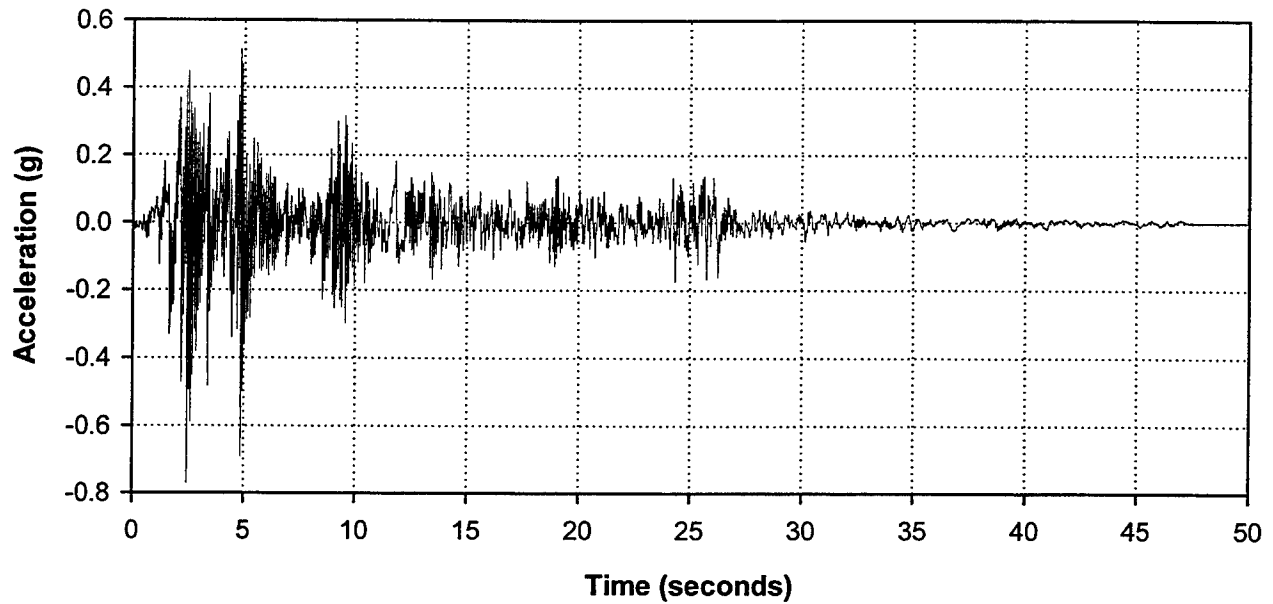
Figure 3a. Response of 12.2 hz SDOF oscillator to El Centro time history, 2% damping.
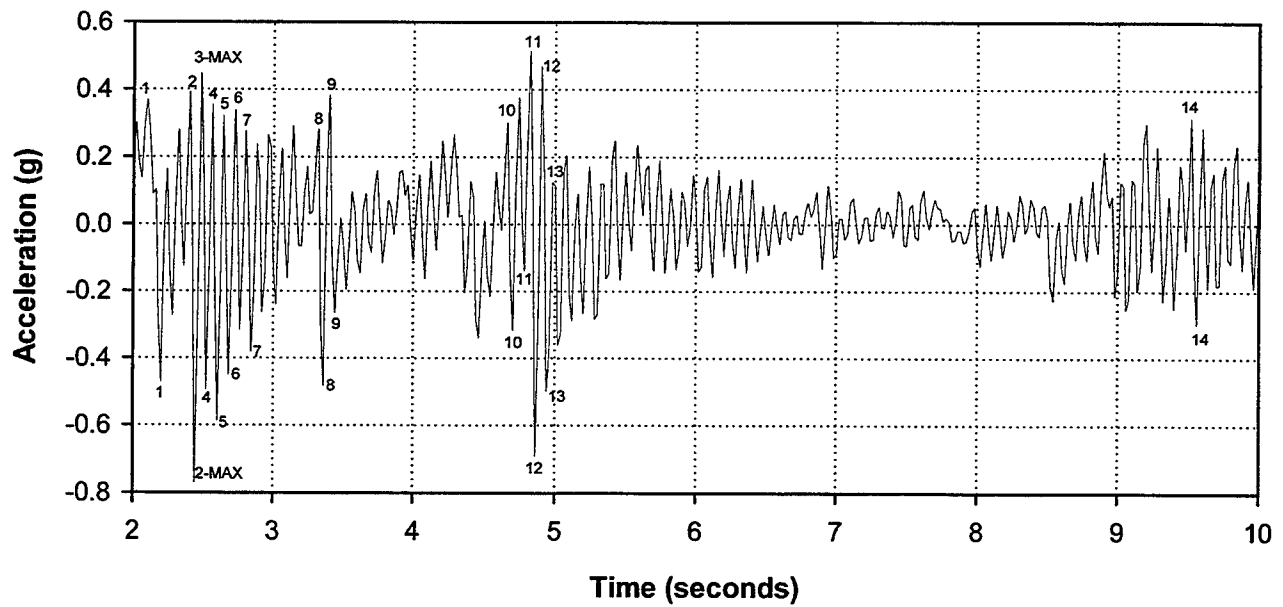
Figure 3b. Response of 12.2 hz SDOF oscillator identifying strong motion cycles.
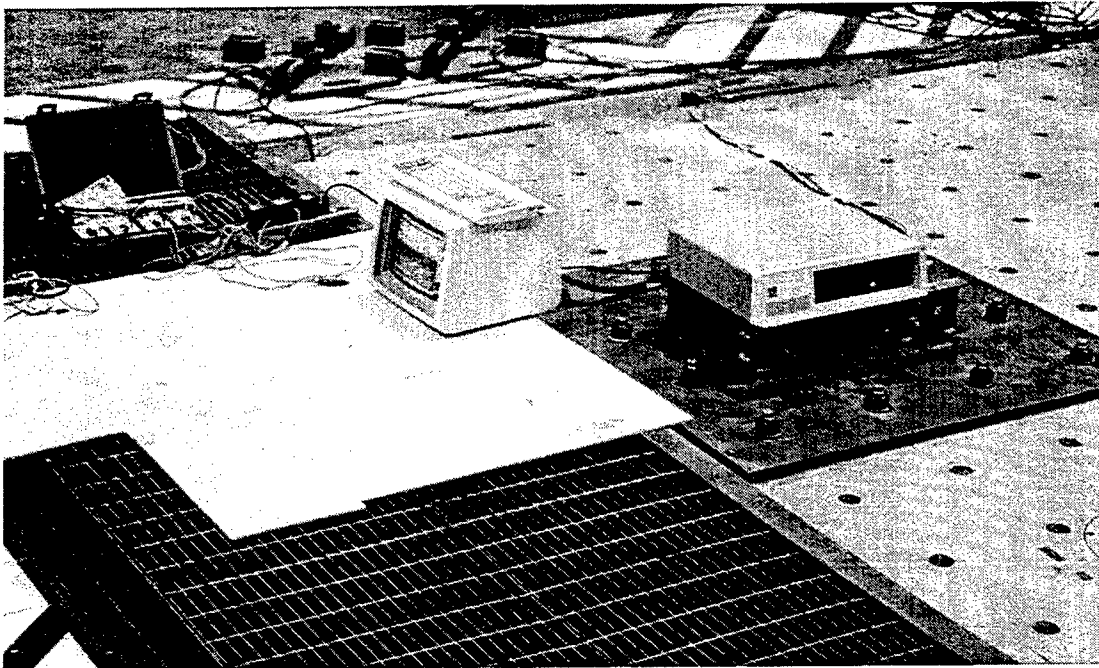
Figure 4a. Configuration of IBM-XT personal computer tested on the USACERL shaketable.
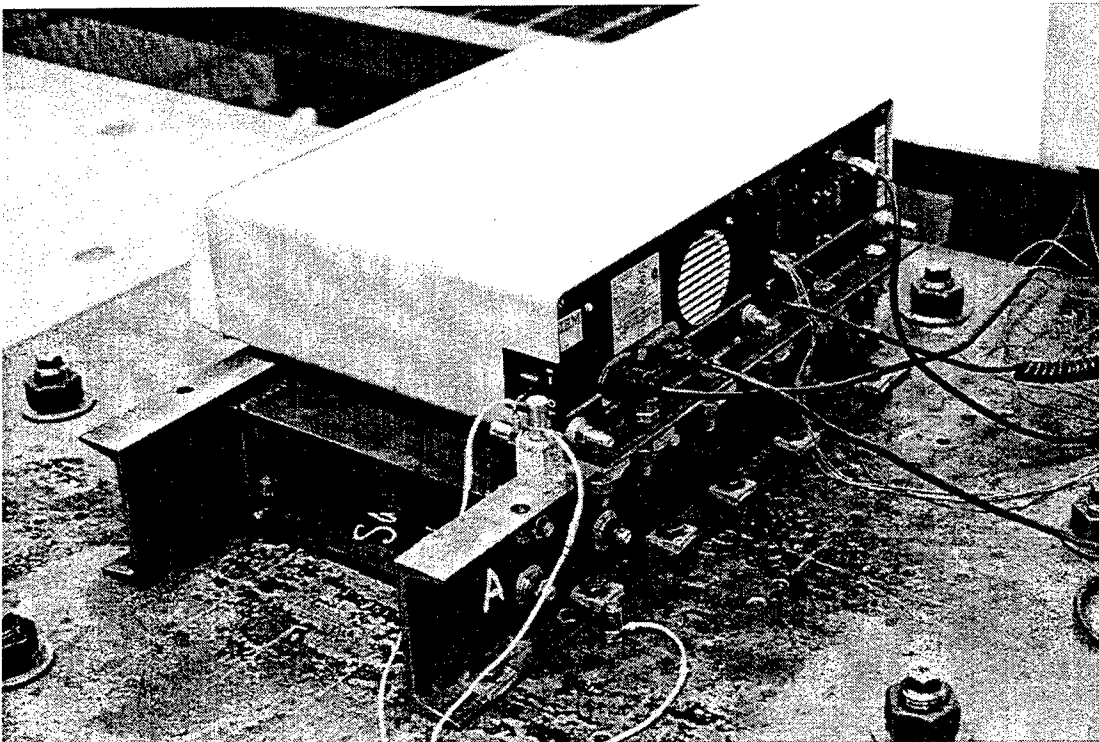
Figure 4b. Close-up showing anchorage and some instrumentation of the IBM computer.
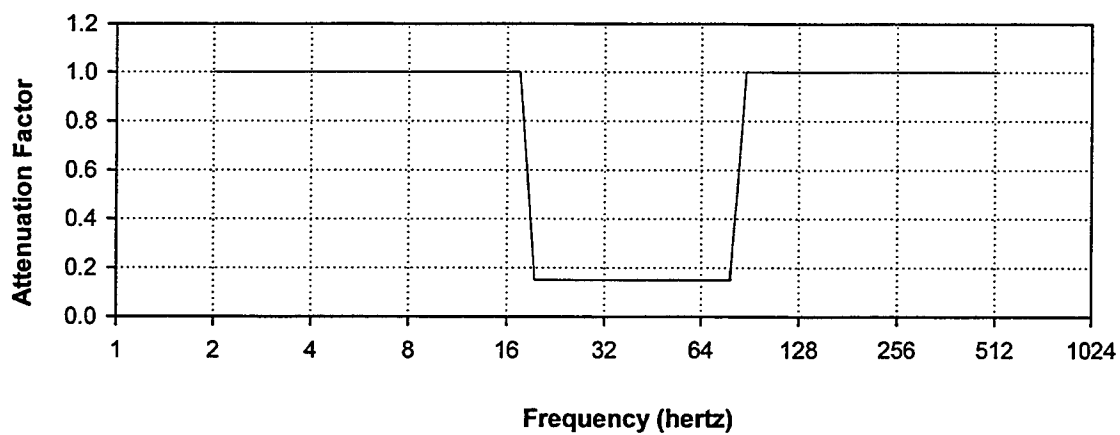
Figure 5a. Attenuation function for Fragility Test 67.
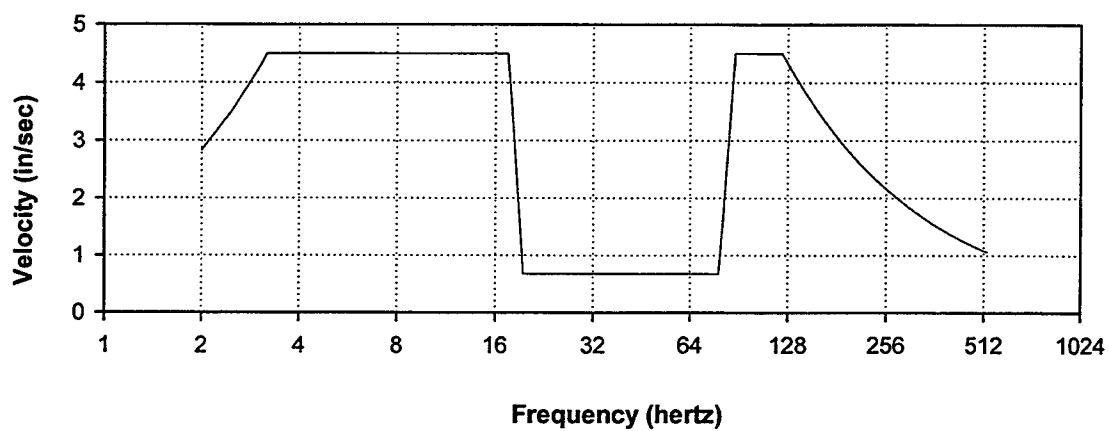
Figure 5b. Scaled envelope for Fragility Test 67.
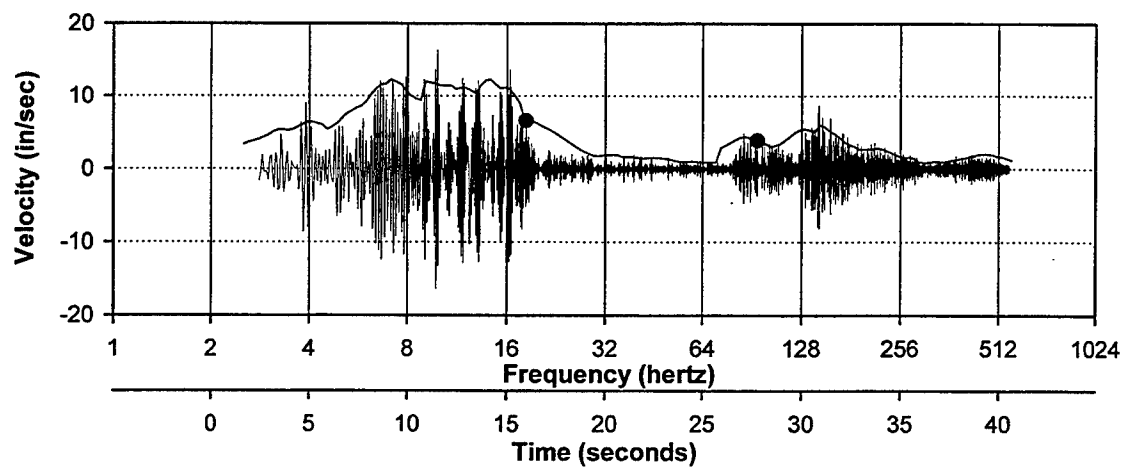
Figure 5c. Fragility Test 67 narrow-band random record and SDOF response envelope.
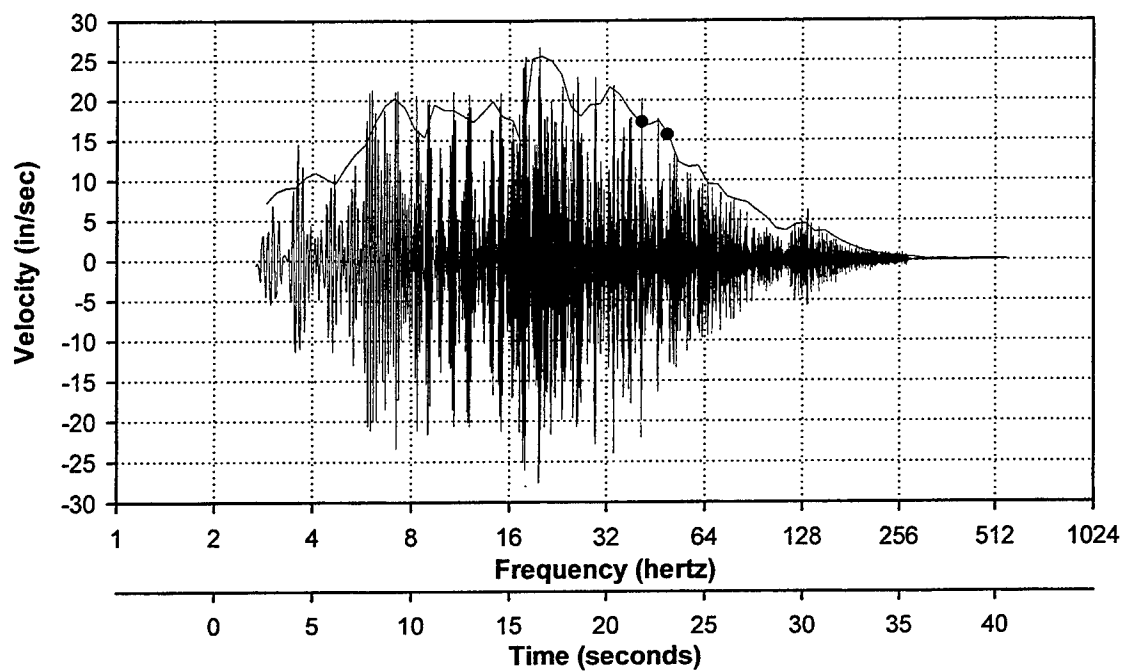
Figure 6a. Test 72 support motion, SDOF oscillator envelope and failure data.
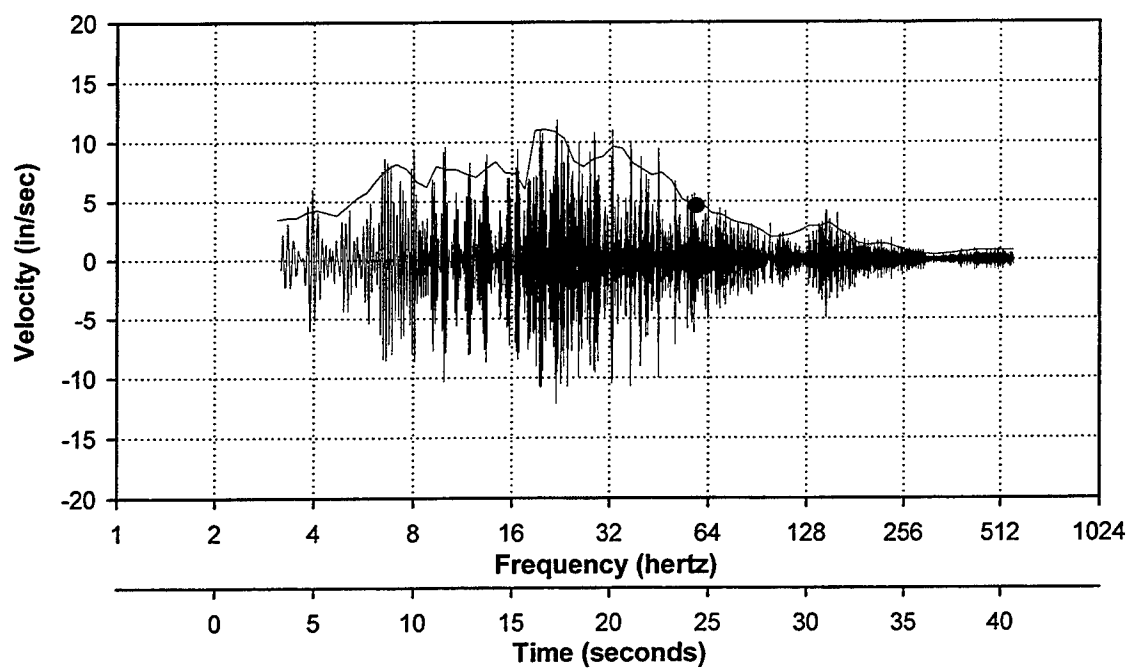
Figure 6b. Test 40 support motion, SDOF oscillator envelope and failure data.
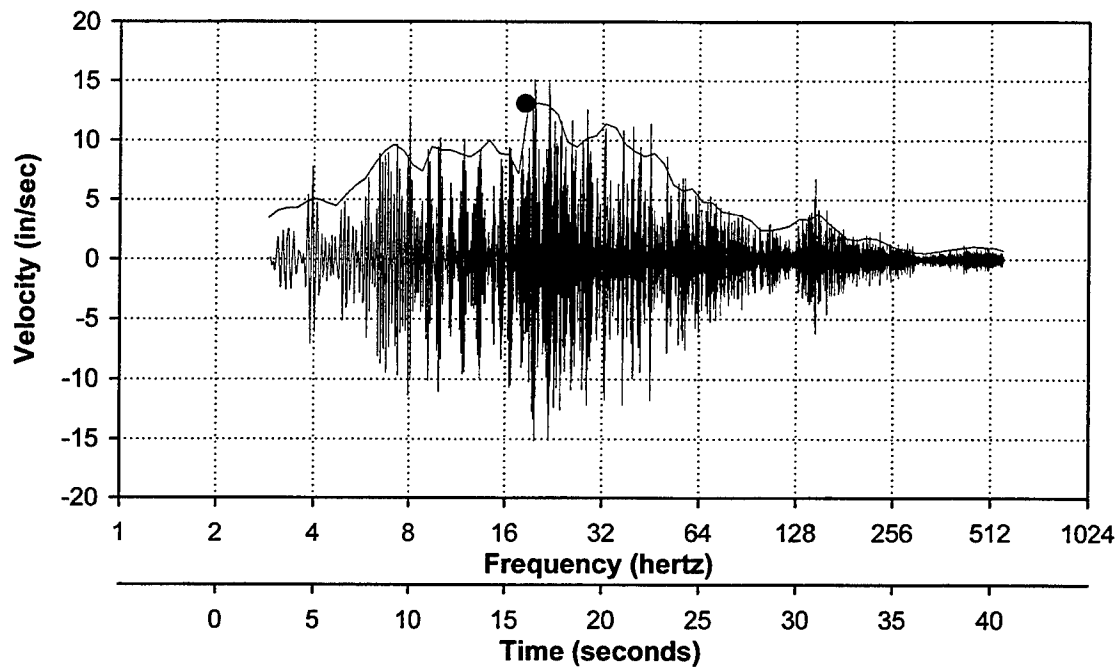
Figure 6c. Test 41 support motion, SDOF oscillator envelope and failure data.
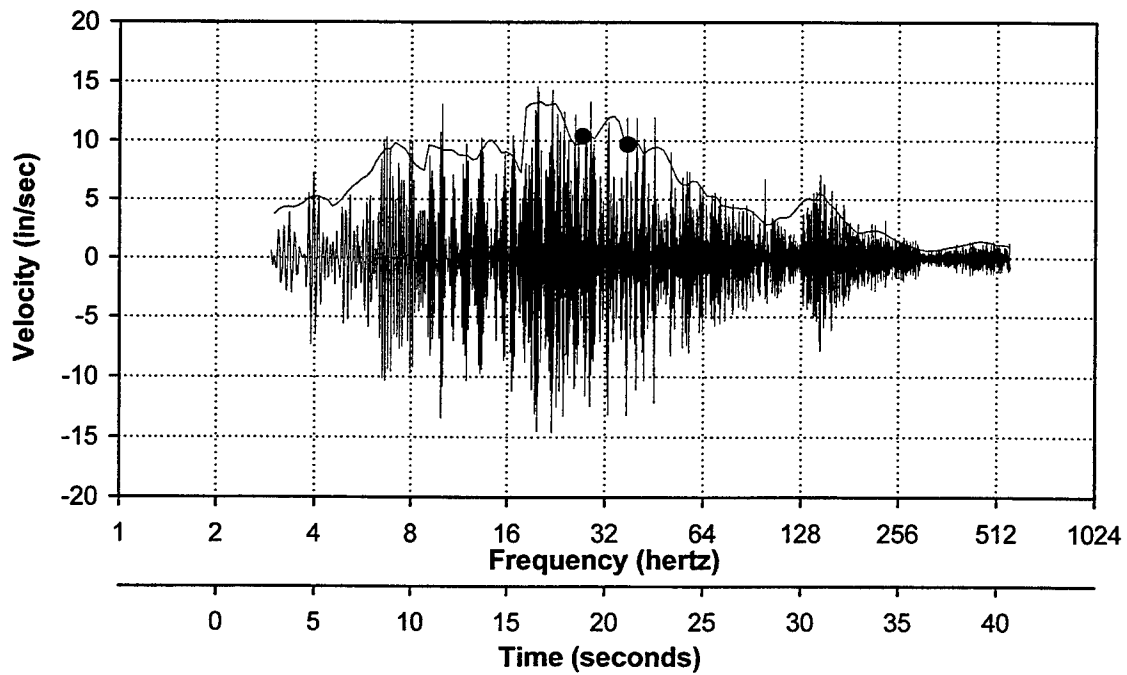
Figure 6d. Test 43 support motion, SDOF oscillator envelope and failure data.
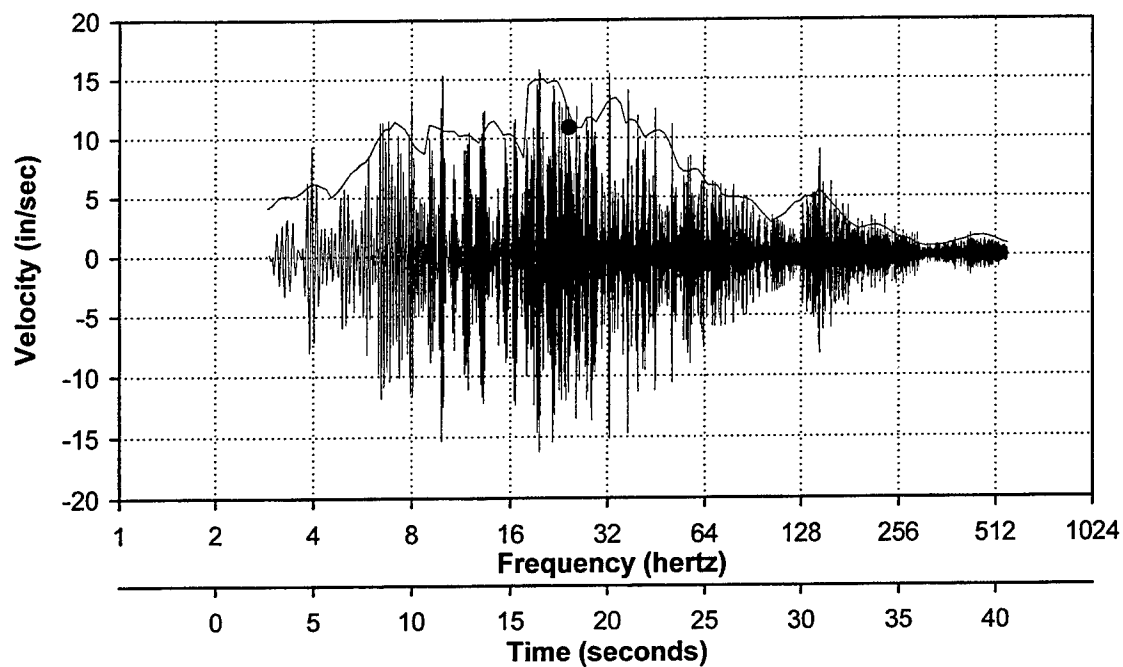
Figure 6e. Test 44 support motion, SDOF oscillator envelope and failure data.
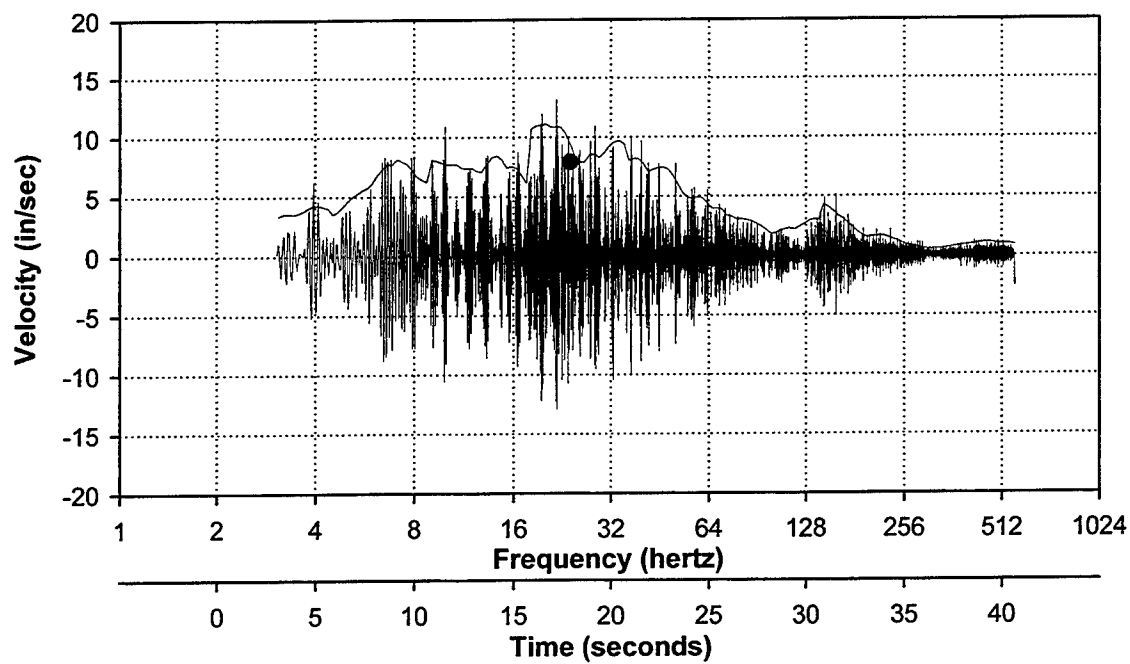
Figure 6f. Test 60 support motion, SDOF oscillator envelope and failure data.
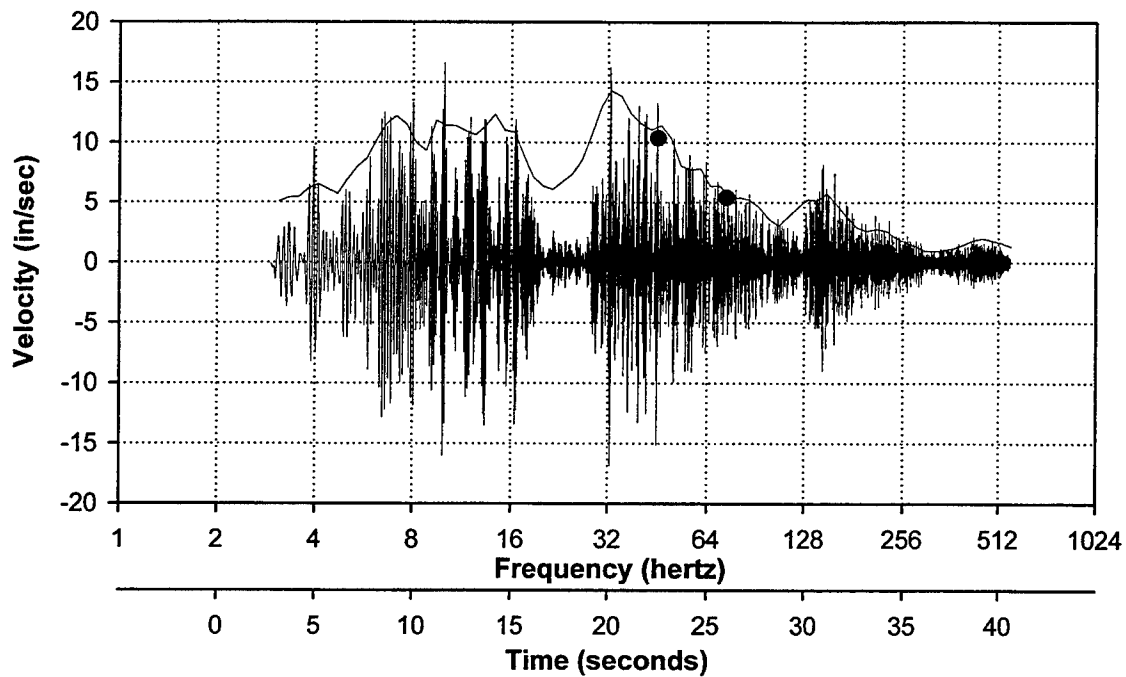
Figure 6g. Test 65 support motion, SDOF oscillator envelope and failure data.
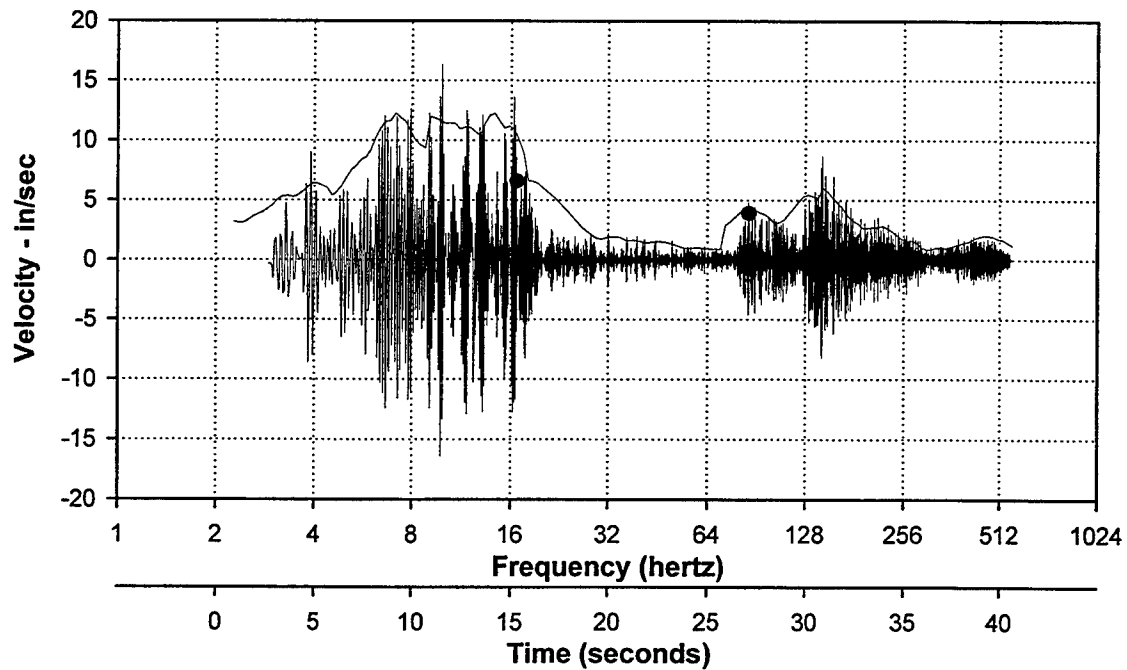
Figure 6h. Test 67 support motion, SDOF oscillator envelope and failure data.
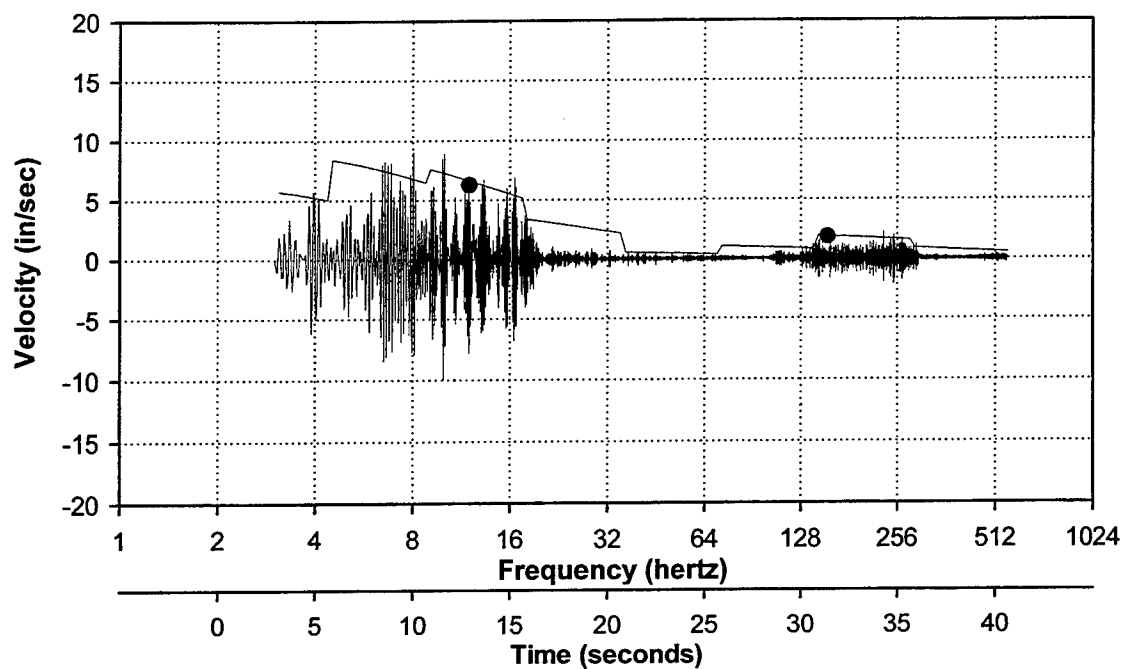
Figure 6i. Test 76 support motion, SDOF oscillator envelope and failure data.
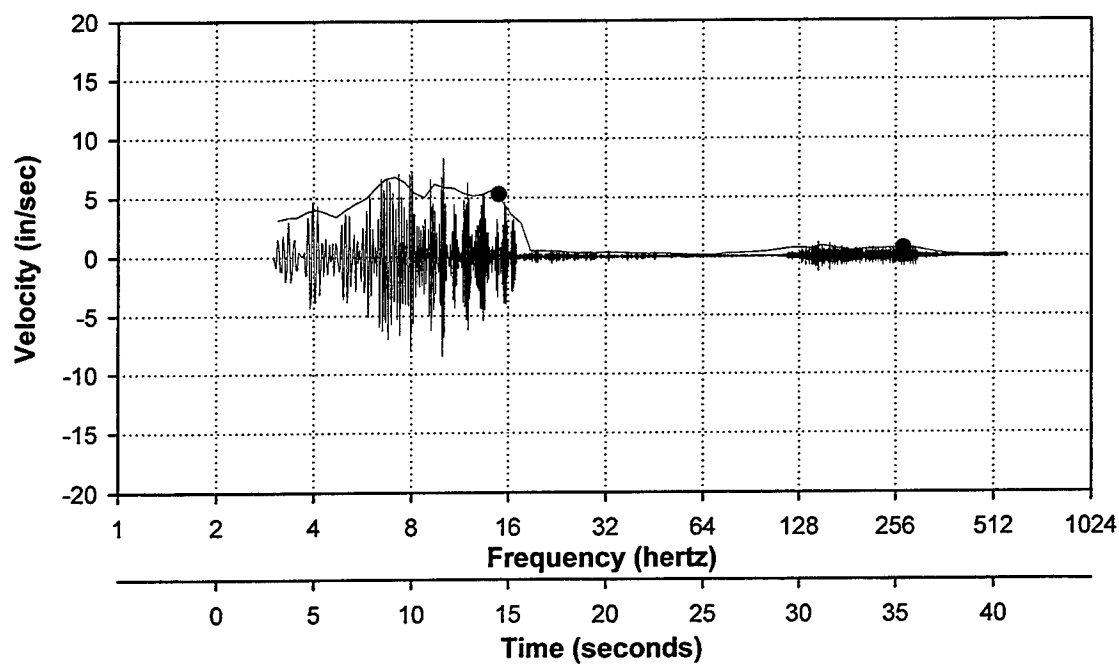
Figure 6j. Test 80 support motion, SDOF oscillator envelope and failure data.
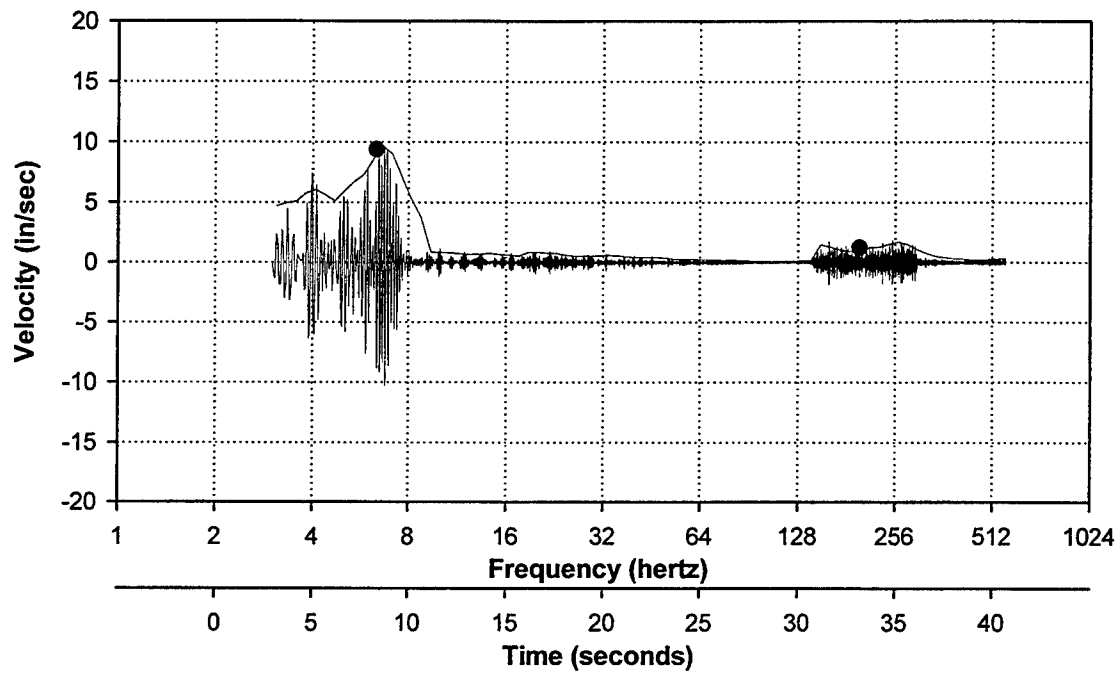
Figure 6k. Test 86 support motion, SDOF oscillator envelope and failure data.
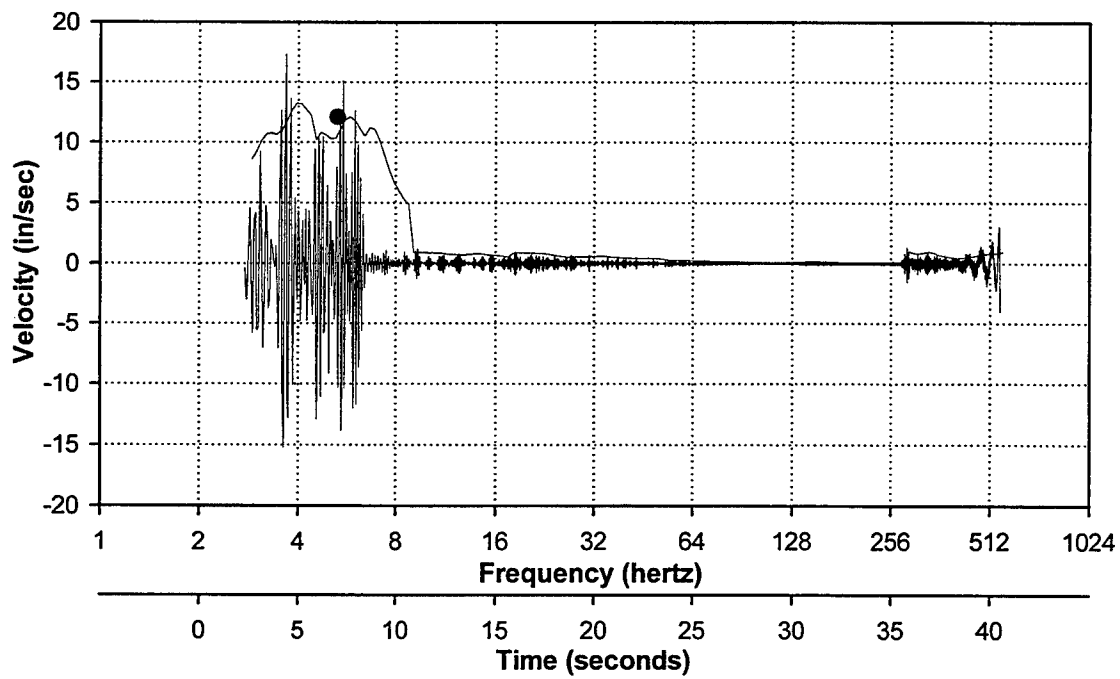
Figure 6l. Test 101 support motion, SDOF oscillator envelope and failure data.
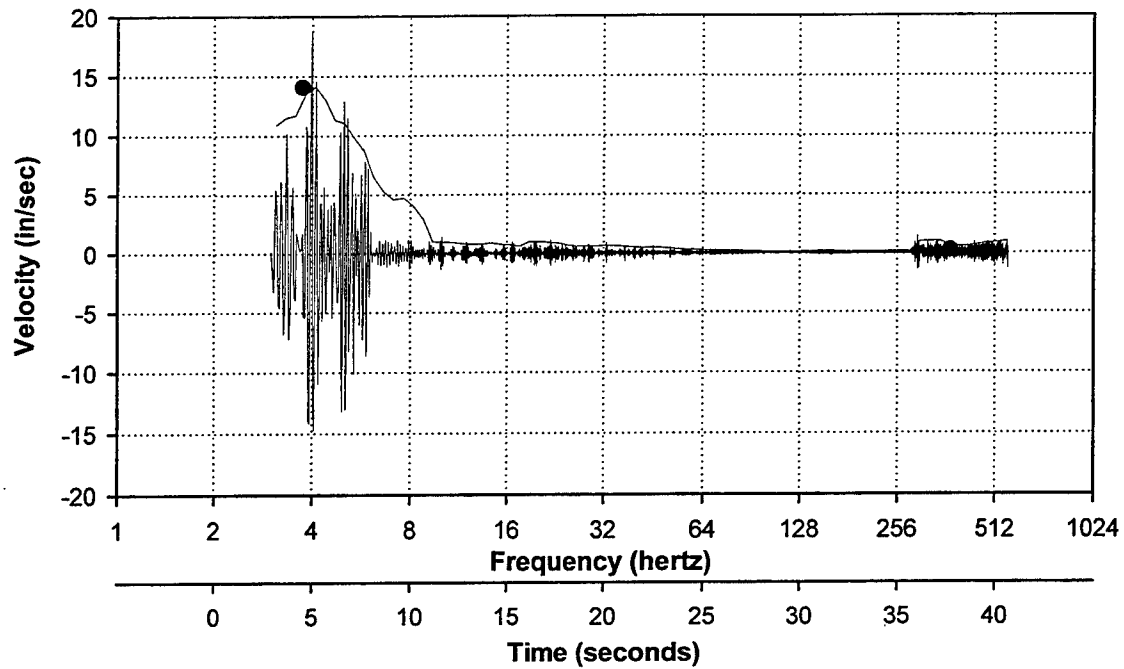
Figure 6m. Test 105 support motion, SDOF oscillator envelope and failure data.
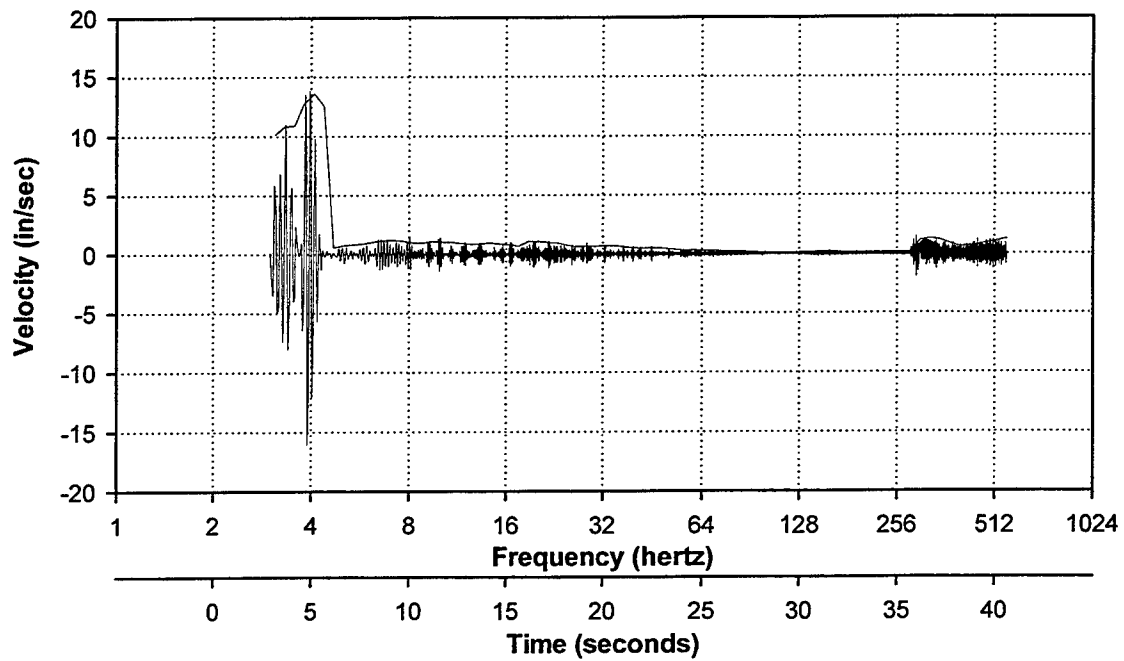
Figure 6n. Test 107 support motion, SDOF oscillator envelope and failure data.
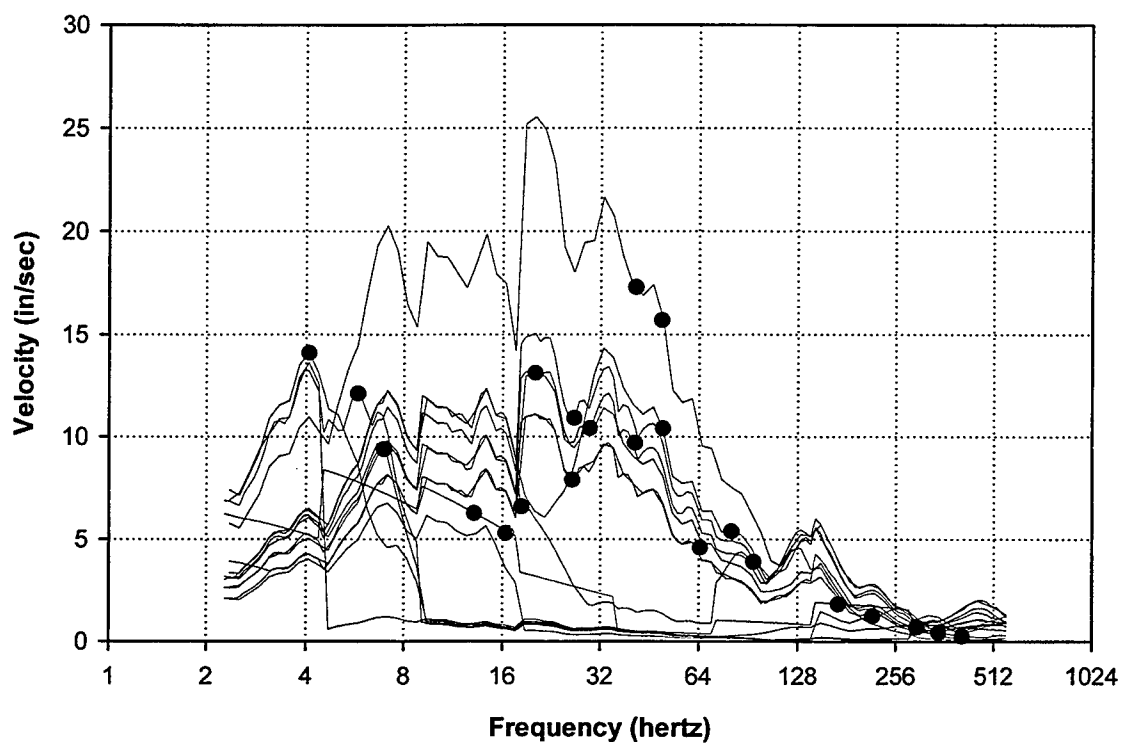
Figure 7. SDOF envelope of support motion and failure data.
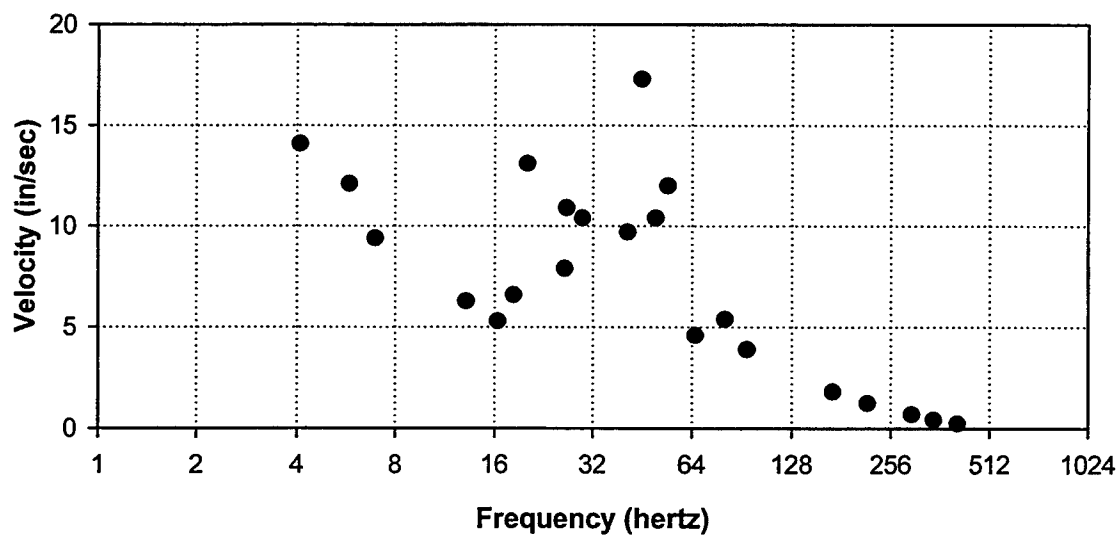
Figure 8. Equipment fragility data.
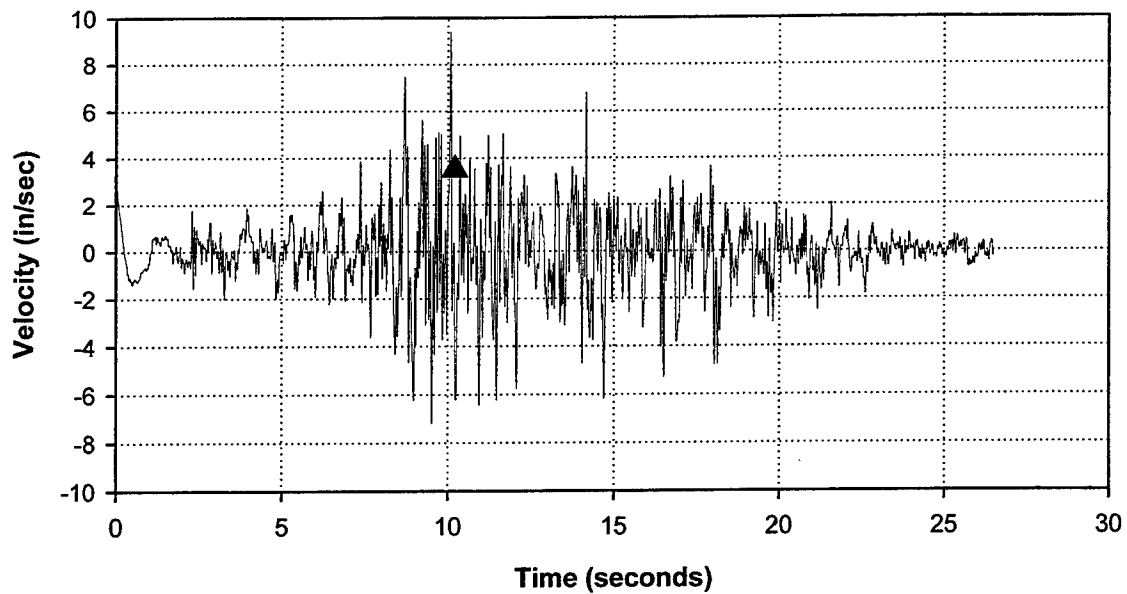
Figure 9a. Lucerne seismic record with failure point.
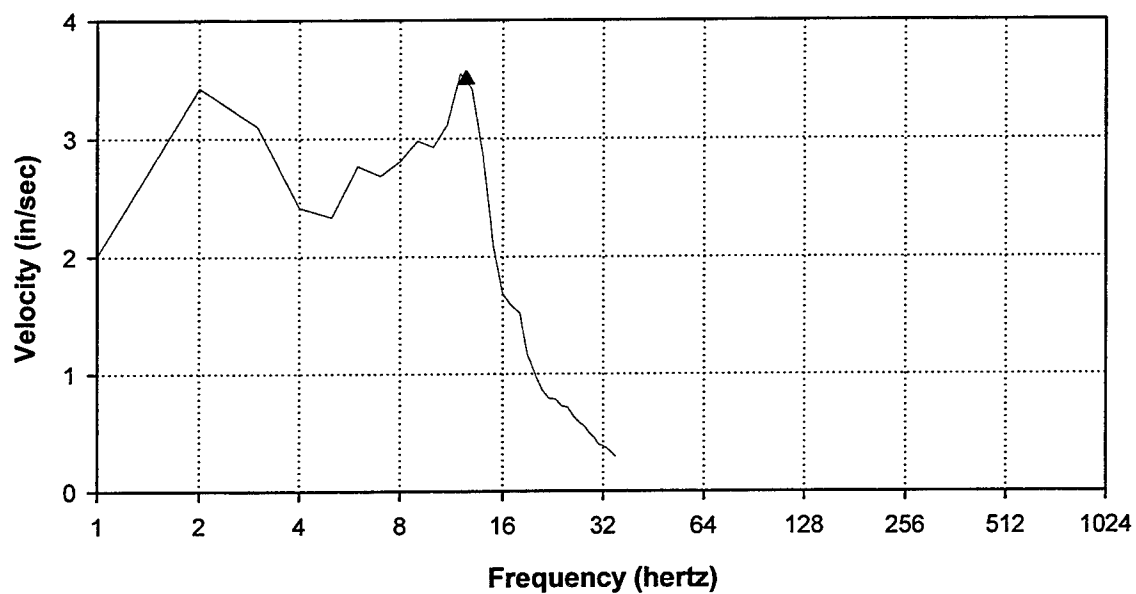
Figure 9b. SDOF envelope of Lucerne seismic record with failure point.
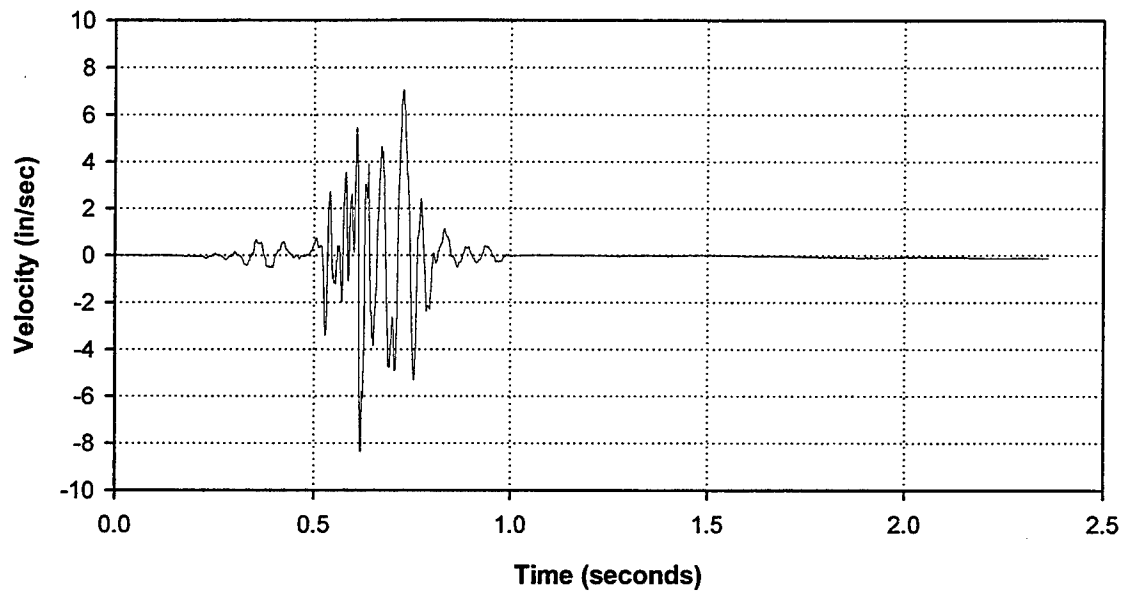
Figure 10a. Shock record.
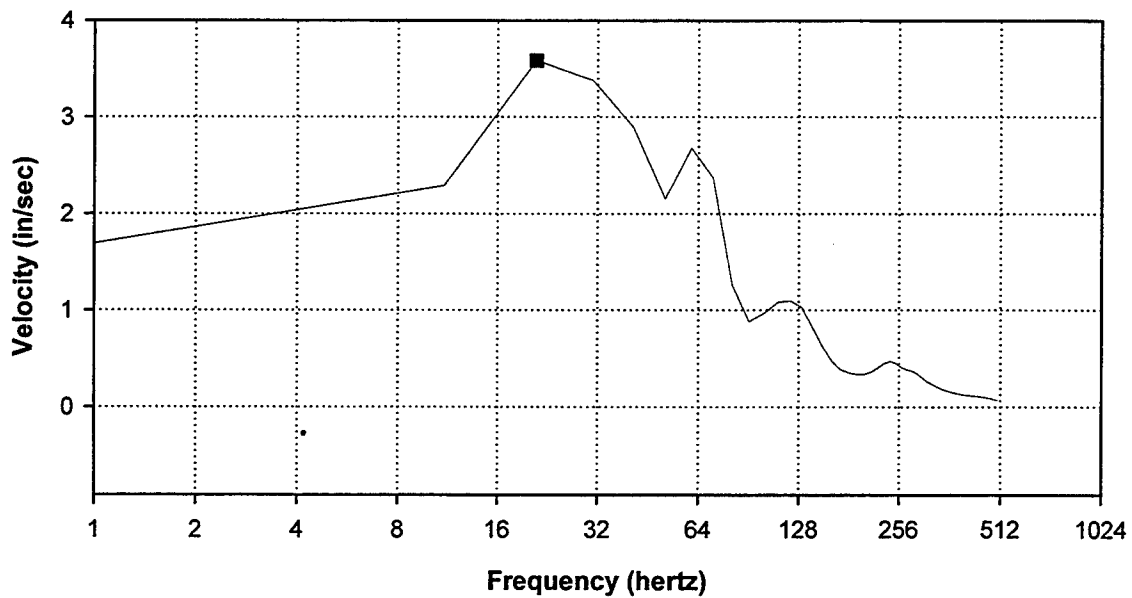
Figure 10b. SDOF envelope of shock record with failure point.
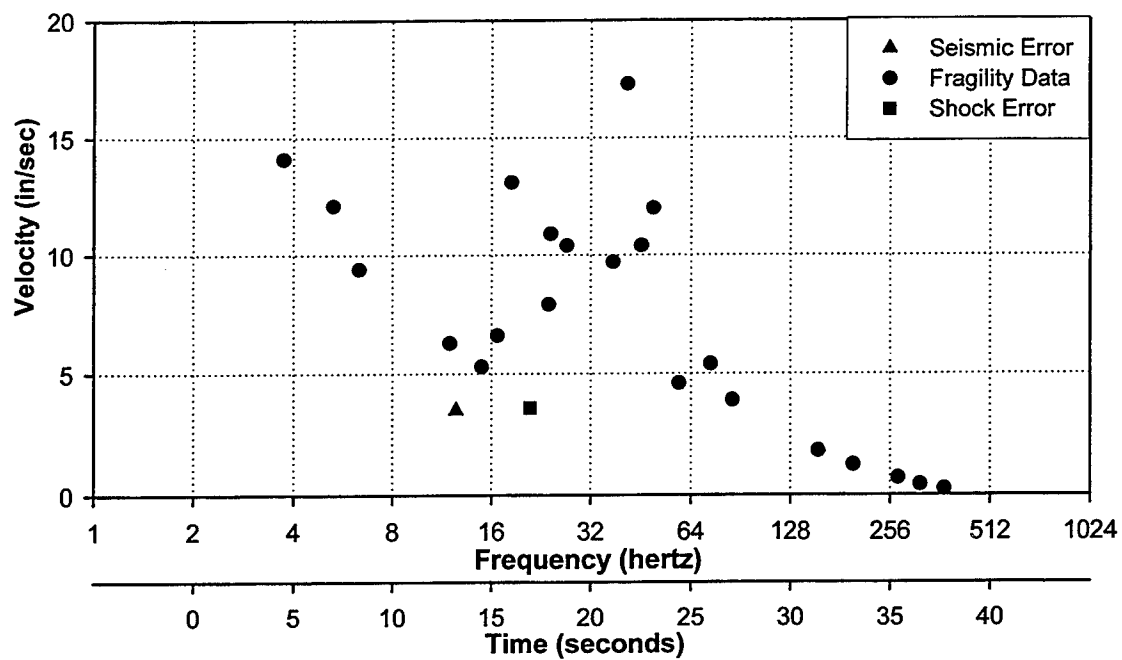
Figure 11. Fragility data with seismic and shock failures.
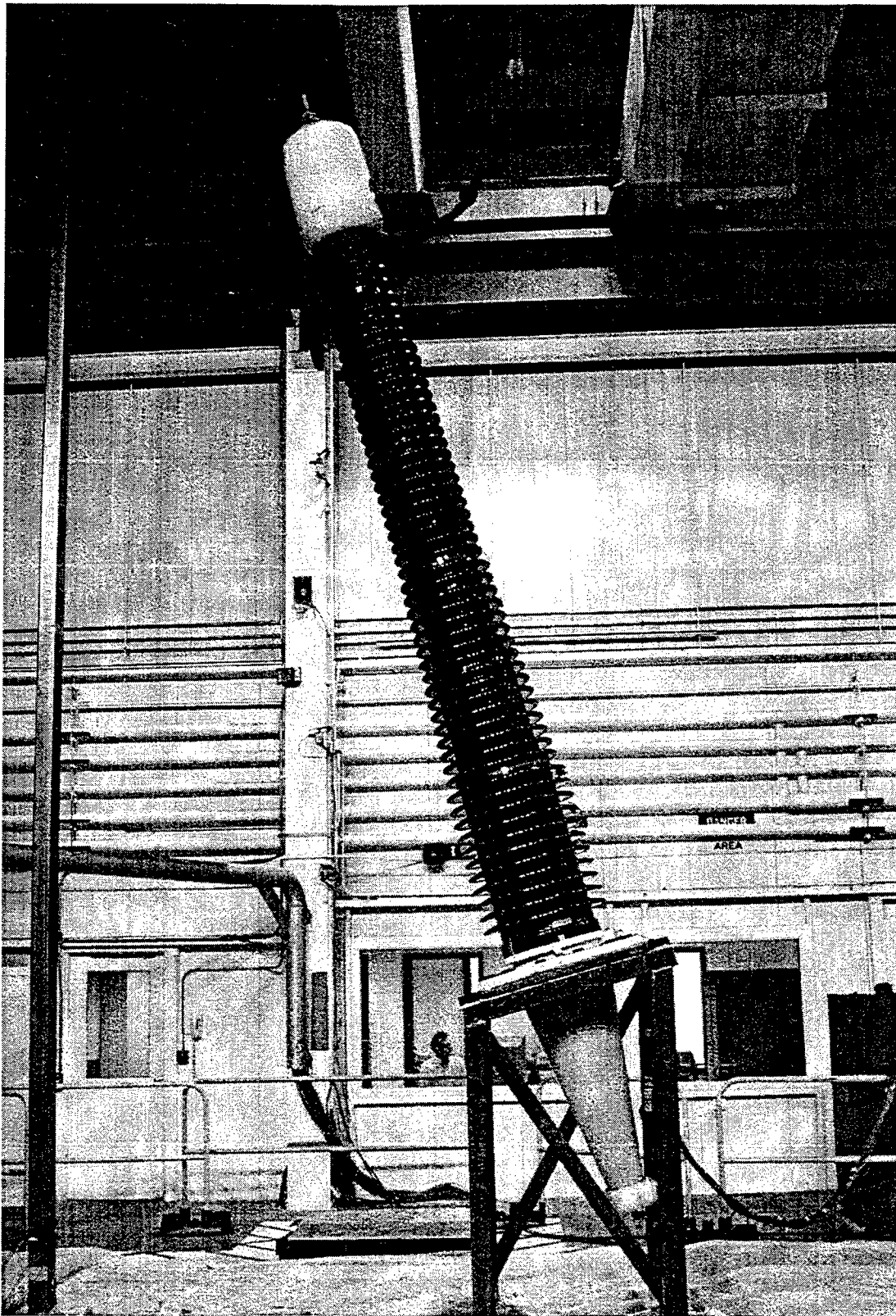
Figure 12. TVA power transformer bushing tested on the USACERL triaxial shake table.
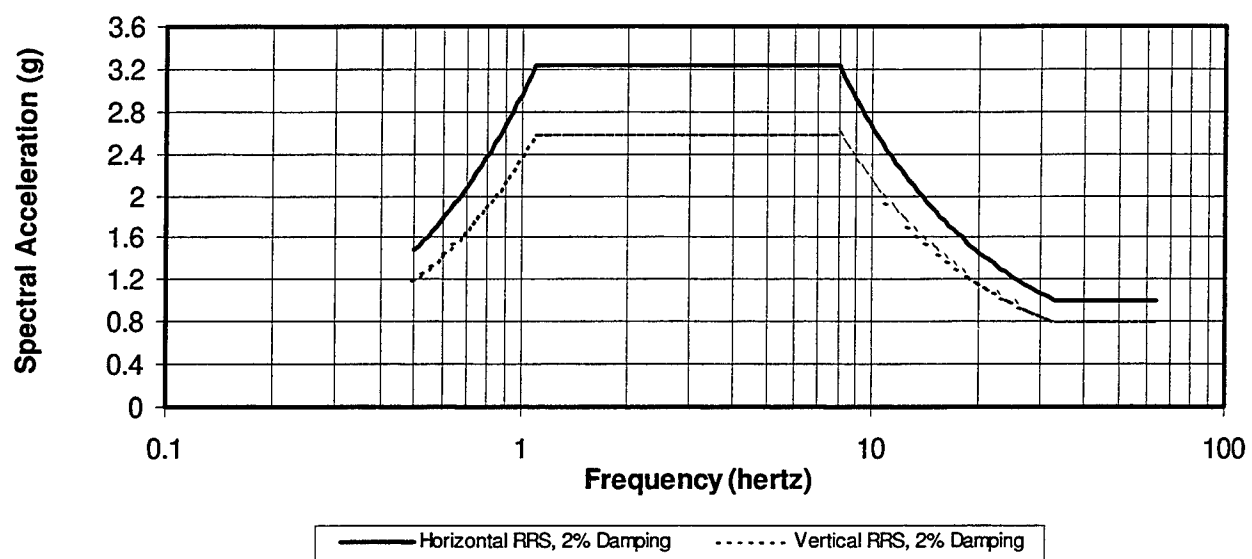
Figure 13. Horizontal and vertical response spectra, IEEE 693 high seismic performance level.
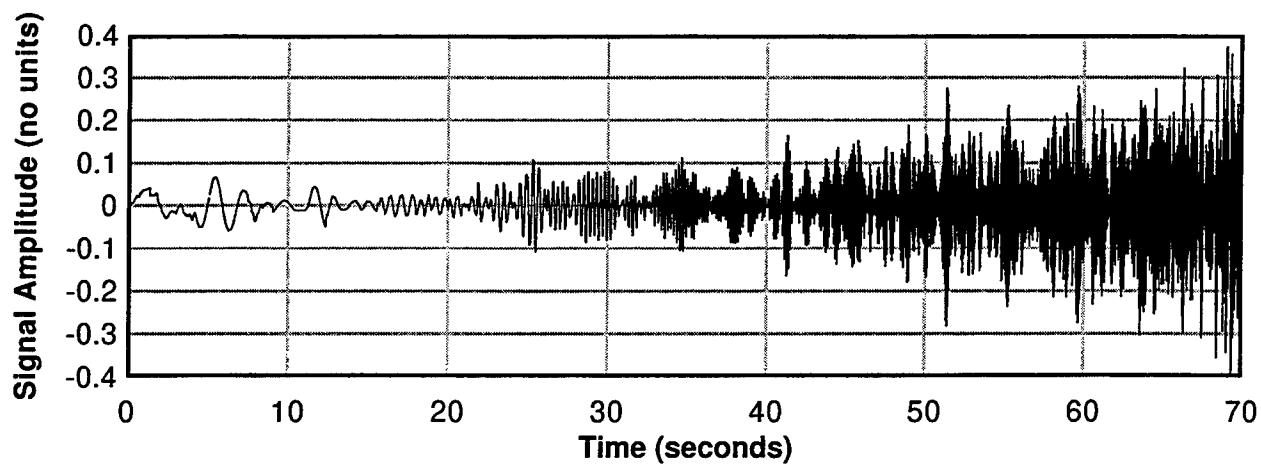
Figure 14a. Generated narrow-band random signal, Ran1.
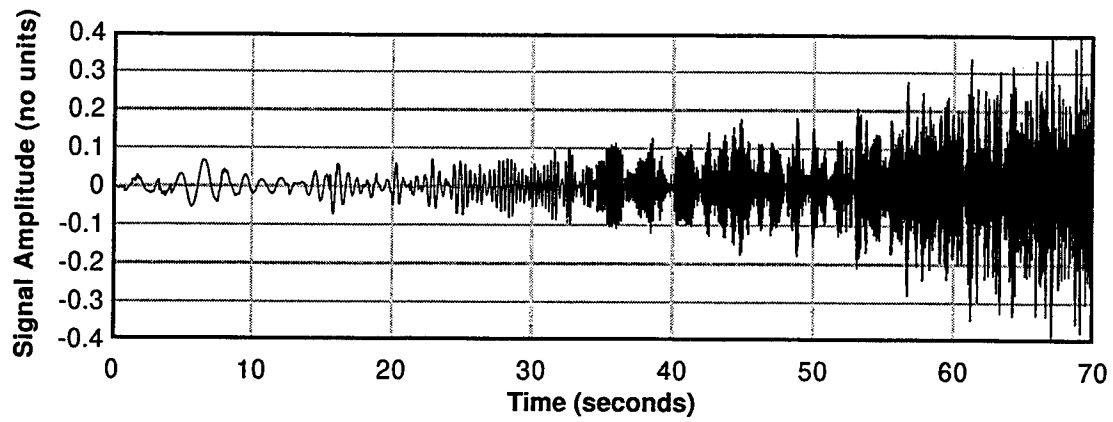
Figure 14b. Generated narrow-band random signal, Ran2.
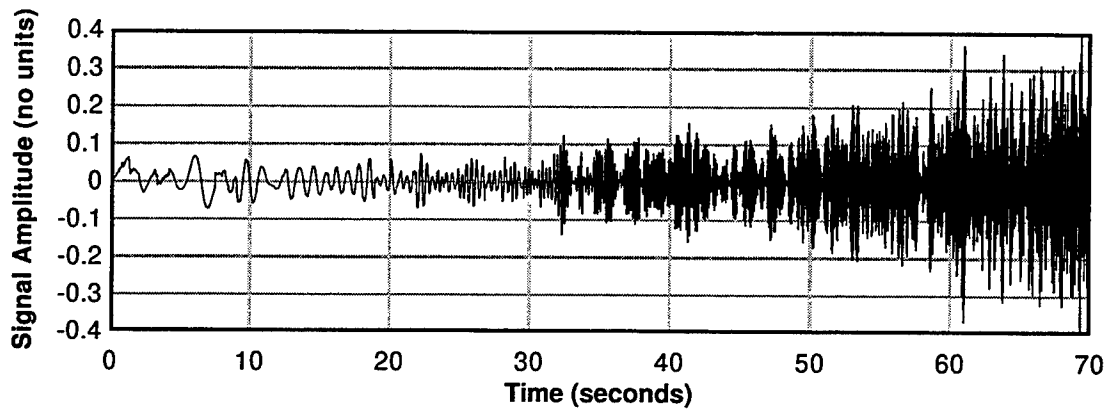
Figure 14c. Generated narrow-band random signal, Ran3.
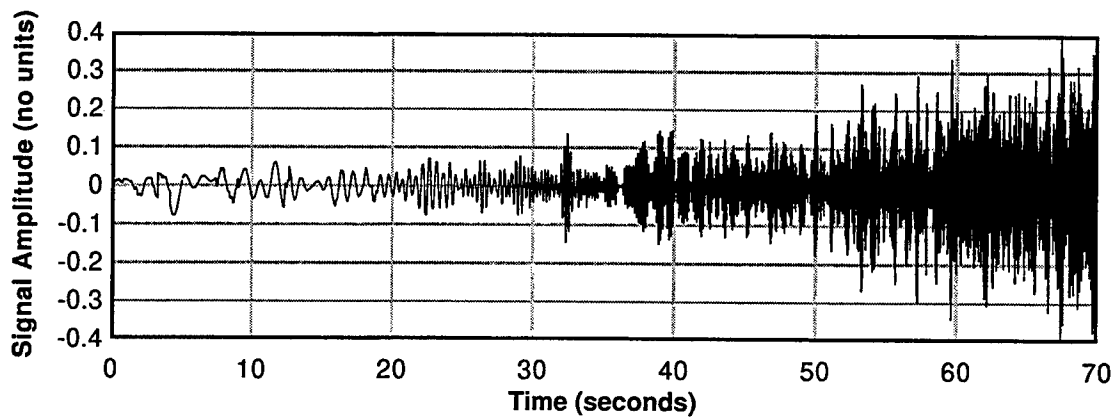
Figure 14d. Generated narrow-band random signal, Ran4.
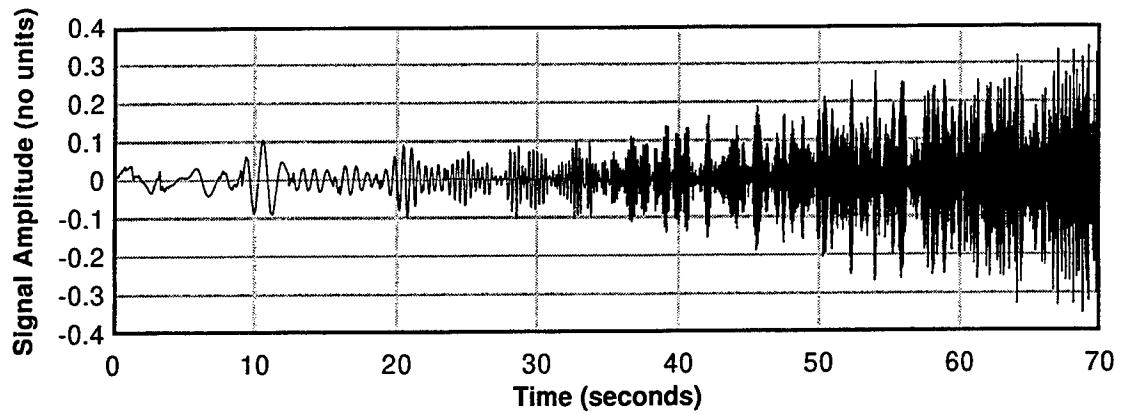
Figure 14e. Generated narrow-band random signal, Ran5.
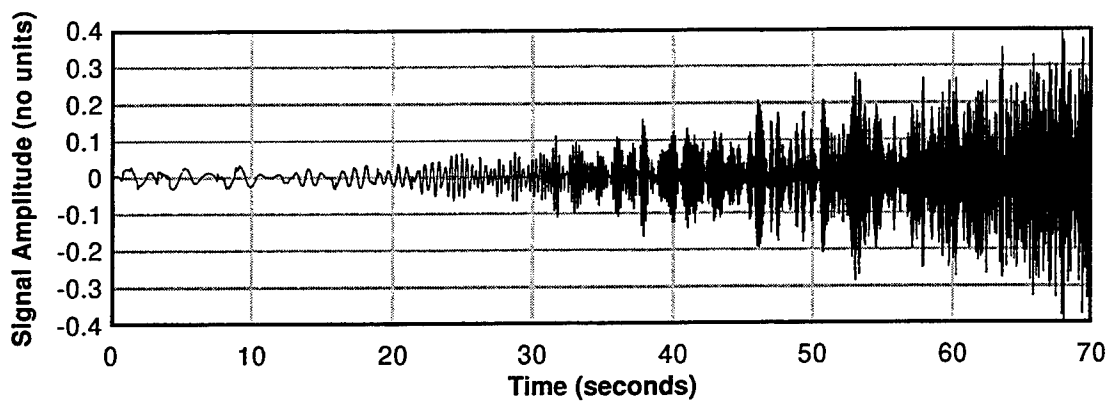
Figure 14f. Generated narrow-band random signal, Ran6.
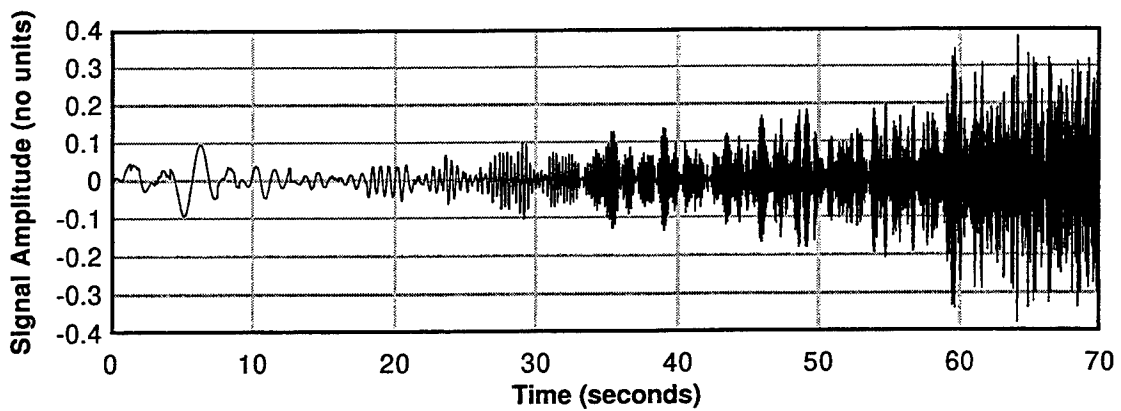
Figure 14g. Generated narrow-band random signal, Ran7.
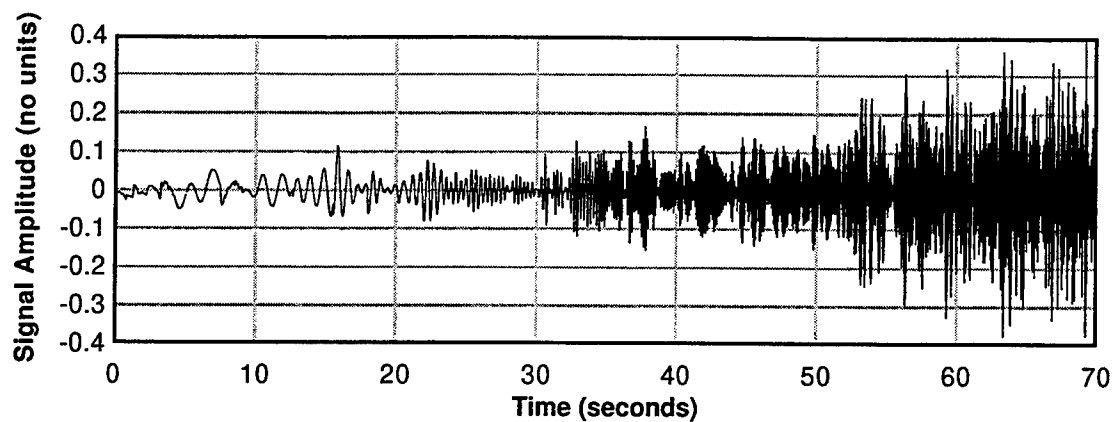
Figure 14h. Generated narrow-band random signal, Ran8.
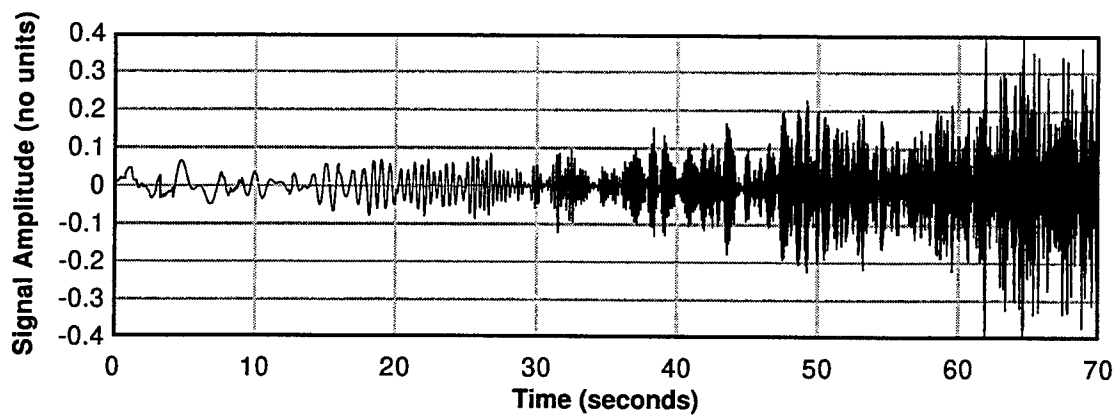
Figure 14i. Generated narrow-band random signal, Ran9.
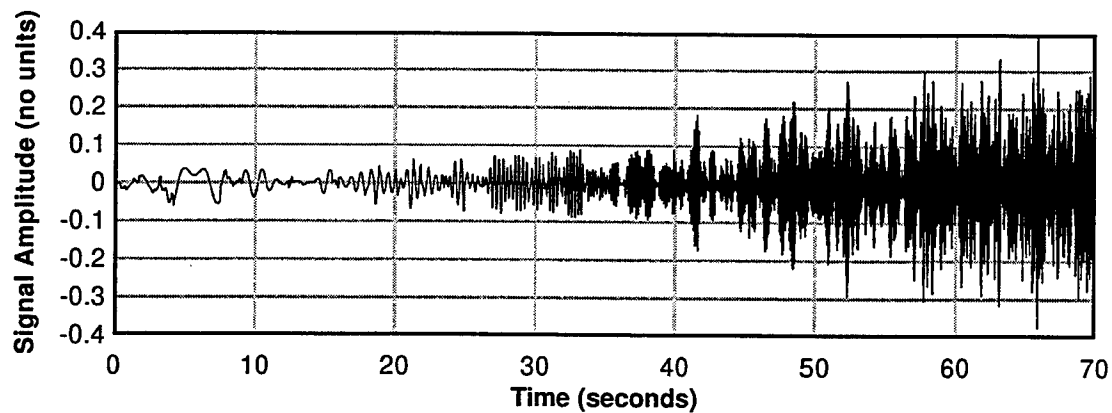
Figure 14j. Generated narrow-band random signal, Ran10.
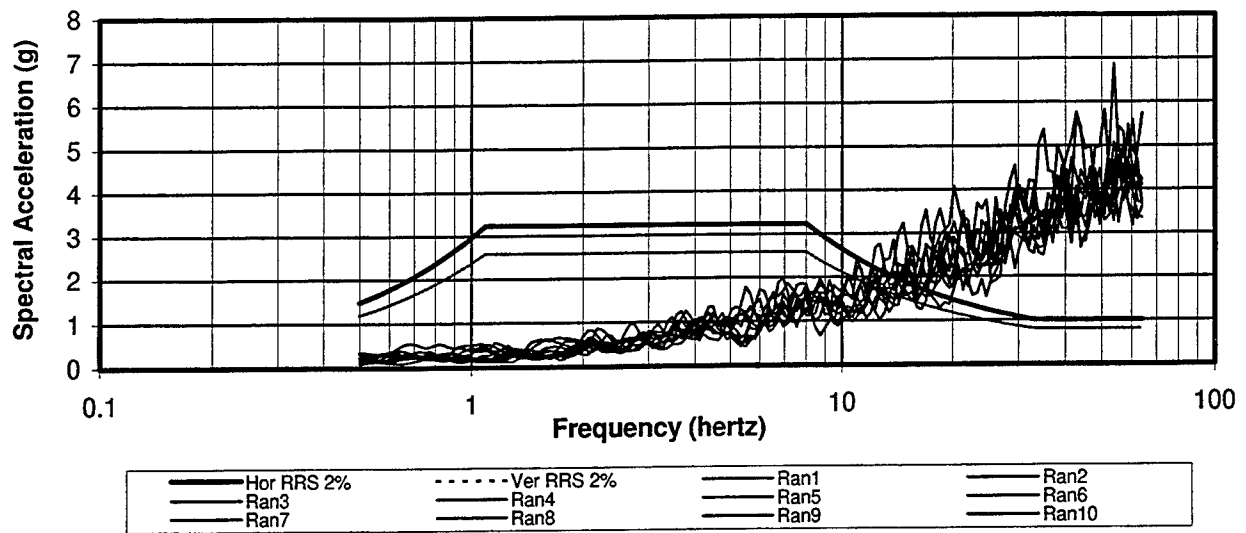
Figure 15. IEEE 693 high seismic performance response spectra and unscaled response spectra.

Scaling Relationships for Narrow-Band Random Tests

Frequency Range, $f_{n-1} - f_n$ (Hz)	Time Range $t_{n-1} - t_n$ (seconds)	Scale Number & Amplitude,		Horizontal Scaling, S_H (g)	Vertical Scaling, S_v (g)
		n	A_n (g)		
		0	12		
0.5 – 1.122	0 – 11.67	1	8	$\dfrac{A_1 - A_0}{t_1 - t_0}(t - t_0) + A_0$	0.8 S_H
1.122 – 8	11.67 – 40	2	2	$\dfrac{A_2 - A_1}{t_2 - t_1}(t - t_1) + A_1$	0.8 S_H
8 – 33.903	40 – 60.833	3	0.25	$\dfrac{A_3 - A_2}{t_3 - t_2}(t - t_2) + A_2$	0.8 S_H
33.903 – 64	60.833 – 70	4	0.2	$\dfrac{A_4 - A_3}{t_4 - t_3}(t - t_3) + A_3$	0.8 S_H

Note: This information is reproduced from Table 5, Chapter 4.
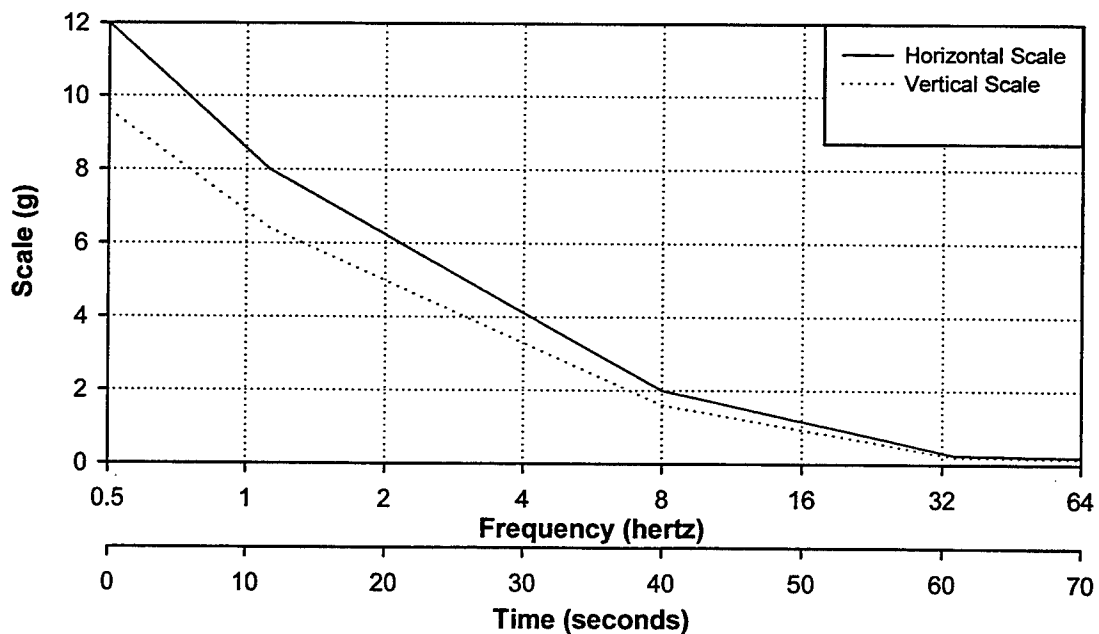
Figure 16. Scaling used for both horizontal (lateral and longitudinal) and vertical records.
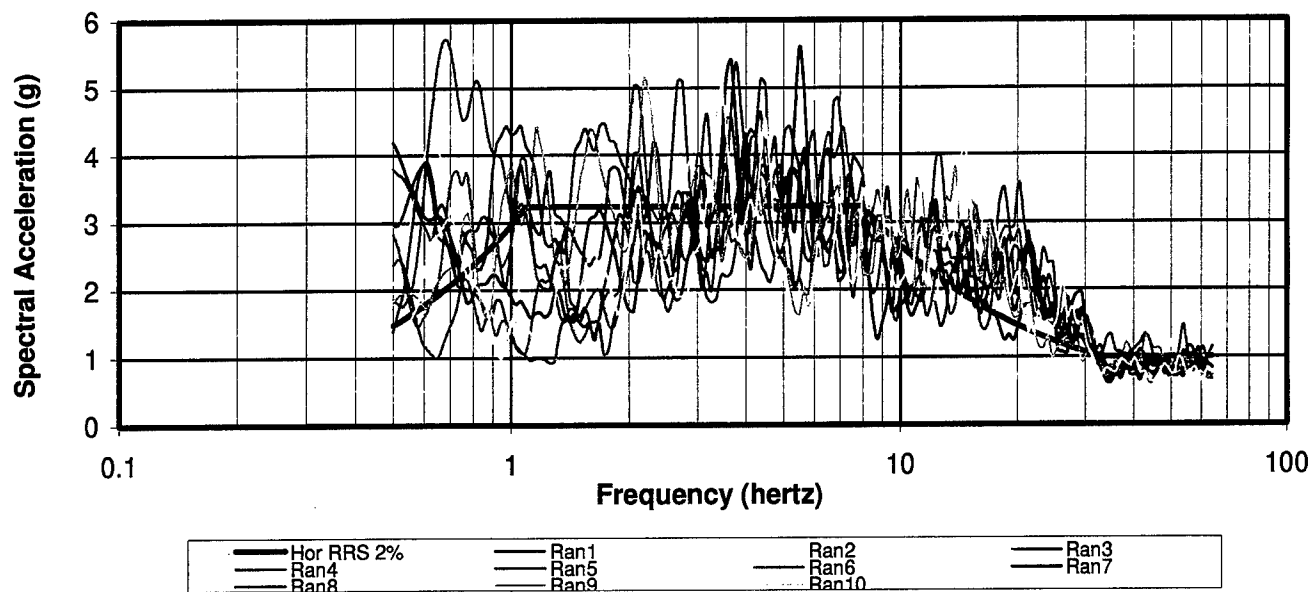
Figure 17a. IEEE 693 high seismic performance response spectra and scaled response spectra.
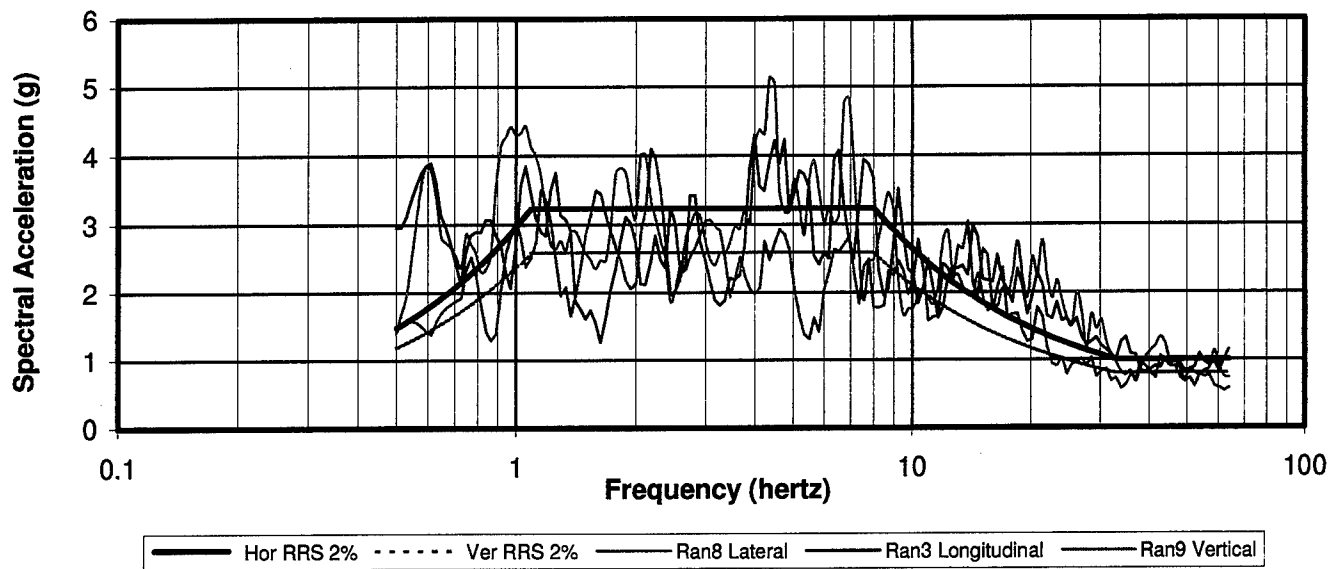
Figure 17b. IEEE 693 spectra and selected scaled response spectra.
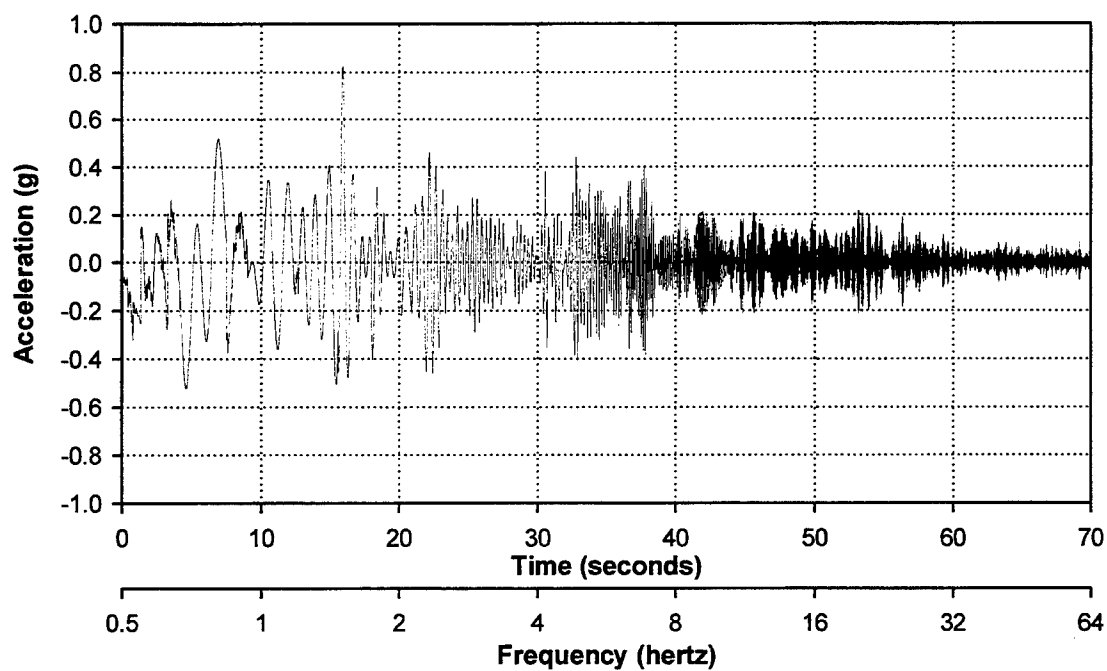
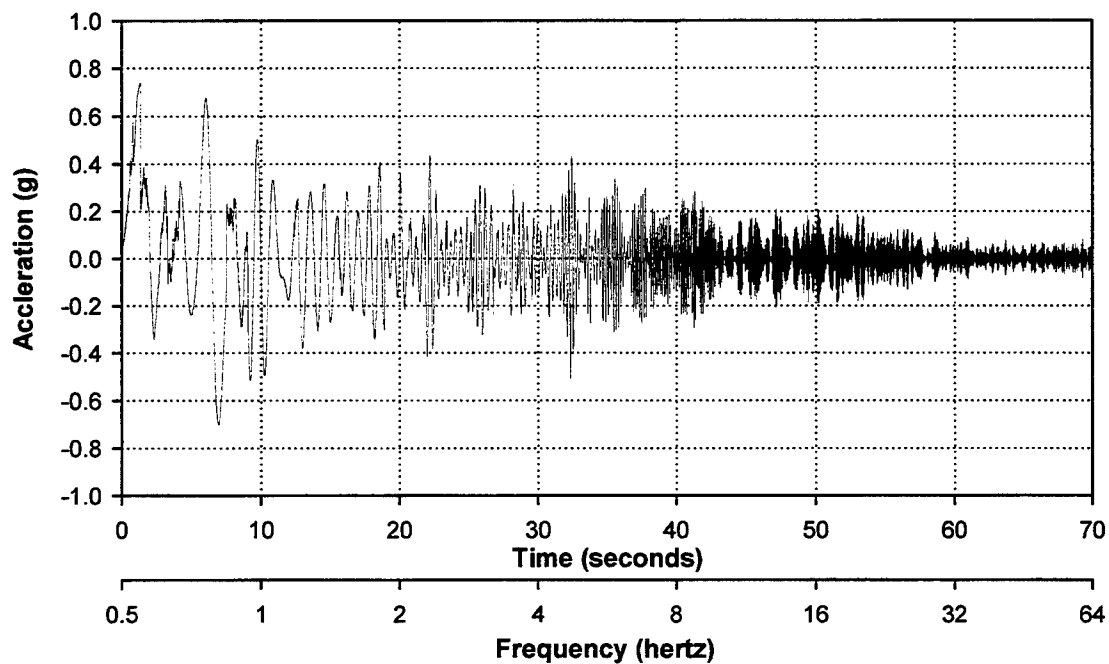Figure 18a. Lateral narrow-band random scaled signal, Ran8.

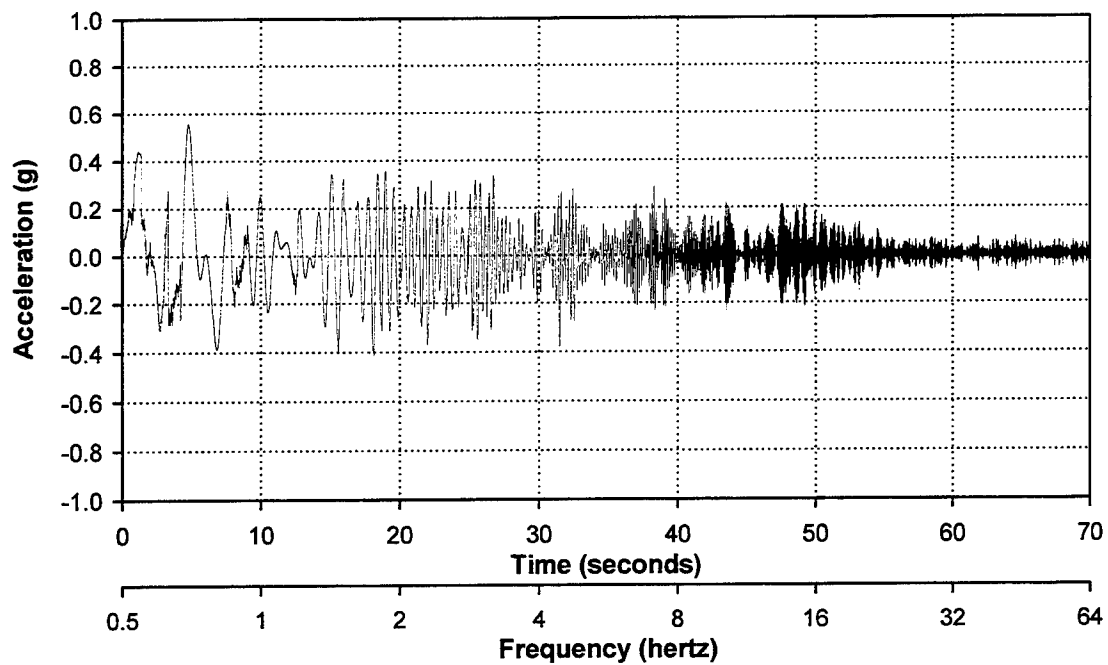Figure 18b. Longitudinal narrow-band random scaled signal, Ran3.

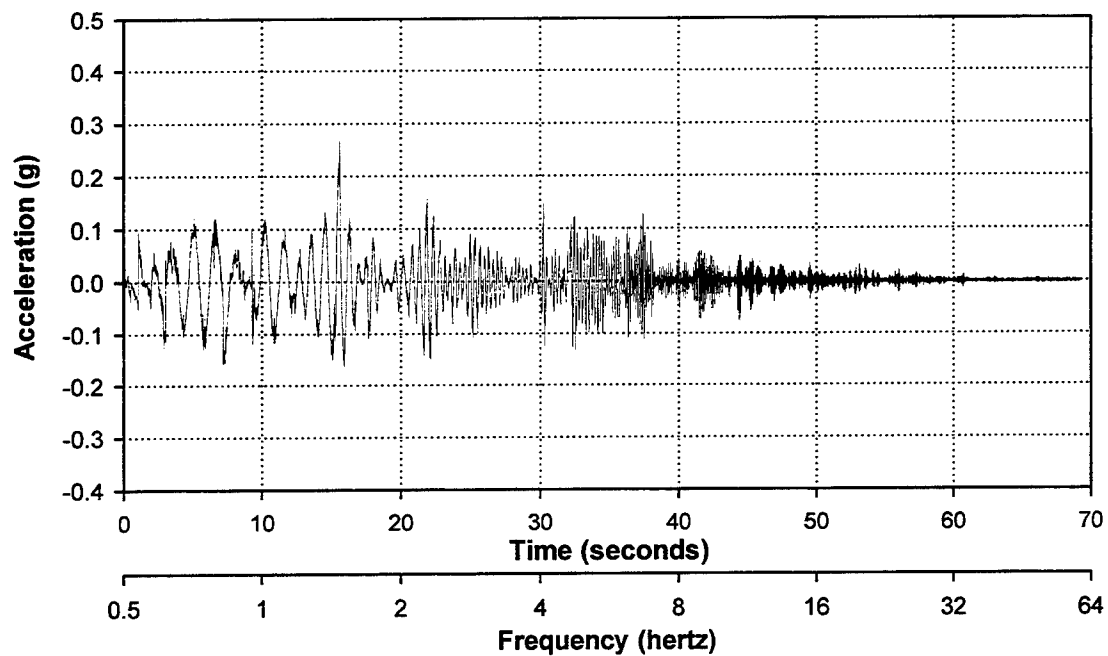Figure 18c. Vertical narrow-band random scaled signal, Ran9.

Figure 19a.   Achieved lateral acceleration with input motions at 29% of Figure 18a.
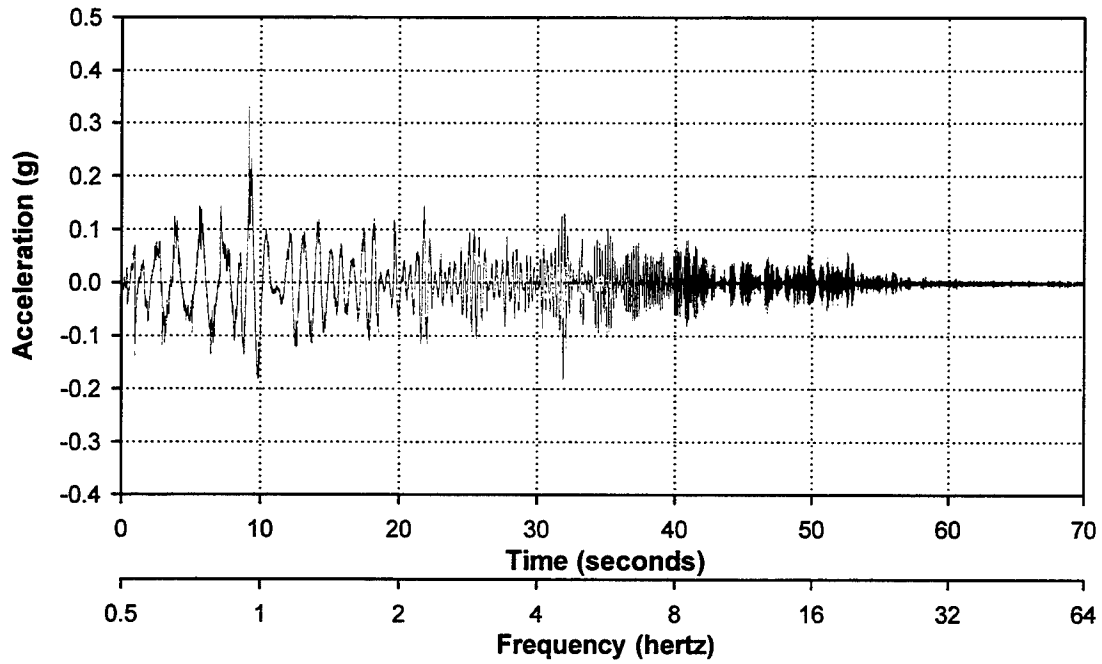
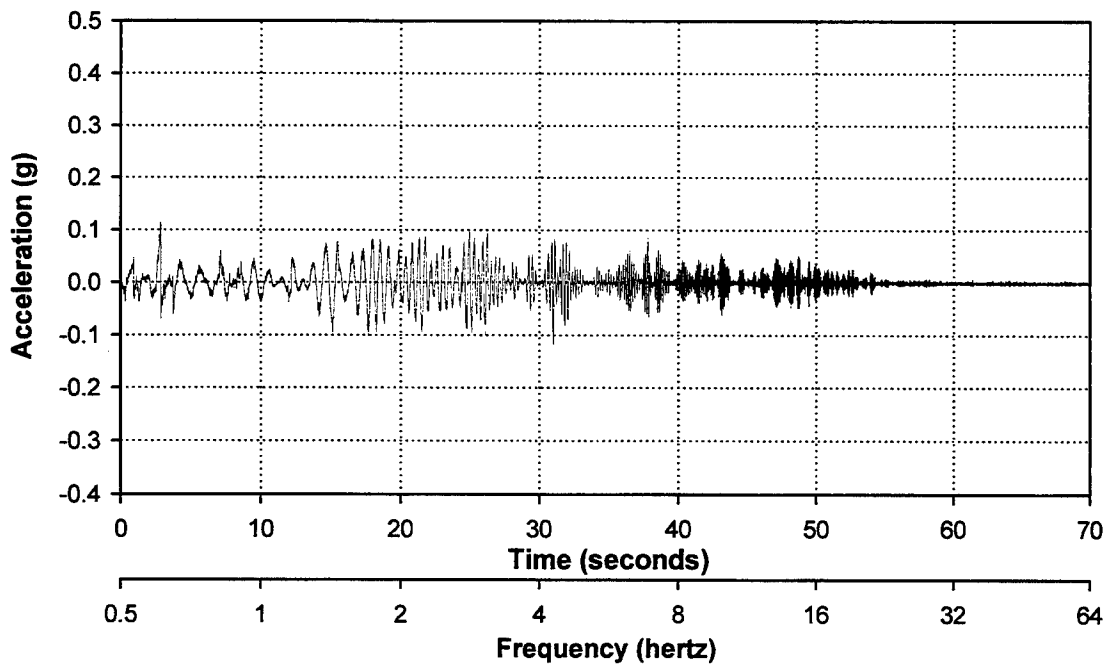Figure 19b. Achieved longitudinal acceleration with input motions at 29% of Figure18b.

Figure 19c. Achieved vertical acceleration with input motions at 29% of Figure18c.
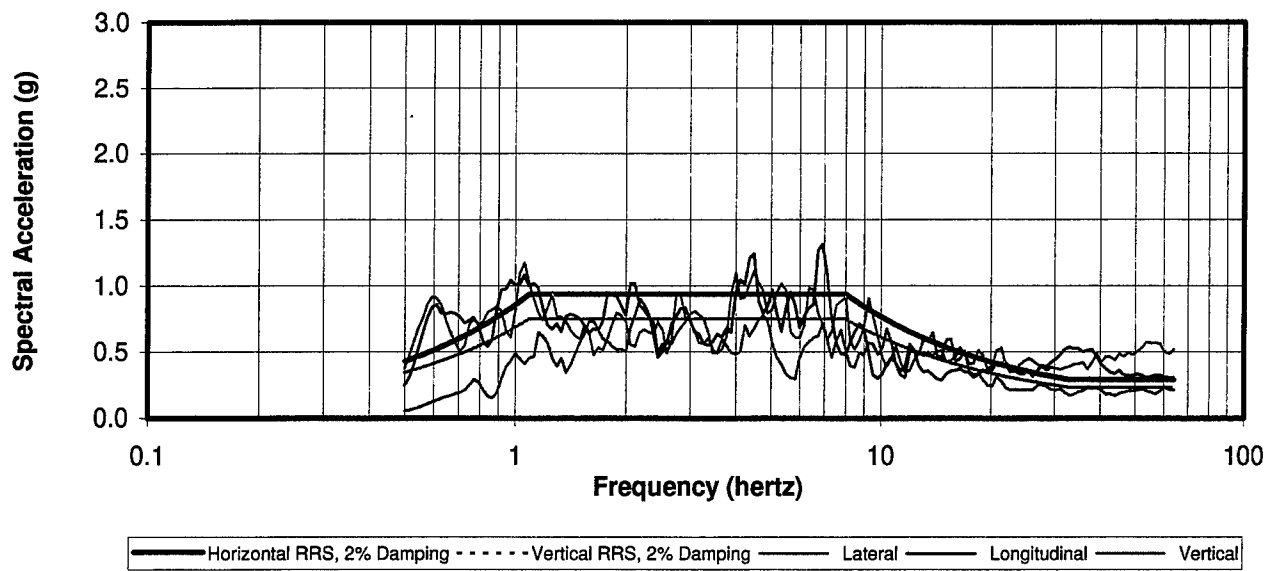
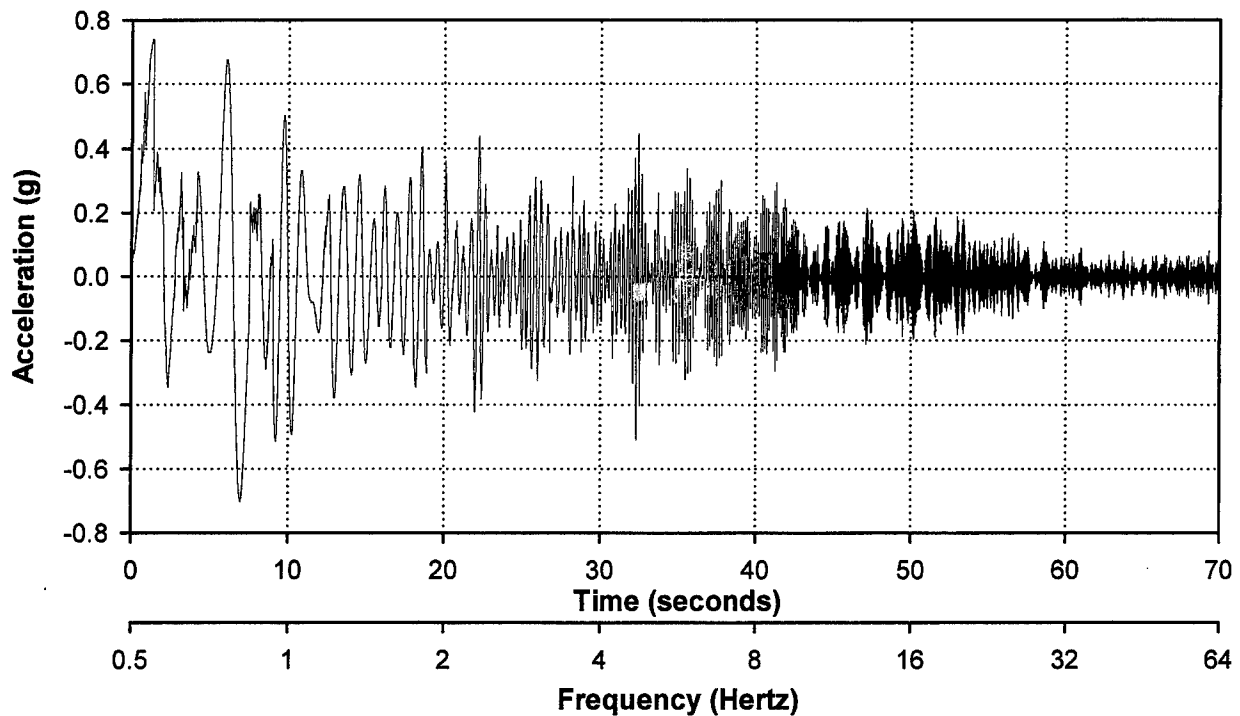**Figure 20. Test response spectra from 29% Figure 18 motions and 29% IEEE 693 spectra.**

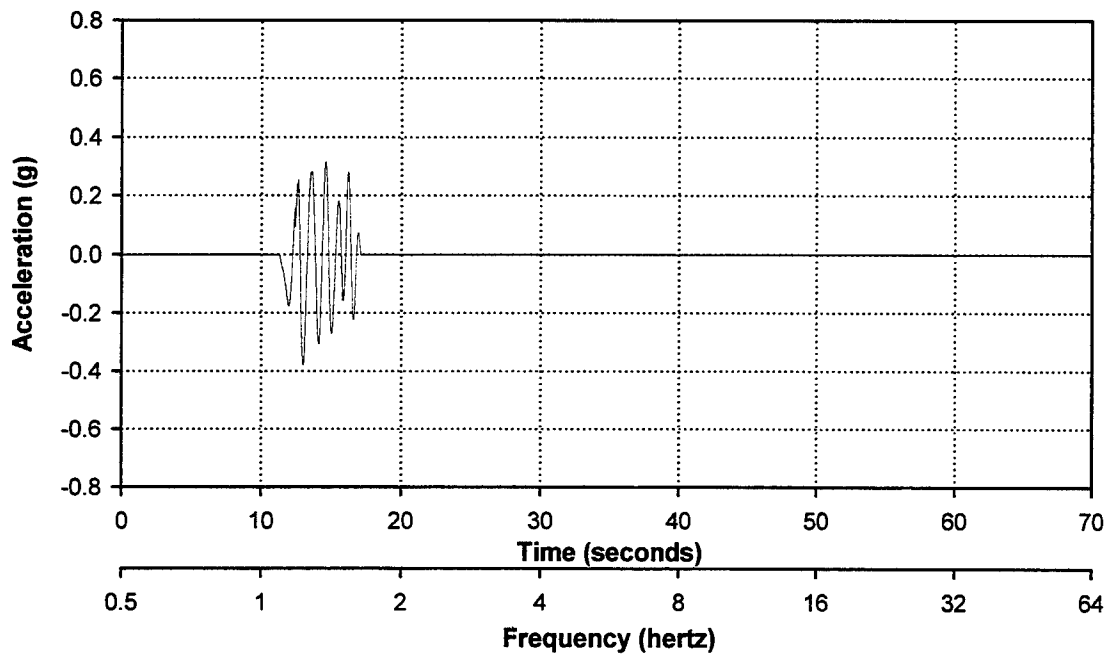**Figure 21a. Original longitudinal narrow-band random scaled signal, Ran3 (from Figure 18b).**

Figure 21b. First region (Ran31) of narrow-band random scaled signal.

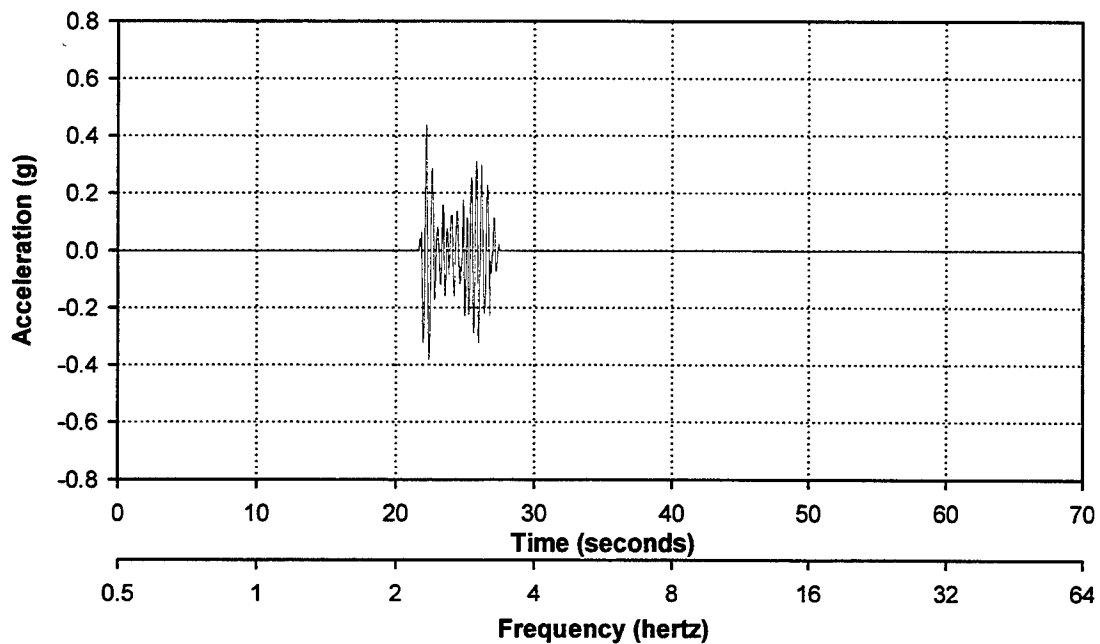**Figure 21c. Second region (Ran32) of narrow-band random scaled signal.**
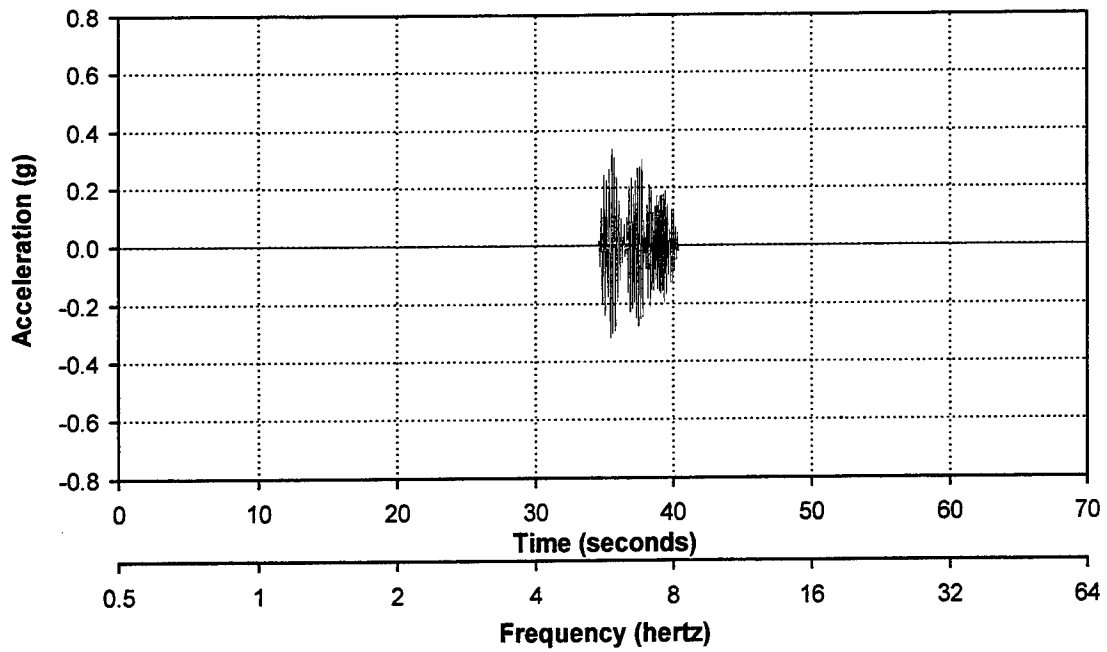
Figure 21d. Third region (Ran33) of narrow-band random scaled signal.

Figure 22a. Approximate attenuation with respect to frequency for the regions of Figure 21.

Figure 22b. Response spectra for Figure 21a and three regions of Figure 21b through 21d.
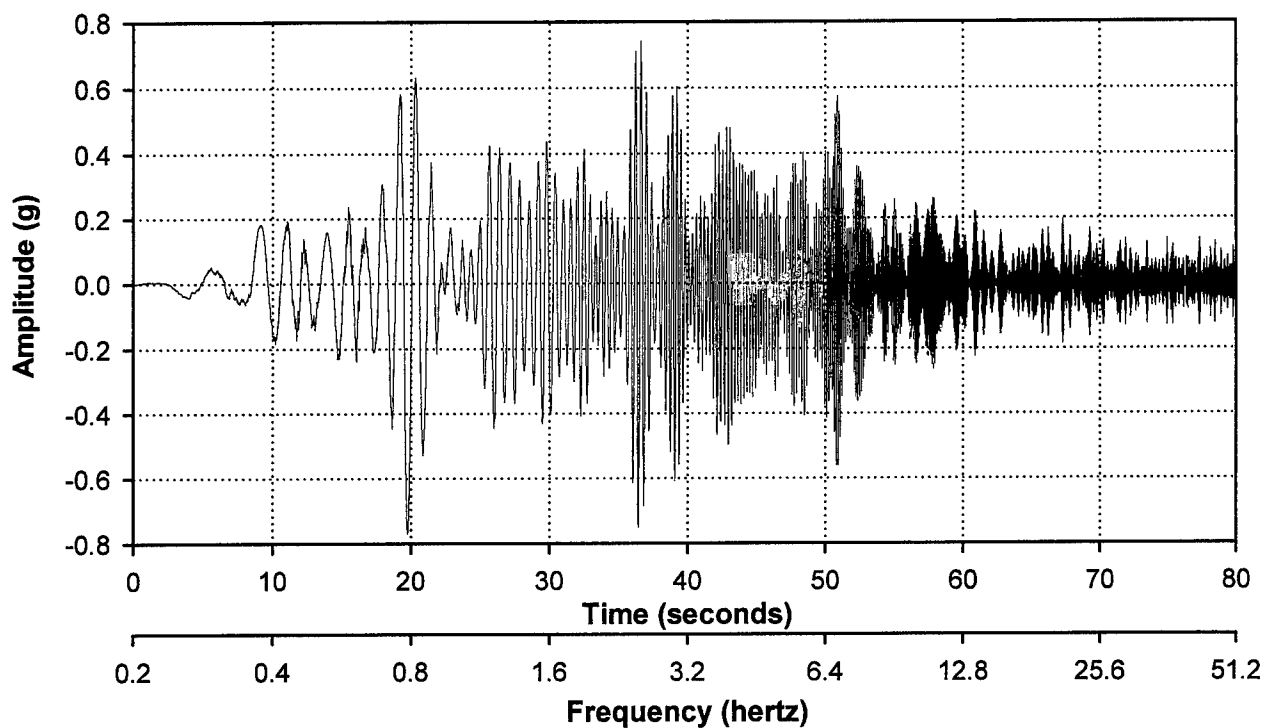
Figure 23a. Narrow-band random record generated by the new Matlab routine scaled to Bellcore (Bel2).
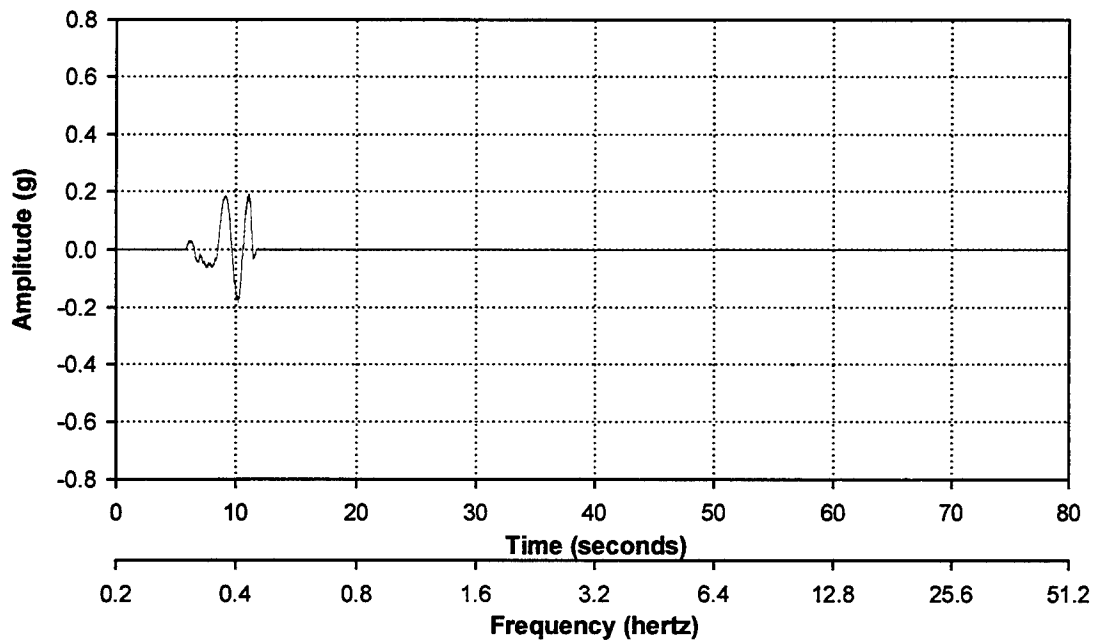
Figure 23b. First region of Bellcore narrow-band random scaled signal (Bel21).
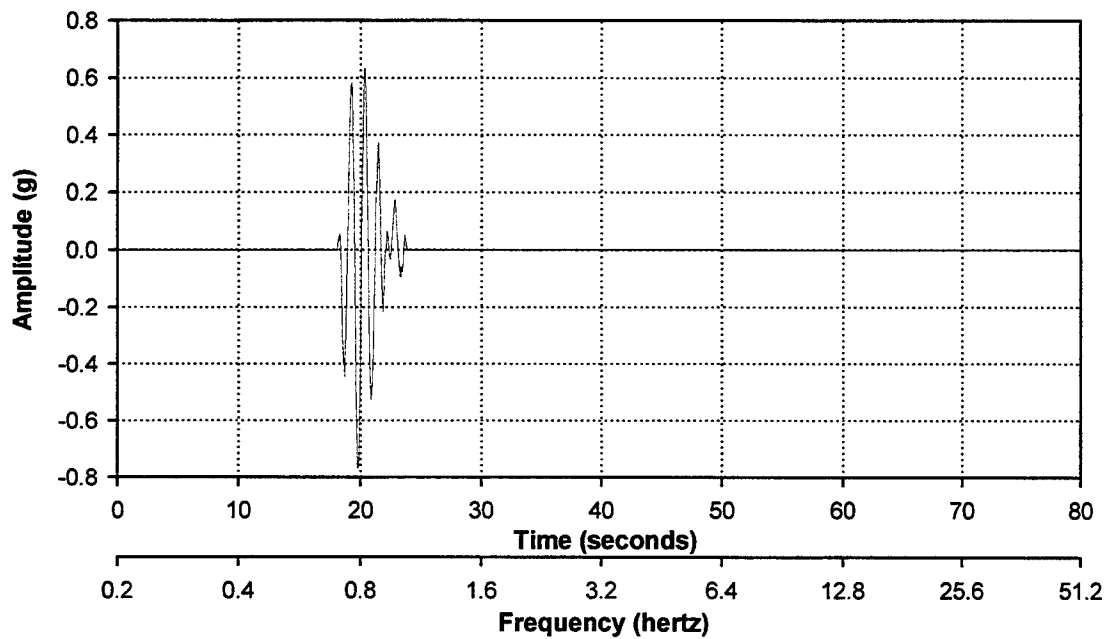
Figure 23c. Second region of Bellcore narrow-band random scaled signal (Bel22).
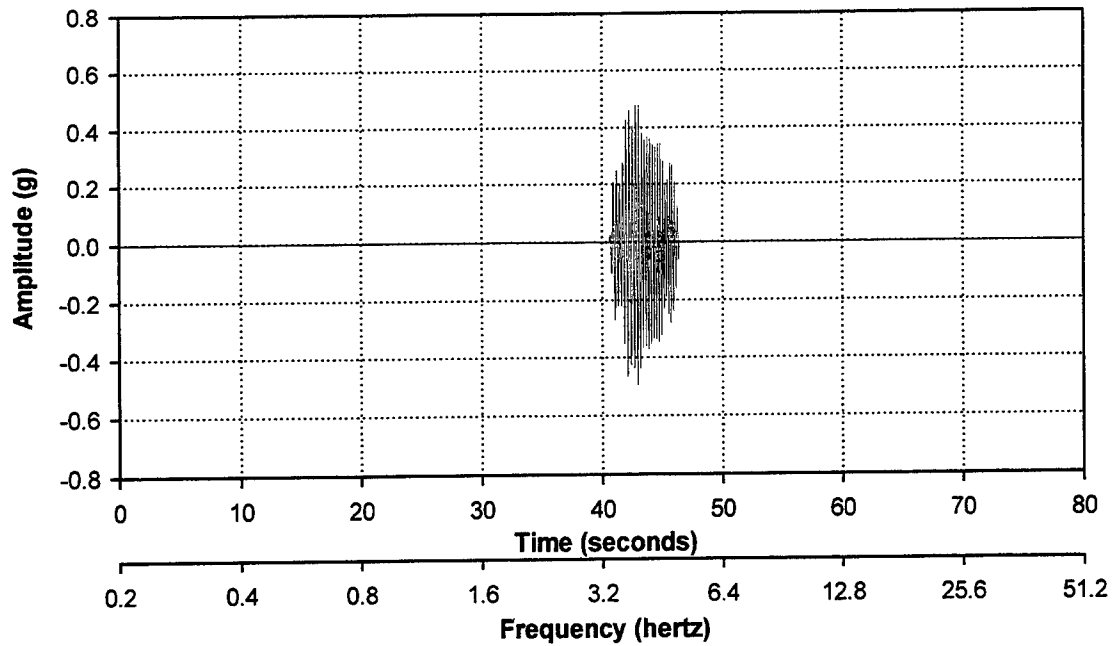
Figure 23d. Third region of Bellcore narrow-band random scaled signal (Bel23).
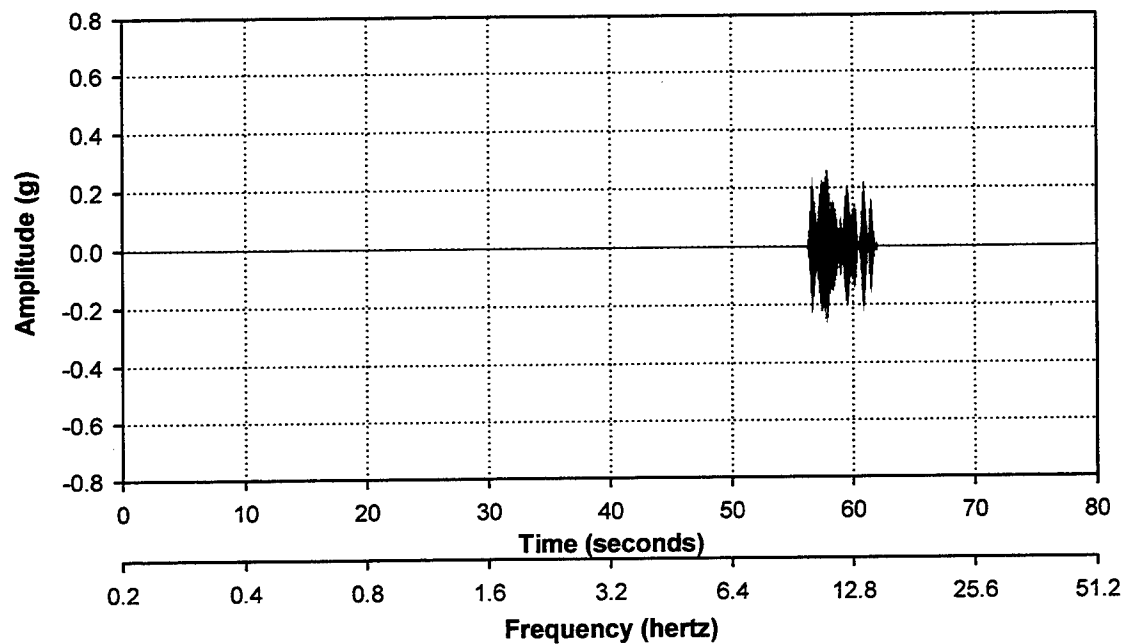
Figure 23e. Fourth region of Bellcore narrow-band random scaled signal (Bel24).
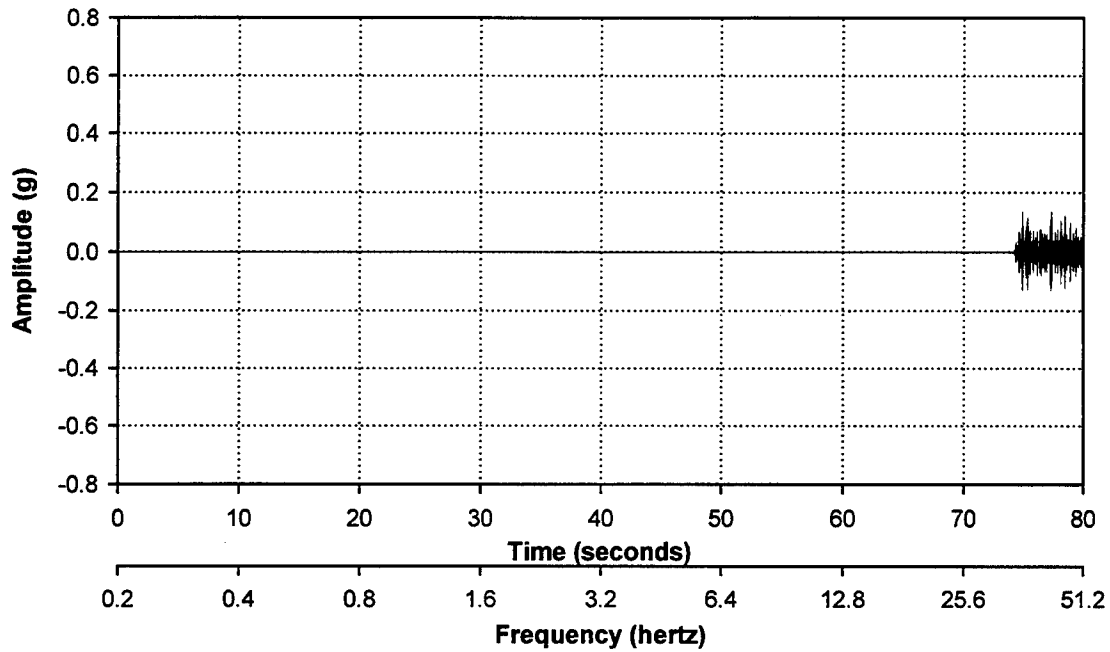
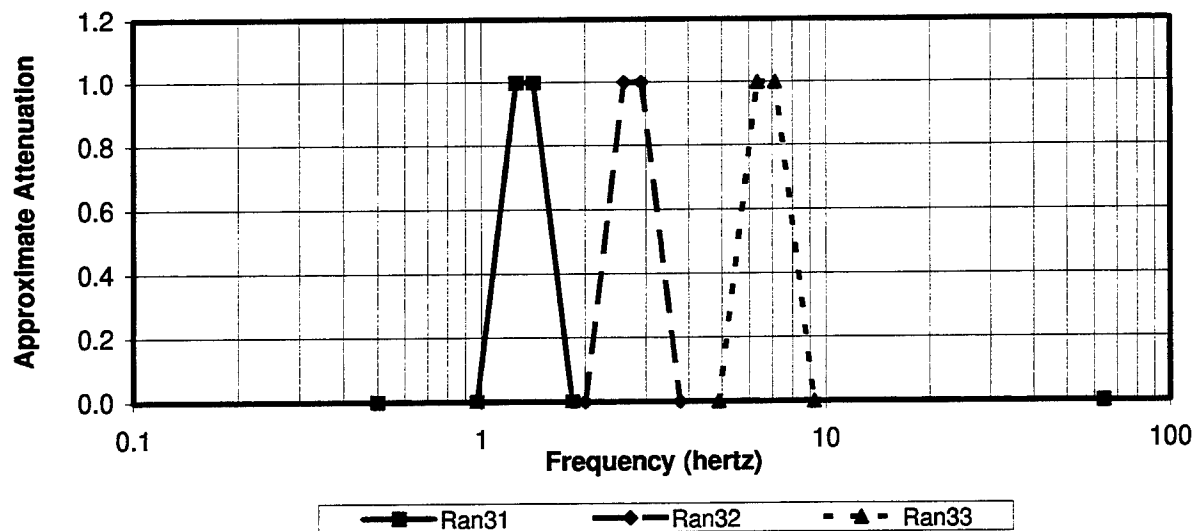Figure 23f. Fifth region of Bellcore narrow-band random scaled signal (Bel25).
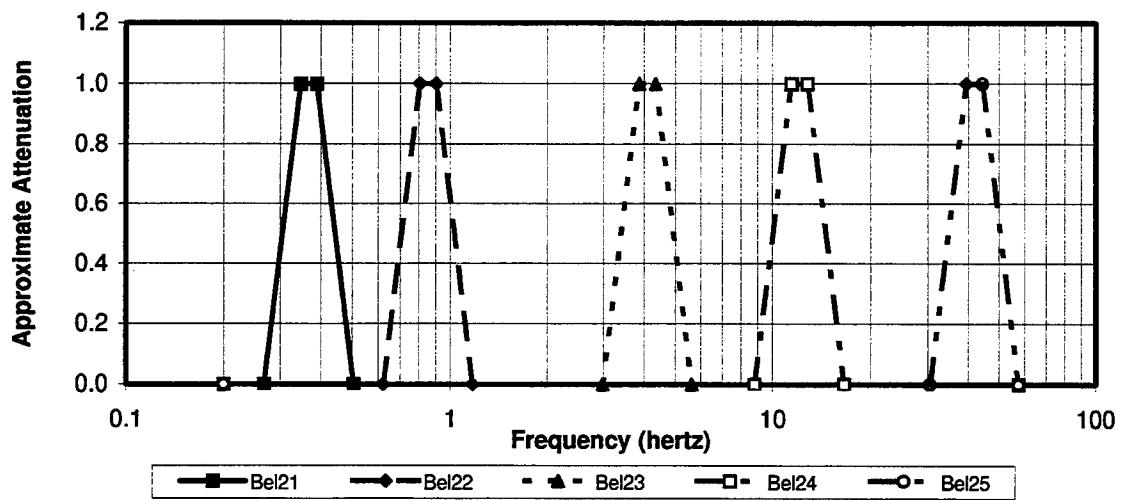
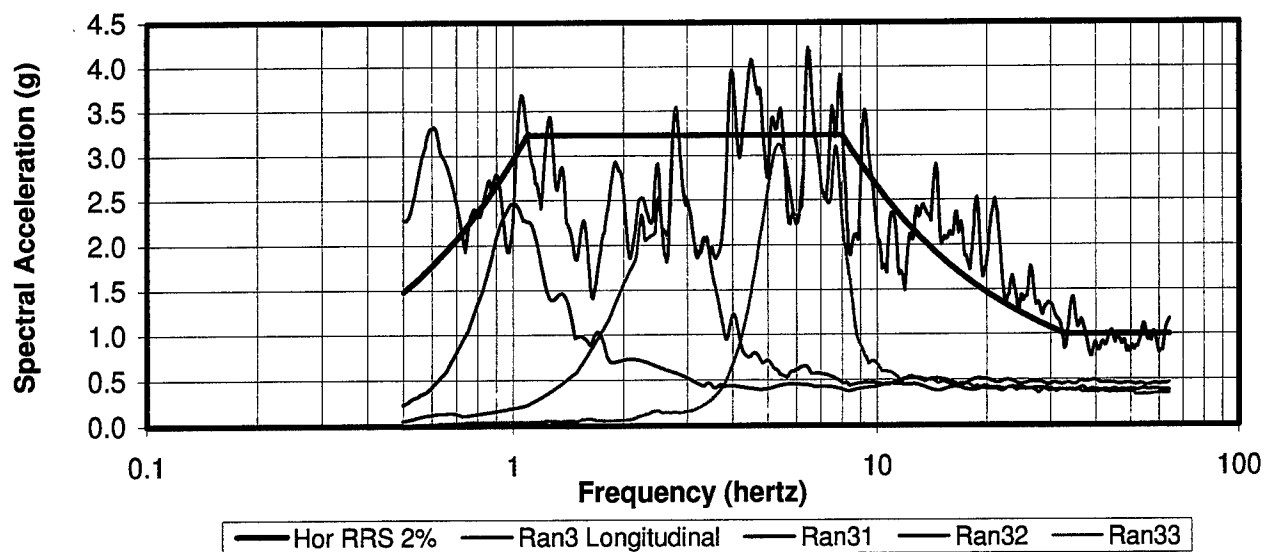Figure 24a. Approximate attenuation with respect to frequency for the regions of Figure 23.
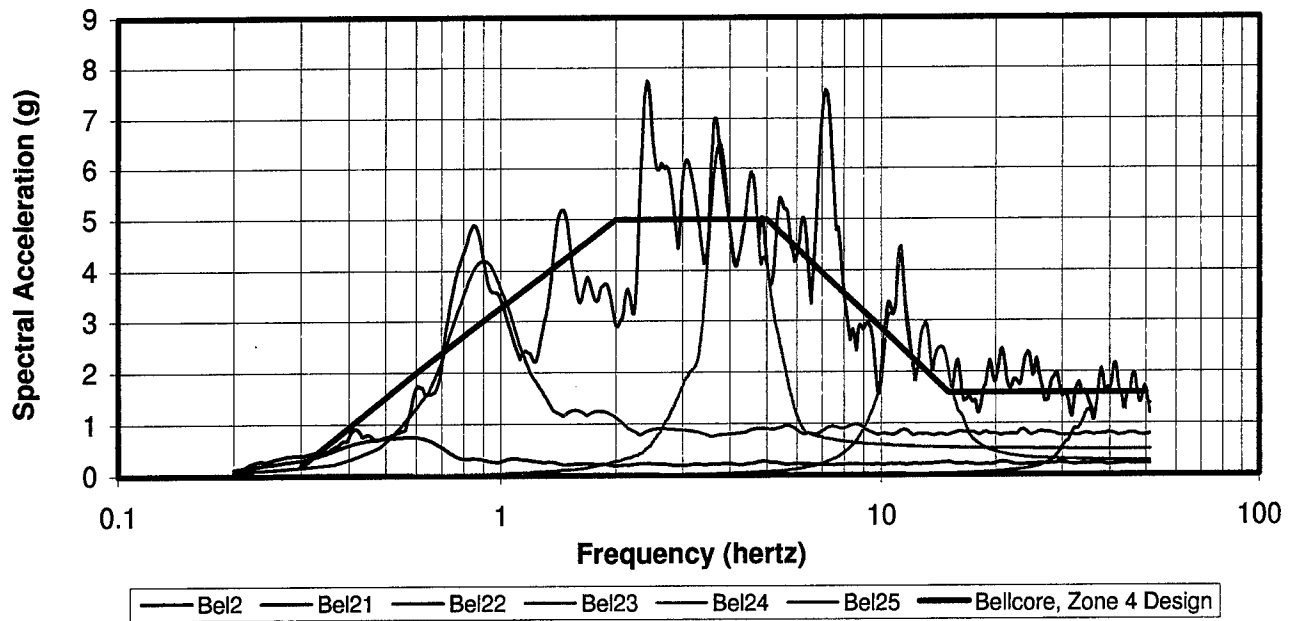
Figure 24b. Response spectra for Figure 23a and five regions of Figures 23b through 23f.
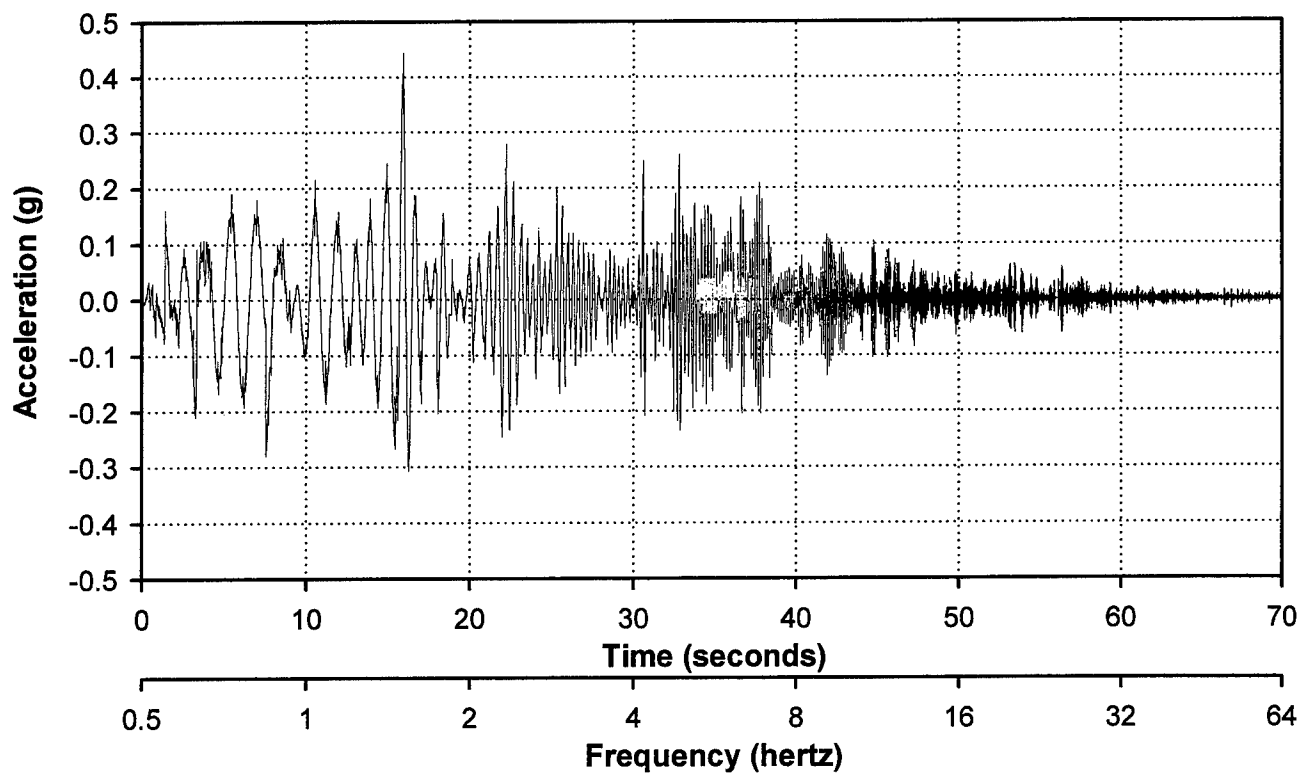
Figure 25a. Achieved lateral acceleration, 50% of Figure 18a (Frag10).
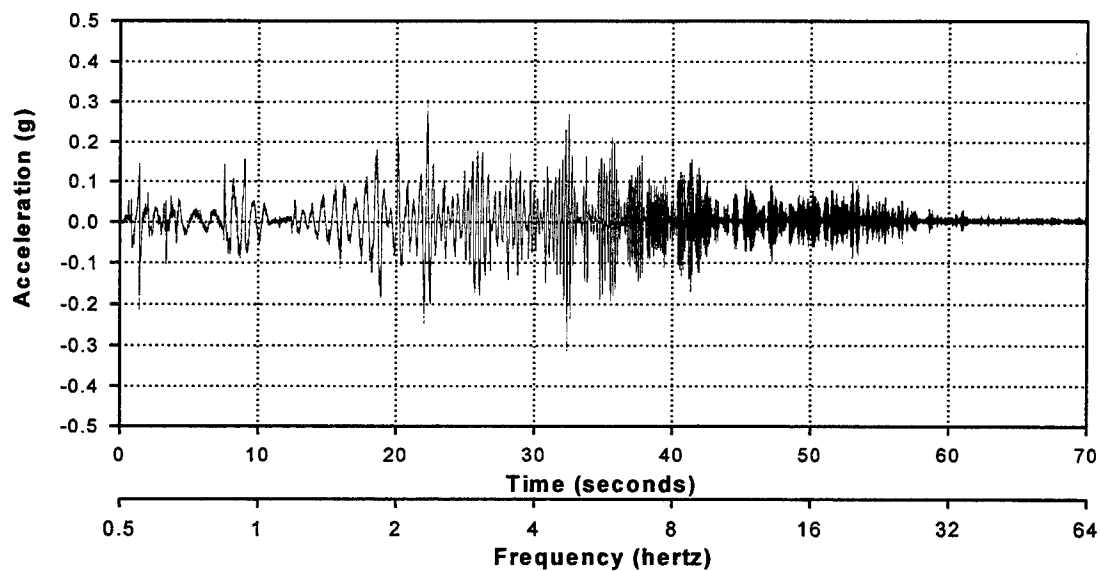
Figure 25b. Achieved longitudinal acceleration, 50% of Figure 18b with 1.2 hz HP filter.
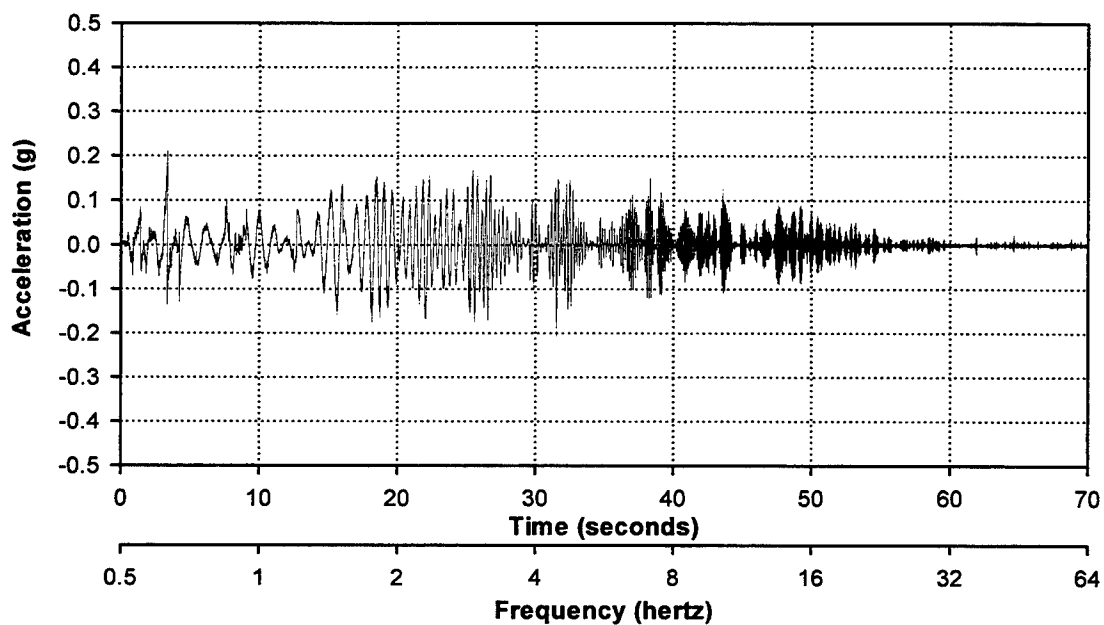
Figure 25c. Achieved vertical acceleration, 50% of Figure 18c.
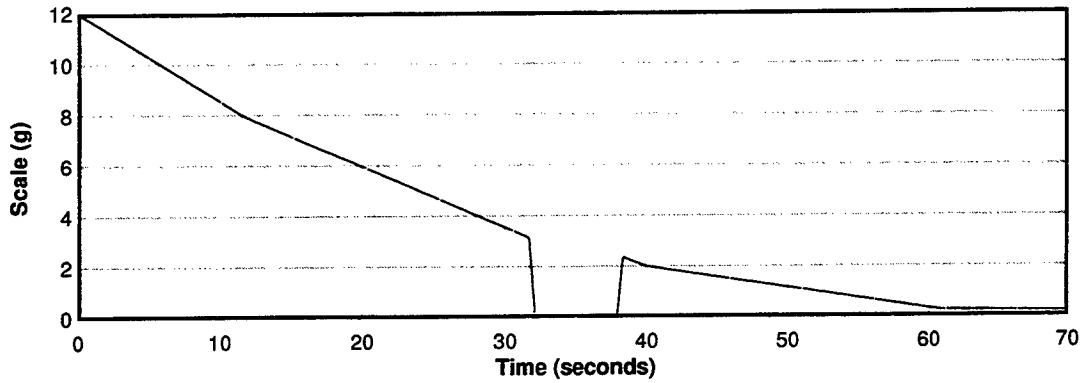
Figure 26a. Scale with Notch 2.
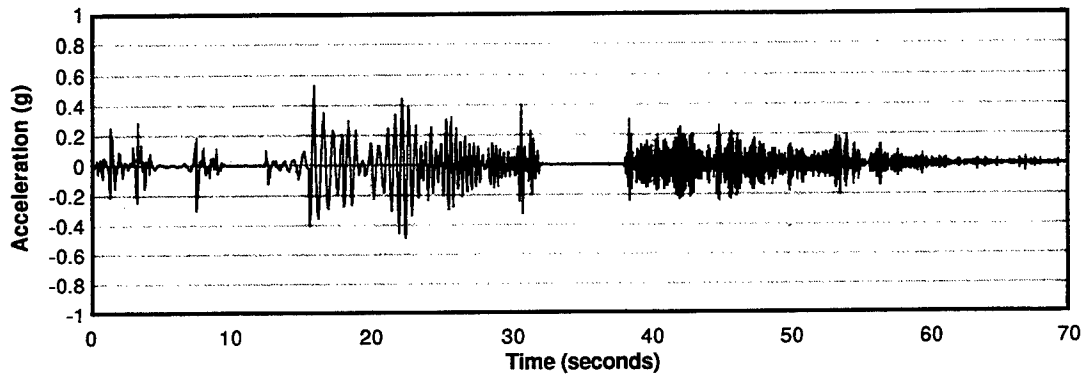
Figure 26b. Lateral achieved acceleration with Notch 2 and 100% of Figure 18a (Frag17).
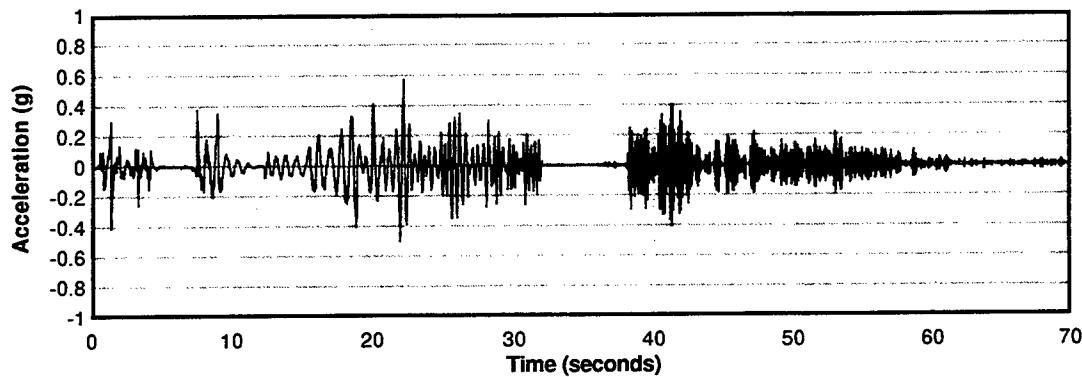
Figure 26c. Longitudinal achieved acceleration with Notch 2 and 100% of Figure 18b (Frag17).
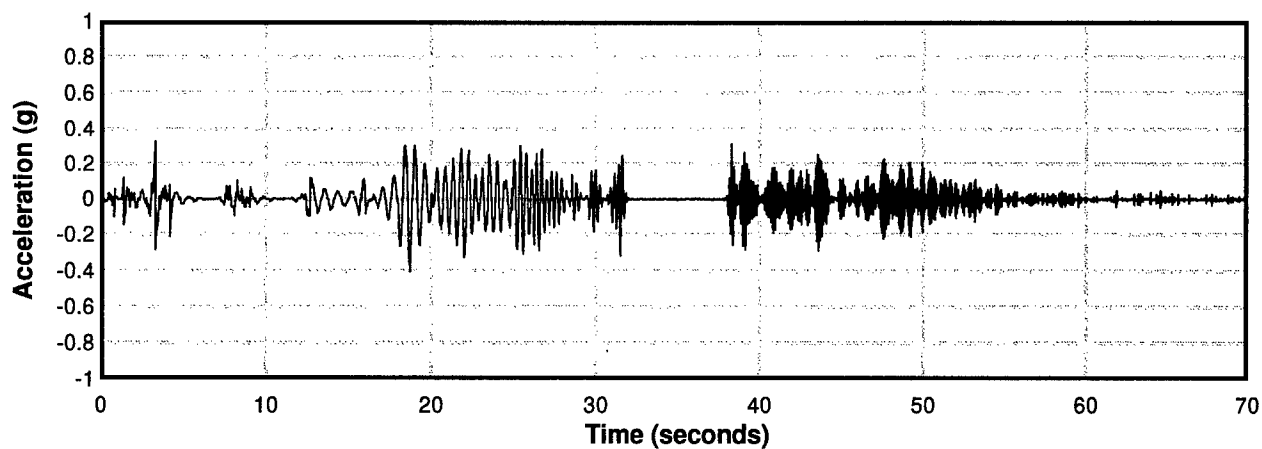
Figure 26d. Vertical achieved acceleration with Notch 2 and 100% of Figure 18c (Frag17).
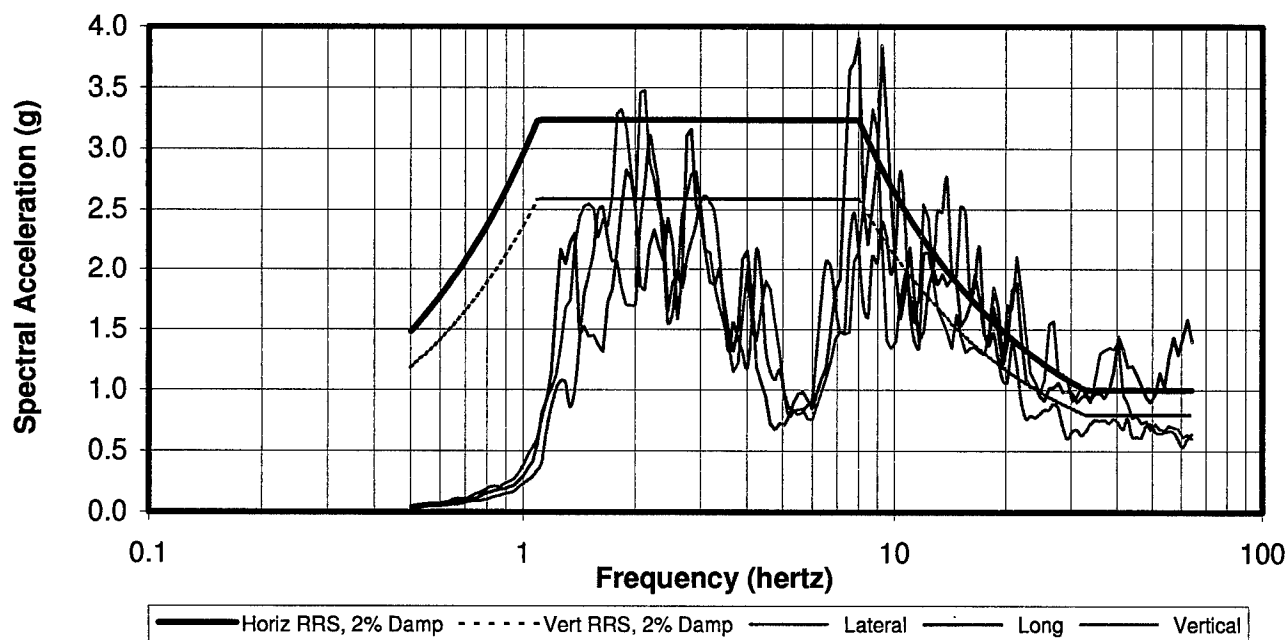
Figure 26e. IEEE 693 spectra and TSR for100% of Figure 18 motions with Notch 2 (Frag17).
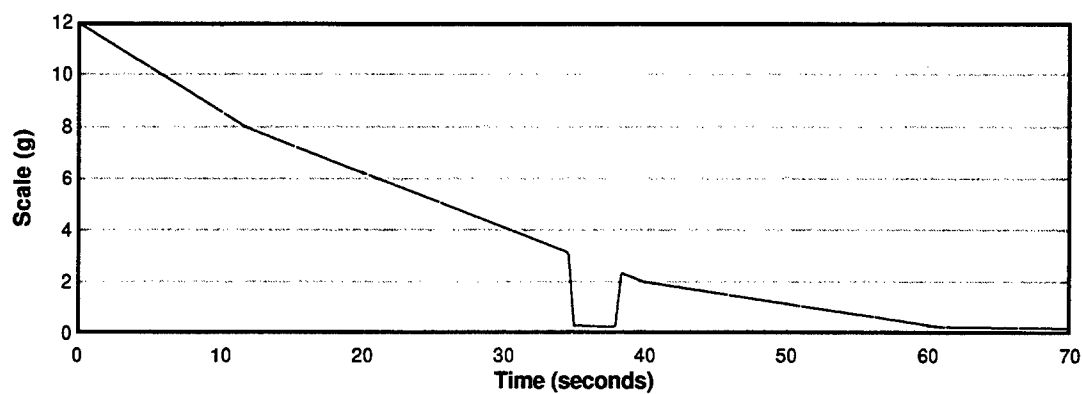
Figure 27a. Scale and Notch 1.
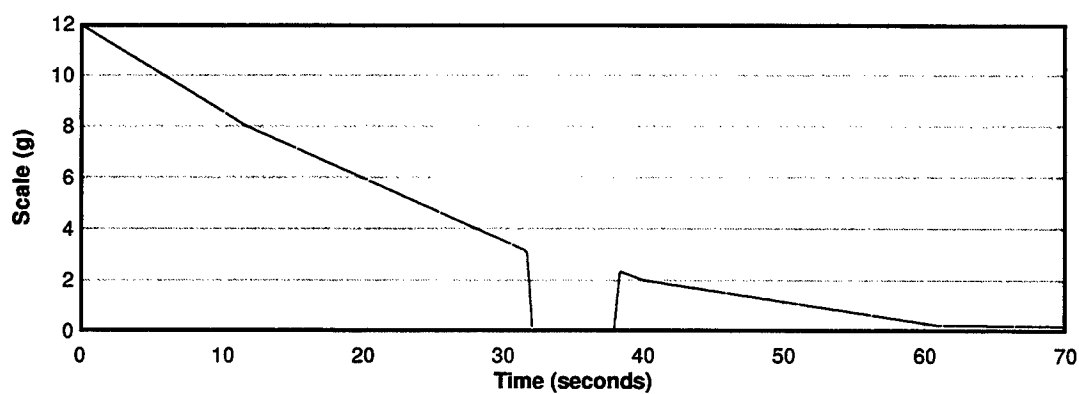
Figure 27b. Scale and Notch 2.
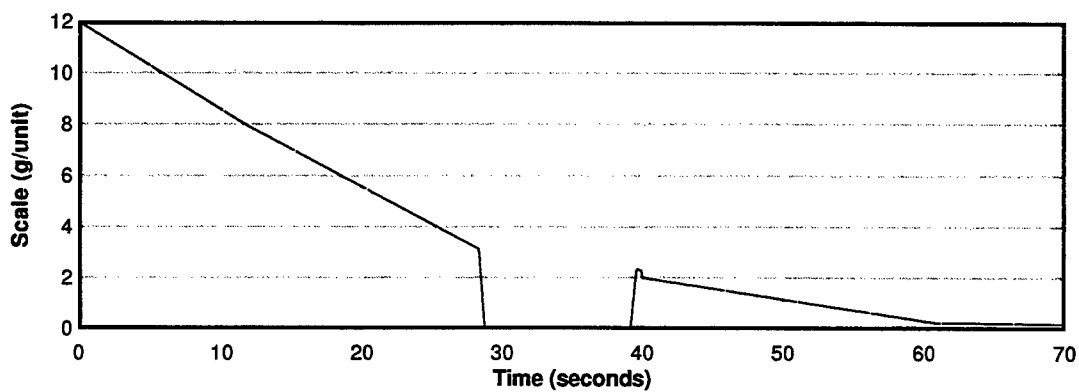
Figure 27c. Scale and Notch 3.
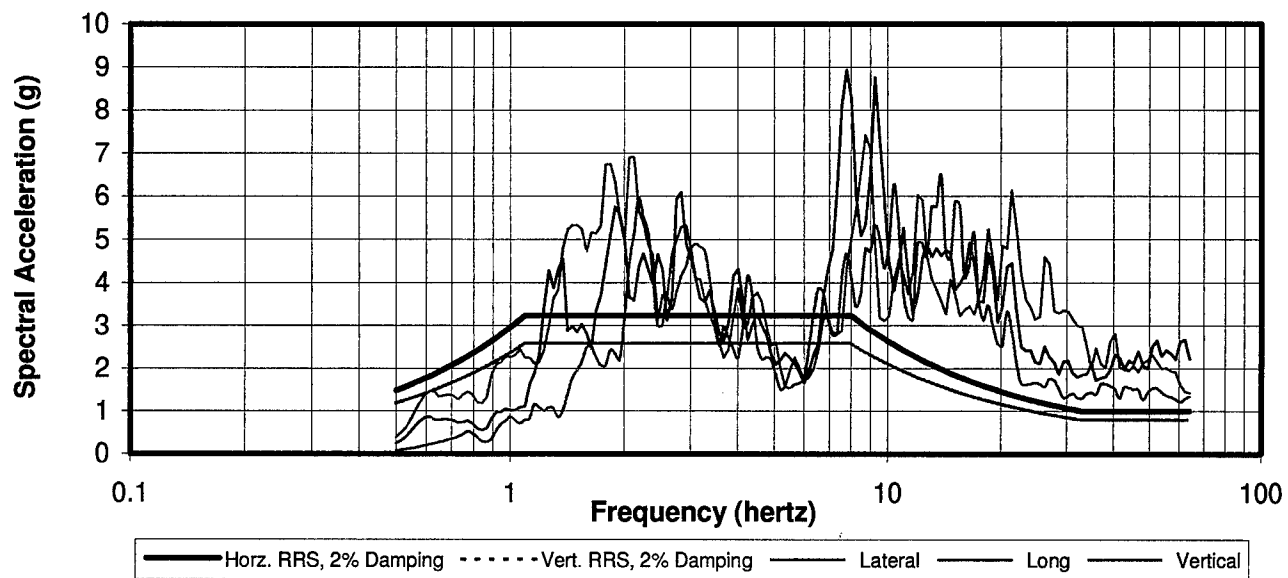
Figure 28a. Maximum TRS through Frag23, 220% of Figure 18.
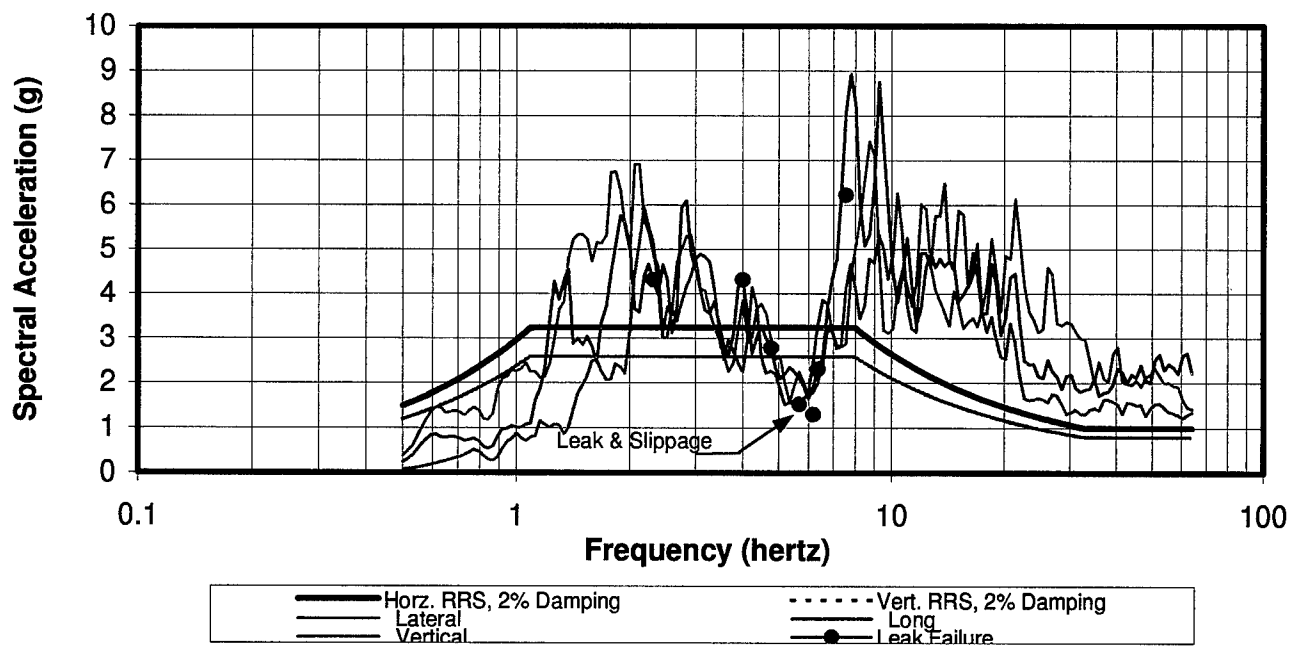
Figure 28b. Maximum TRS through Frag23 and failure data.
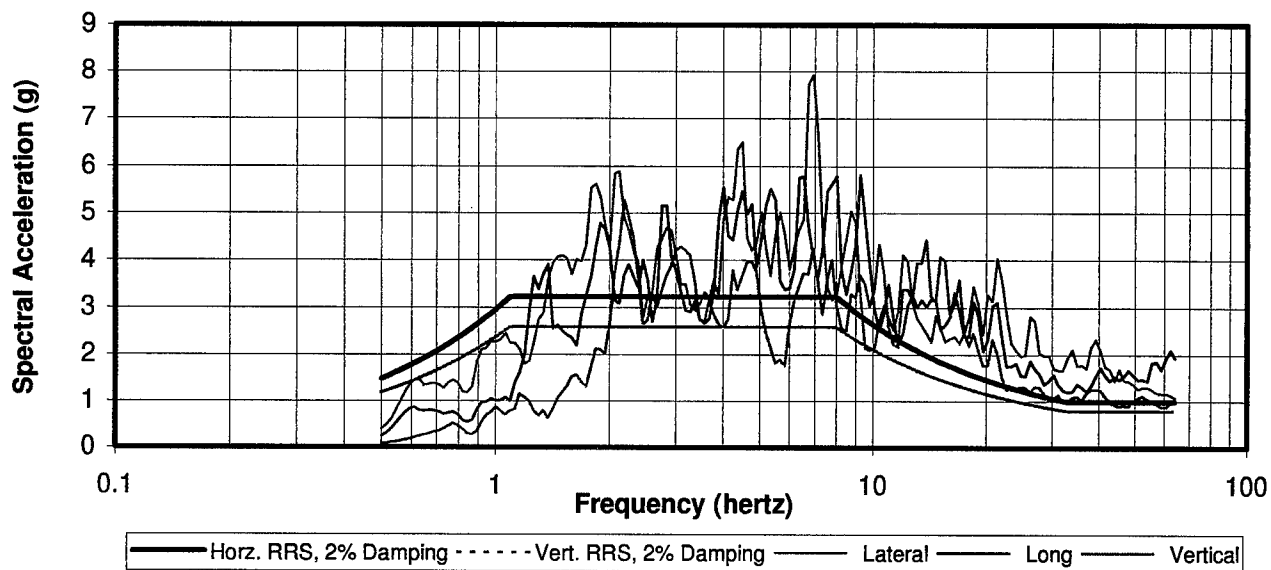
Figure 28c. Maximum TRS without notches.
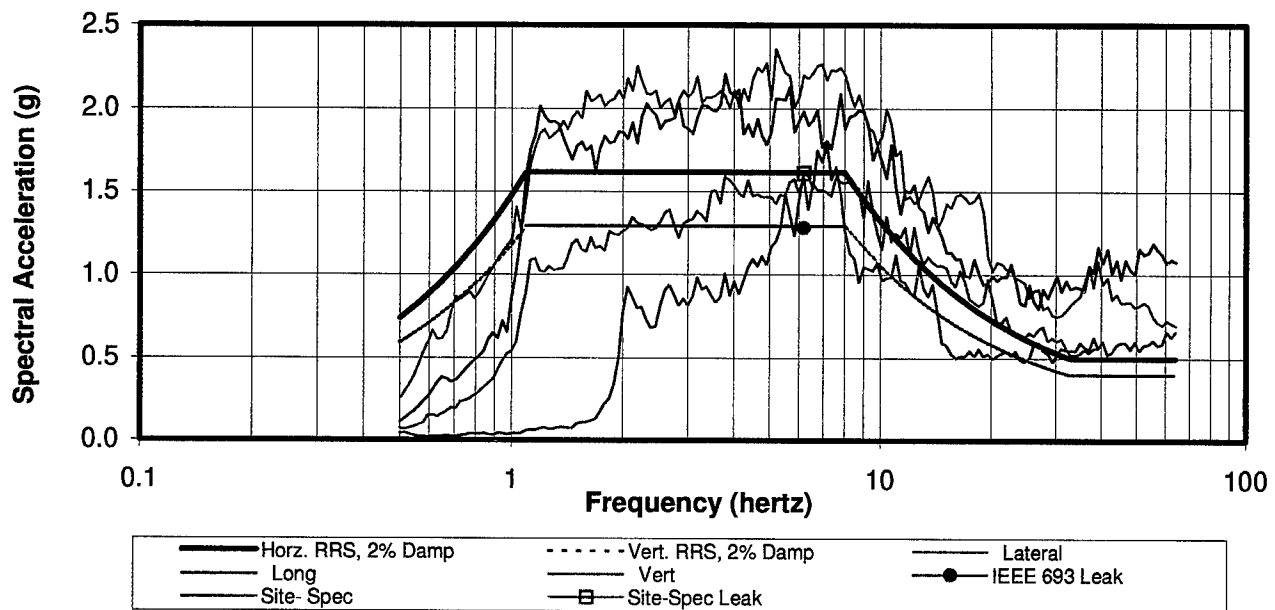
Figure 29a. IEEE 693 (at 50% PL) and site-specific spectra, TRS, and leak failures.
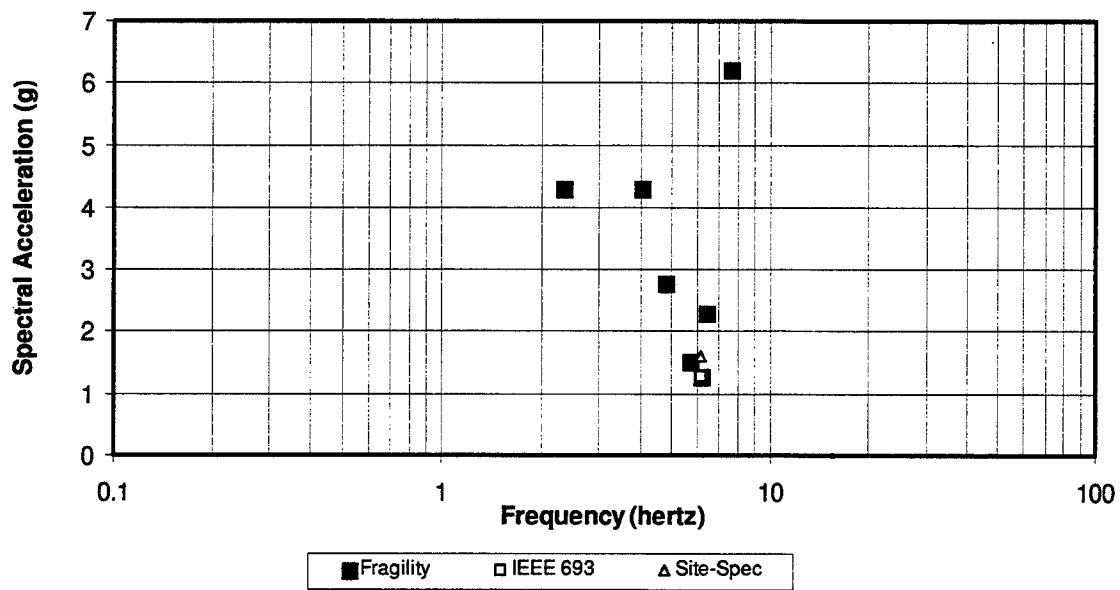
Figure 29b. Failure data from CEFAPP, IEEE 693 and site-specific tests.
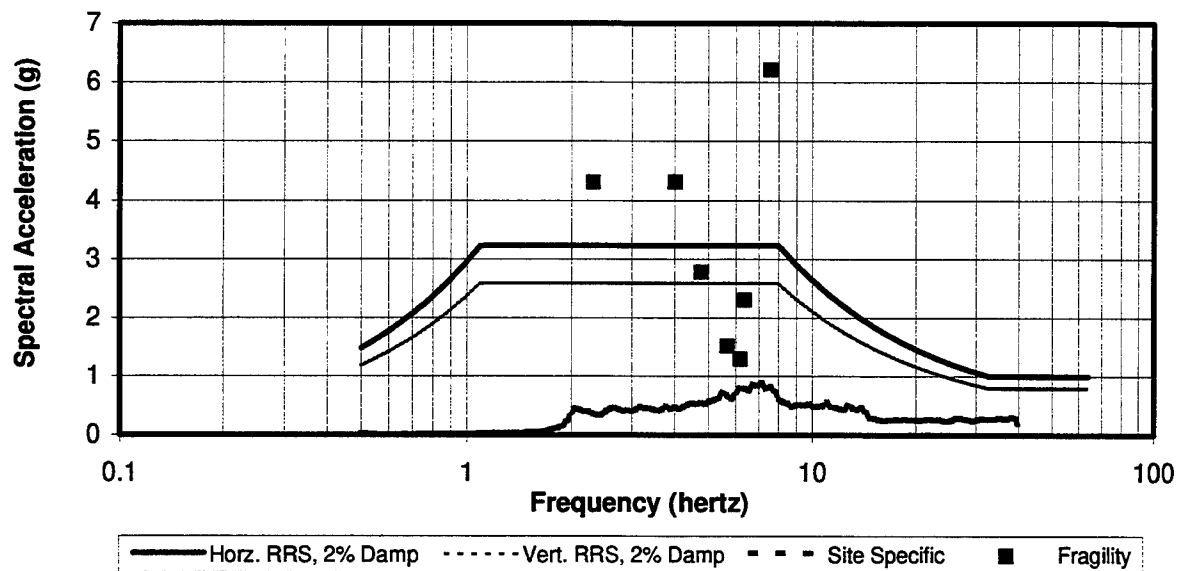
Figure 30. Fragility data with site-specific and IEEE 693 design response spectra.
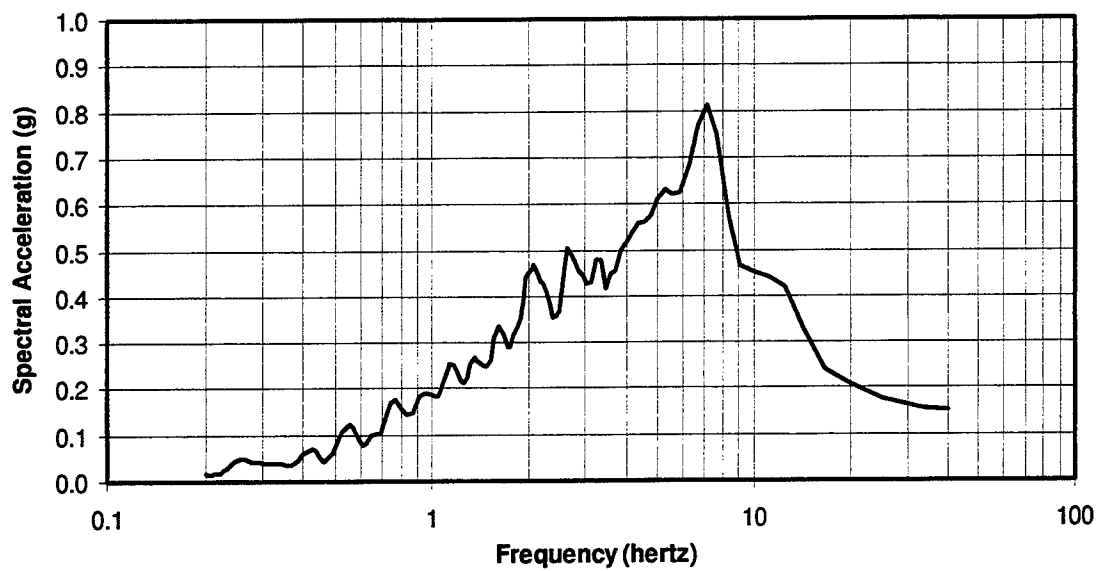
Figure 31. Example of site-specific response spectrum.
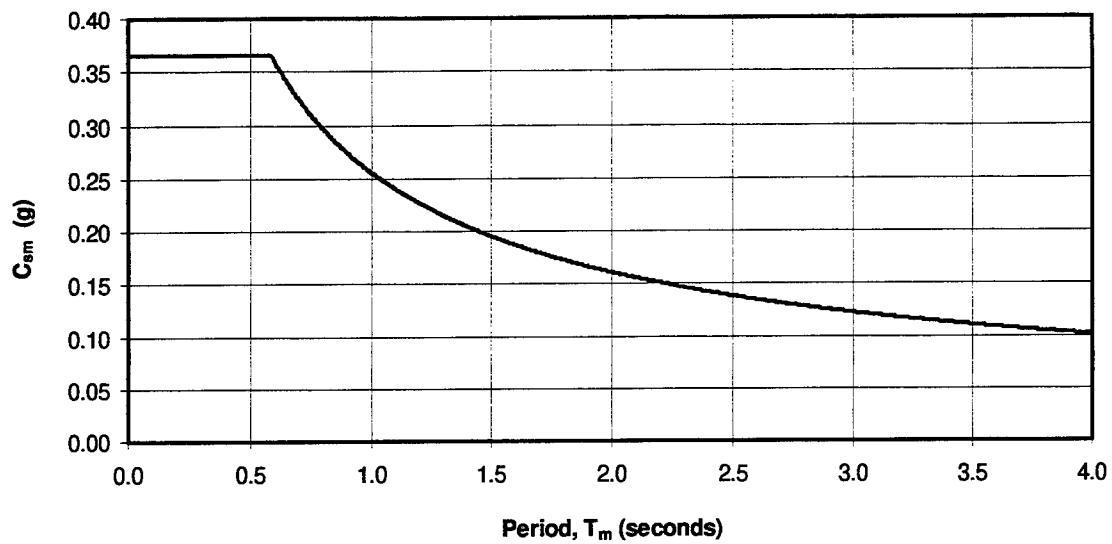
Figure 32a. Example response spectrum based on 1994 NEHRP recommended provisions.
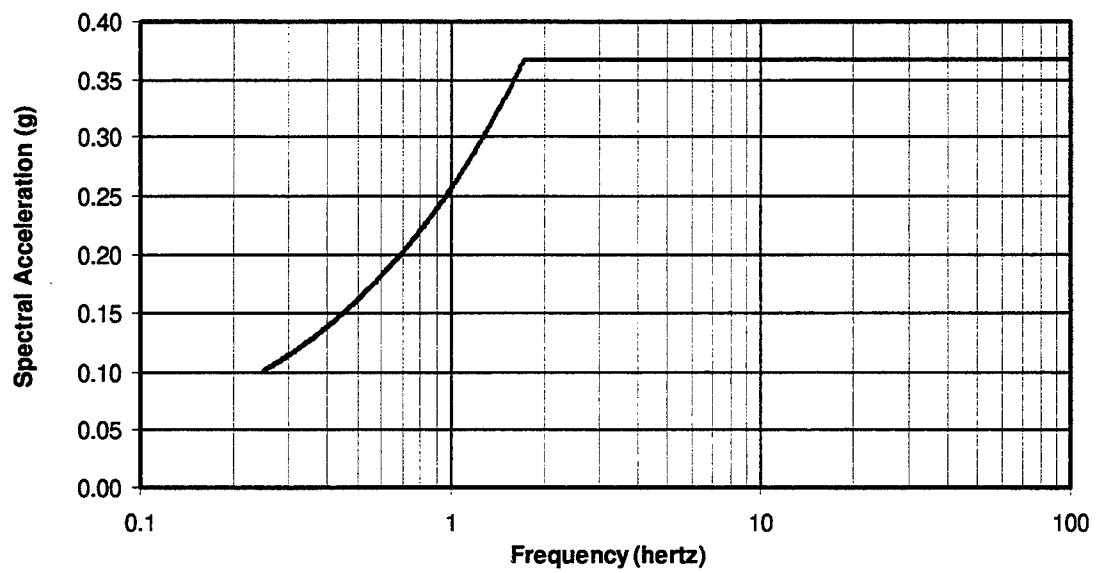
Figure 32b. Example 1994 NEHRP response spectrum plotted with respect to frequency.

0.2 sec Spectral Accel. (%g) with 2% Probability of Exceedance in 50 Years
site: NEHRP B-C boundary
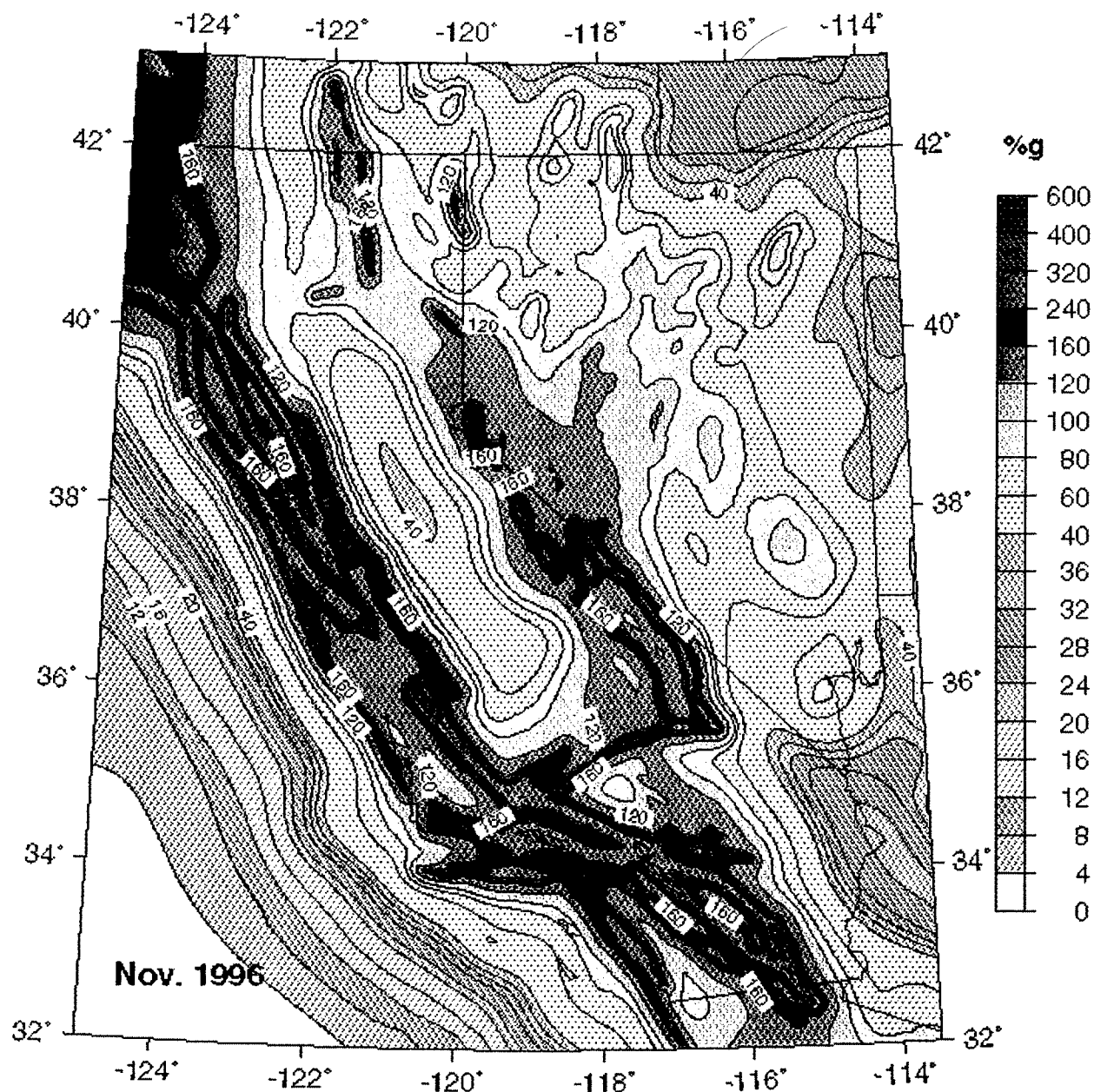
Figure 33a. USGS Spectral Acceleration Map, California and Nevada, 2% PE, 0.2 sec. period.

0.3 sec Spectral Accel. (%g) with 2% Probability of Exceedance in 50 Years
site: NEHRP B-C boundary
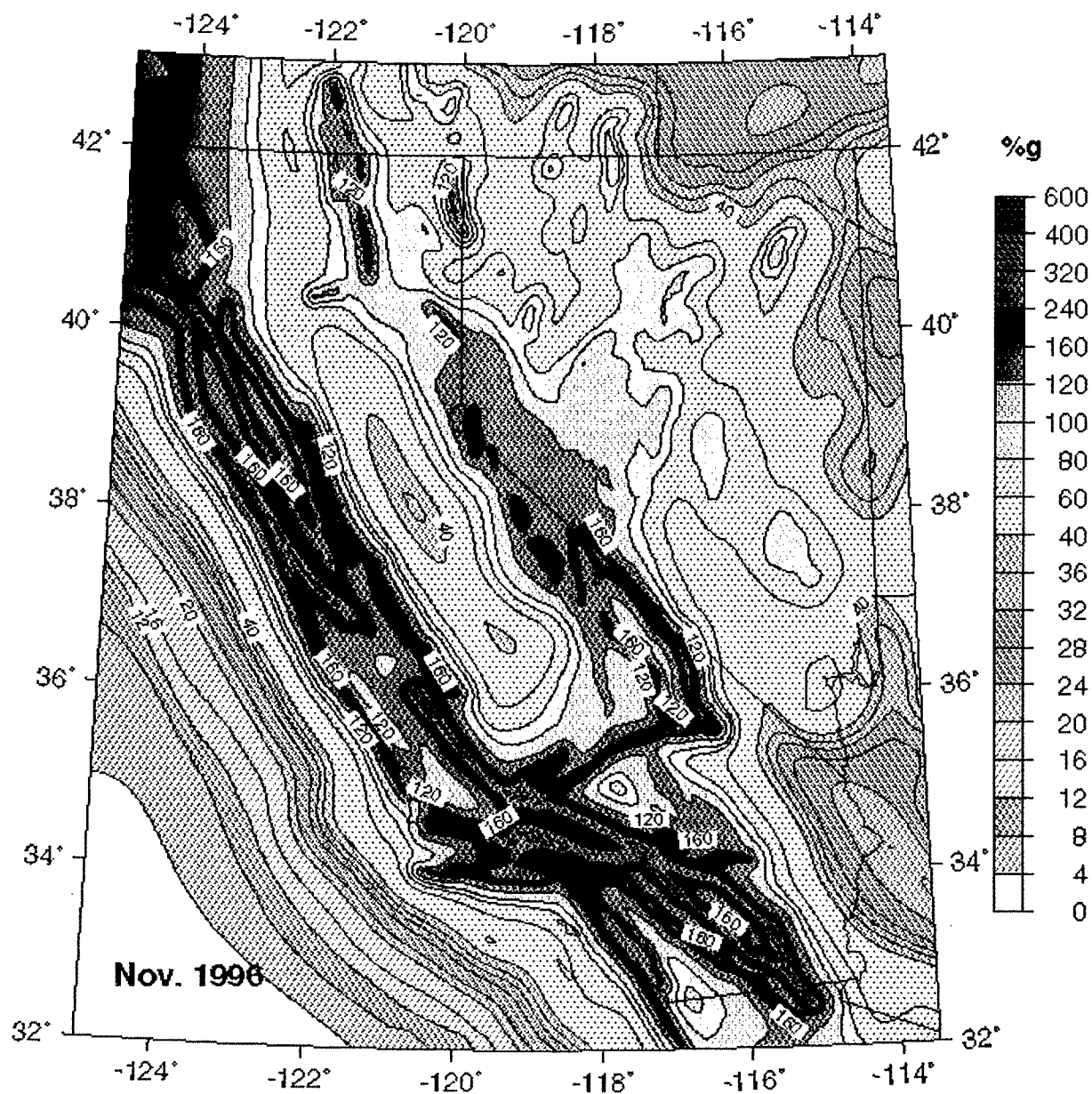
For California portion: U.S. Geological Survey - California Divison of Mines and Geology
For Nevada and surrounding states: USGS

Figure 33b. USGS Spectral Acceleration Map, California and Nevada, 2% PE, 0.3 sec. period.

1.0 sec Spectral Accel. (%g) with 2% Probability of Exceedance in 50 Years
site: NEHRP B-C boundary
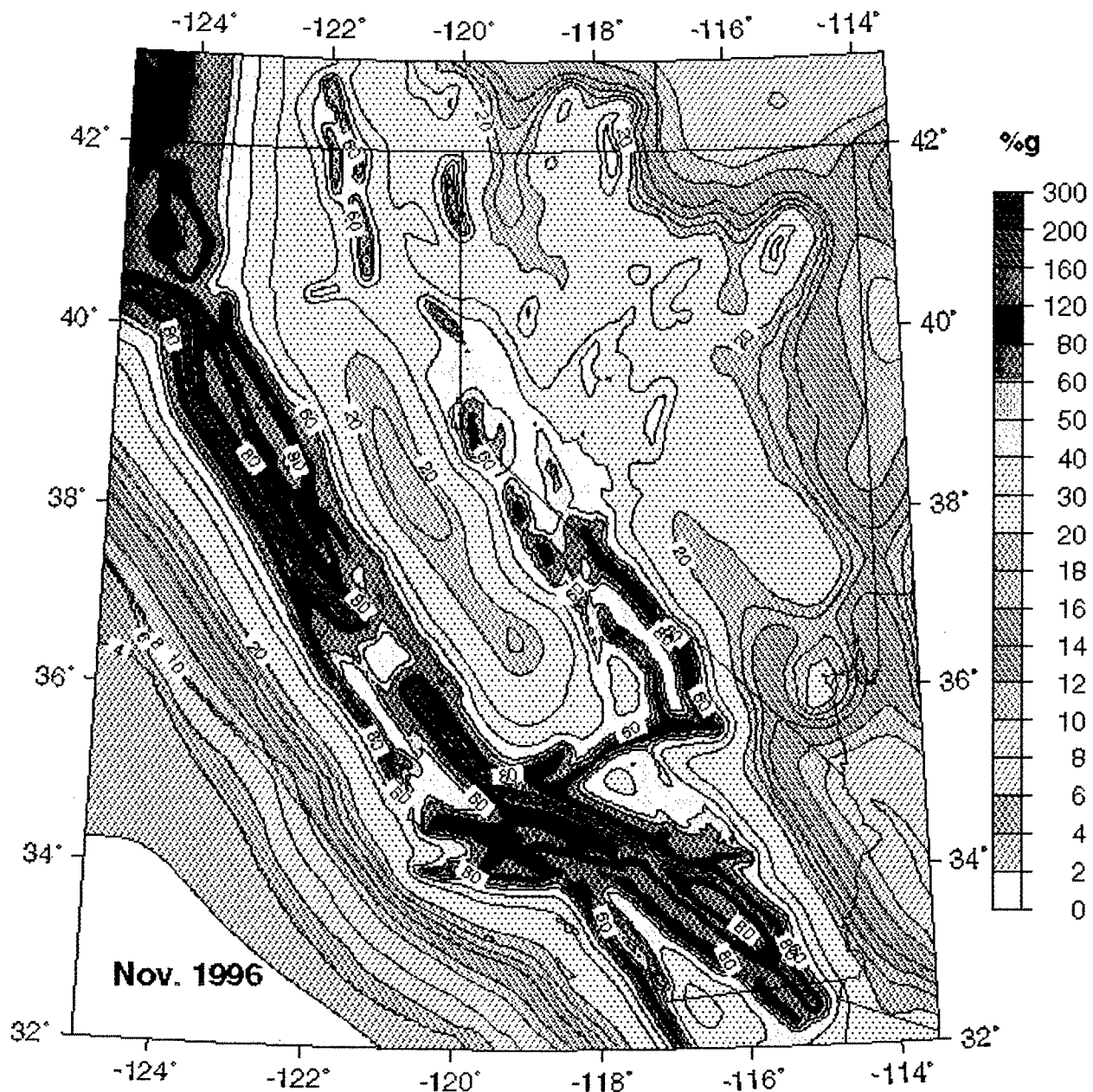
For California portion: U.S. Geological Survey - California Divison of Mines and Geology

For Nevada and surrounding states: USGS

Figure 33c. USGS Spectral Acceleration Map, California and Nevada, 2% PE, 1.0 sec. period.

0.2 sec Spectral Acceleration (%g) with 2% Probability of Exceedance in 50 Years
(site: NEHRP B-C boundary)
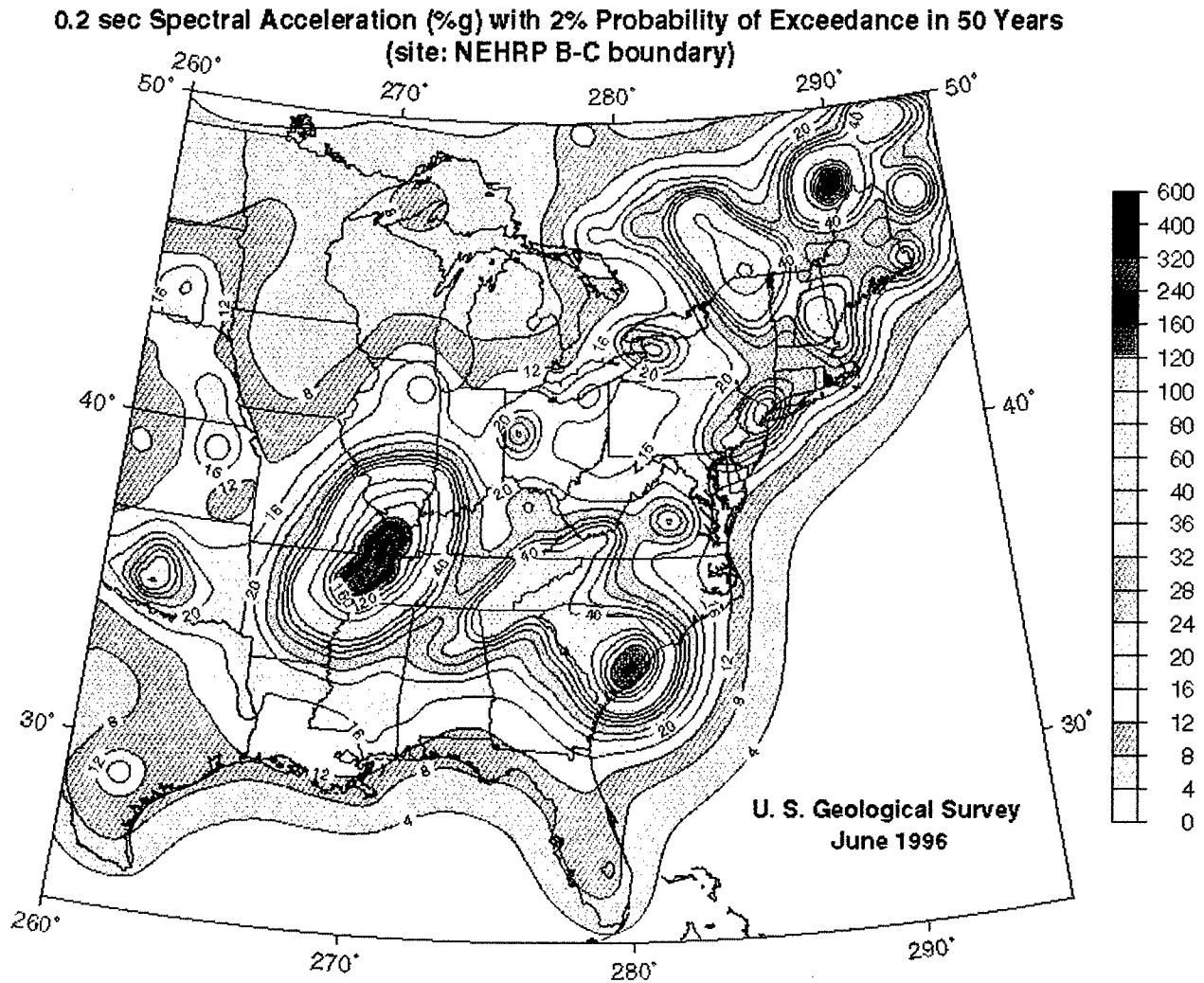
Figure 34a. USGS Spectral Acceleration Map, Central and Eastern U.S., 2% PE, 0.2 sec. period.

0.3 sec Spectral Acceleration (%g) with 2% Probability of Exceedance in 50 Years
(site: NEHRP B-C boundary)
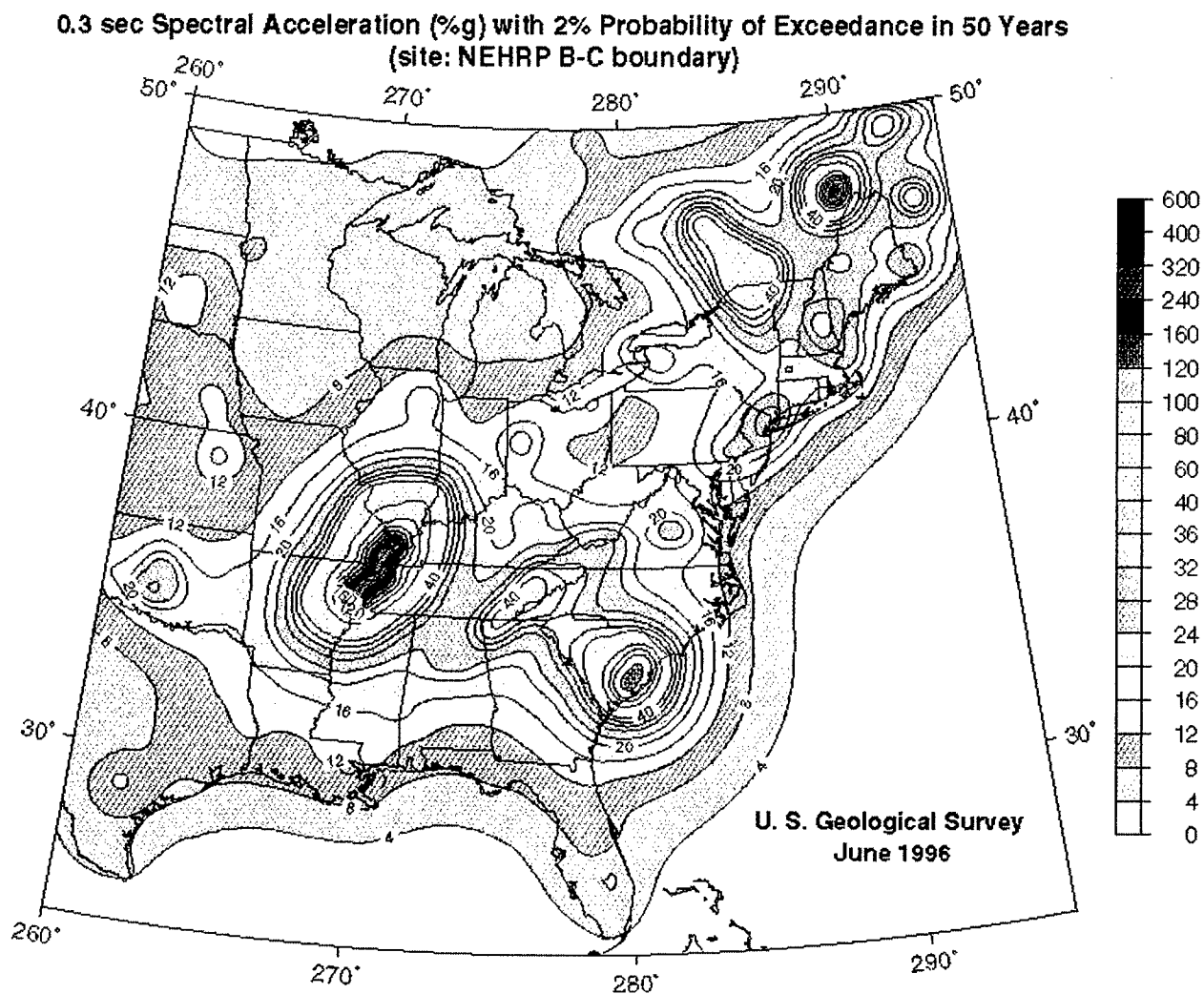
Figure 34b. USGS Spectral Acceleration Map, Central and Eastern U.S., 2% PE, 0.3 sec. period.

1.0 sec Spectral Acceleration (%g) with 2% Probability of Exceedance in 50 Years (site: NEHRP B-C boundary)
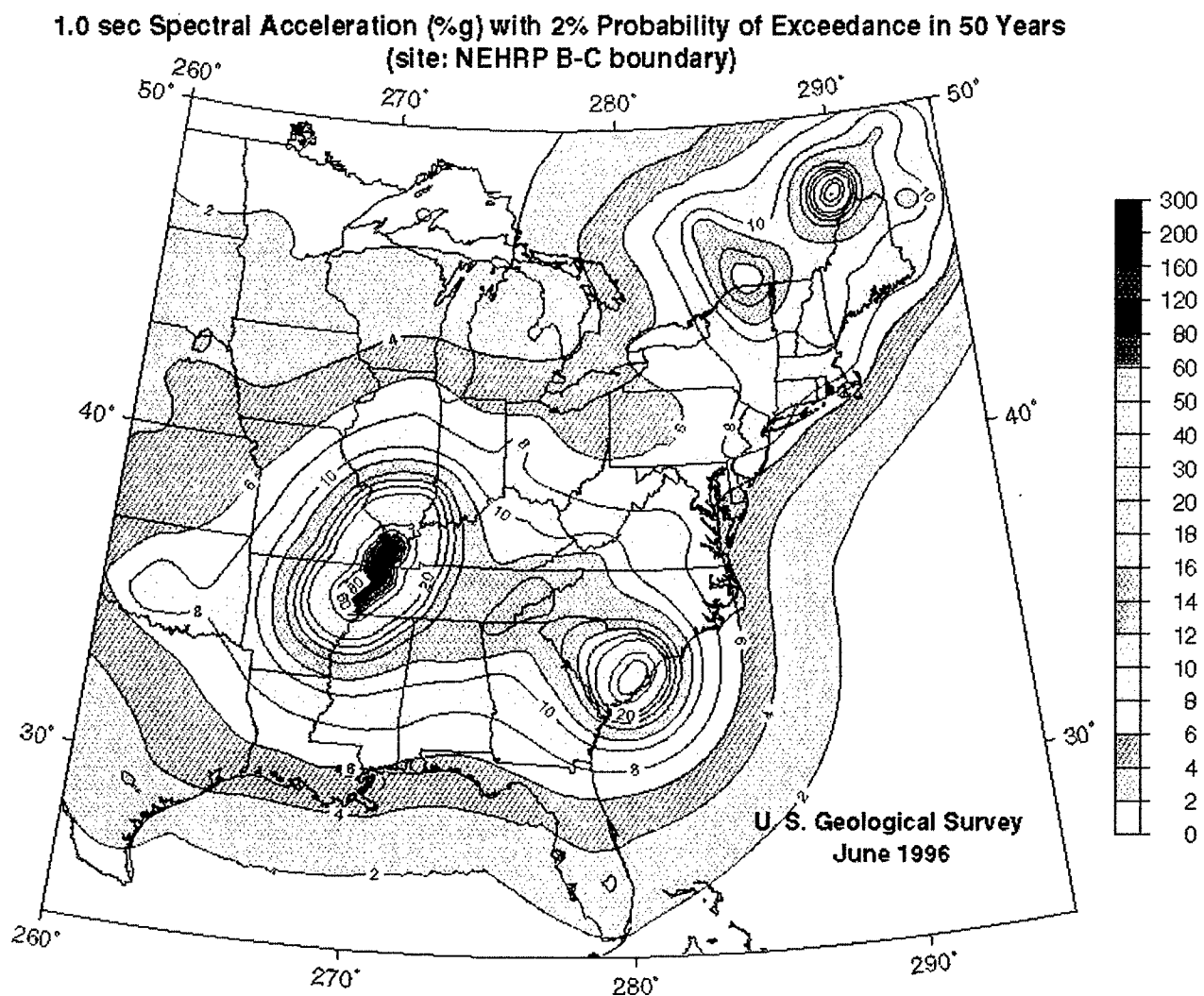
Figure 34c. USGS Spectral Acceleration Map, Central and Eastern U.S., 2% PE, 1.0 sec. period.
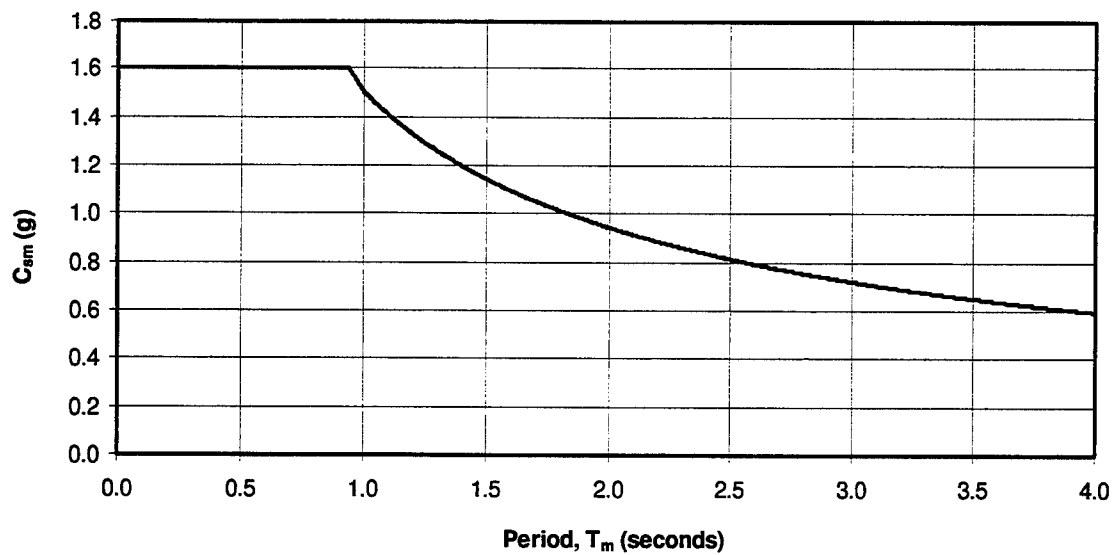
Figure 35a. Example response spectrum based on expected 1997 NEHRP recommended provisions.
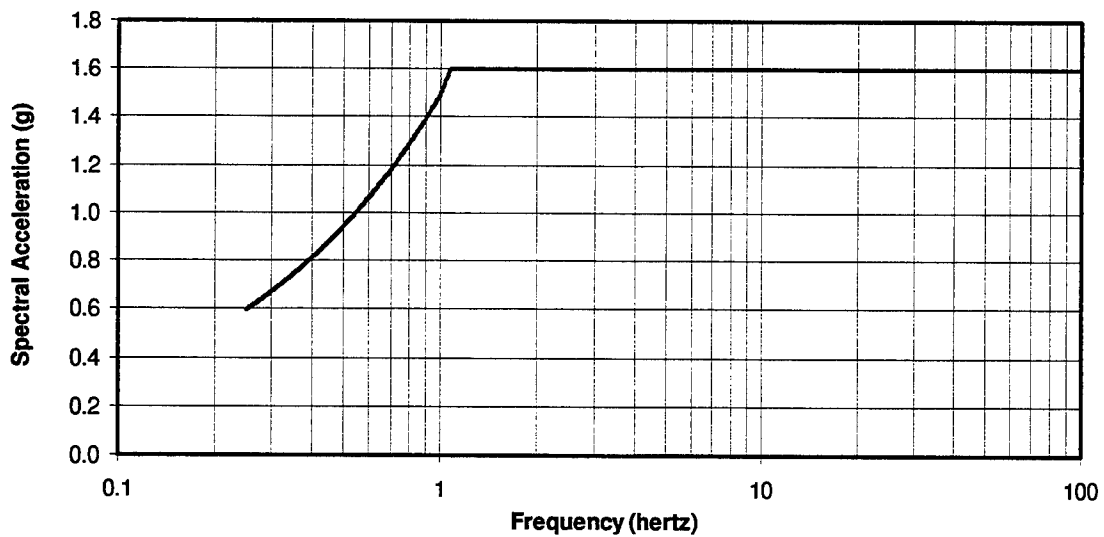
Figure 35b. Example response spectra plotted with respect to frequency.
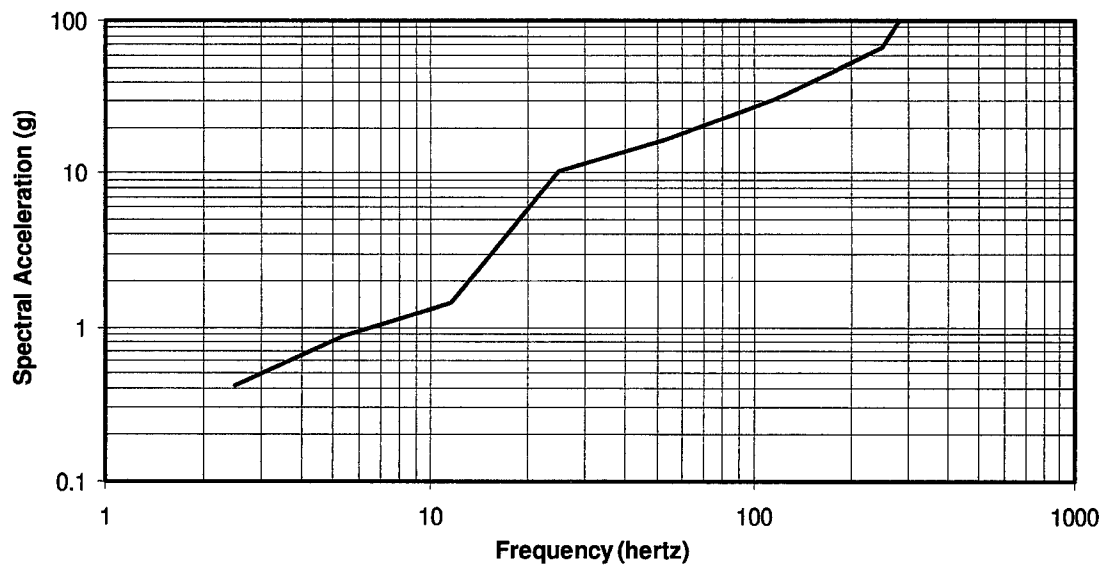
Figure 36. Shock response spectrum for a floor slab.
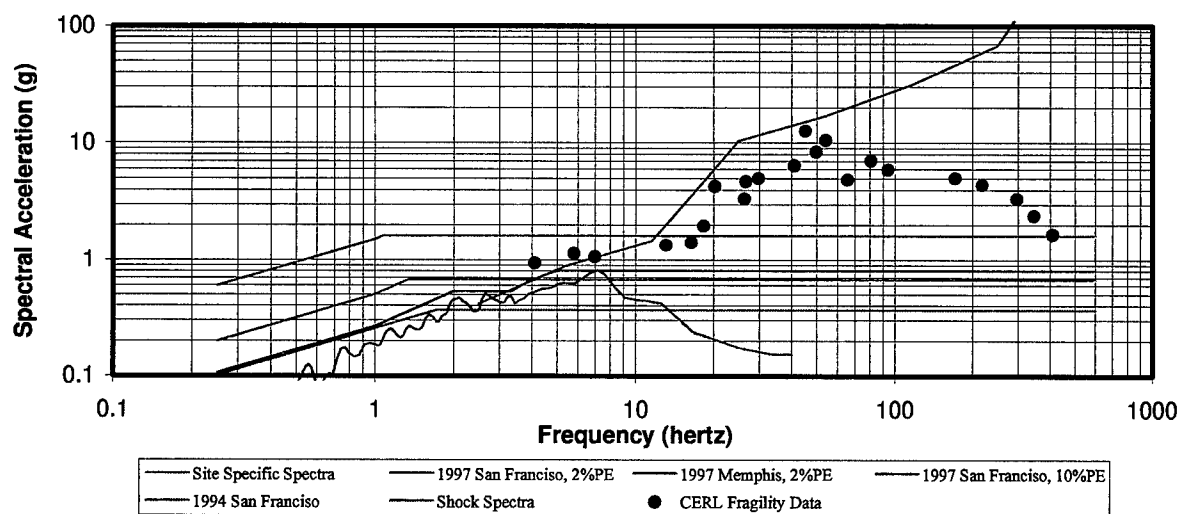
Figure 37. Seismic and shock response spectra with CERL fragility data.
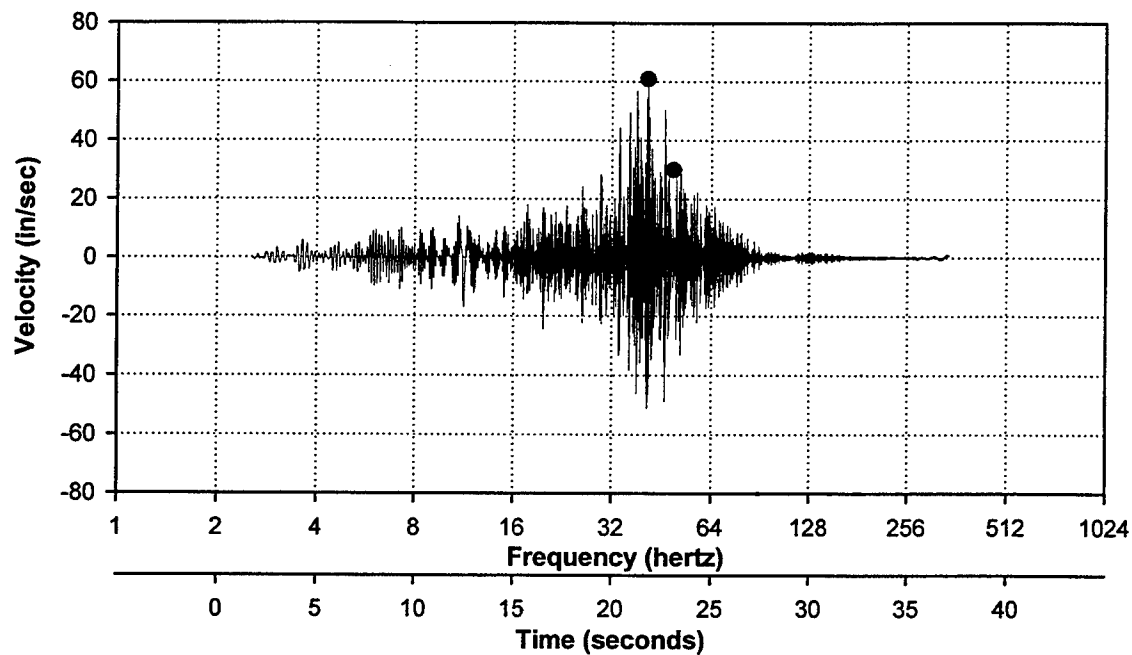
Figure 38a. Fragility Test 72 — hard disk response of test specimen to support motion.
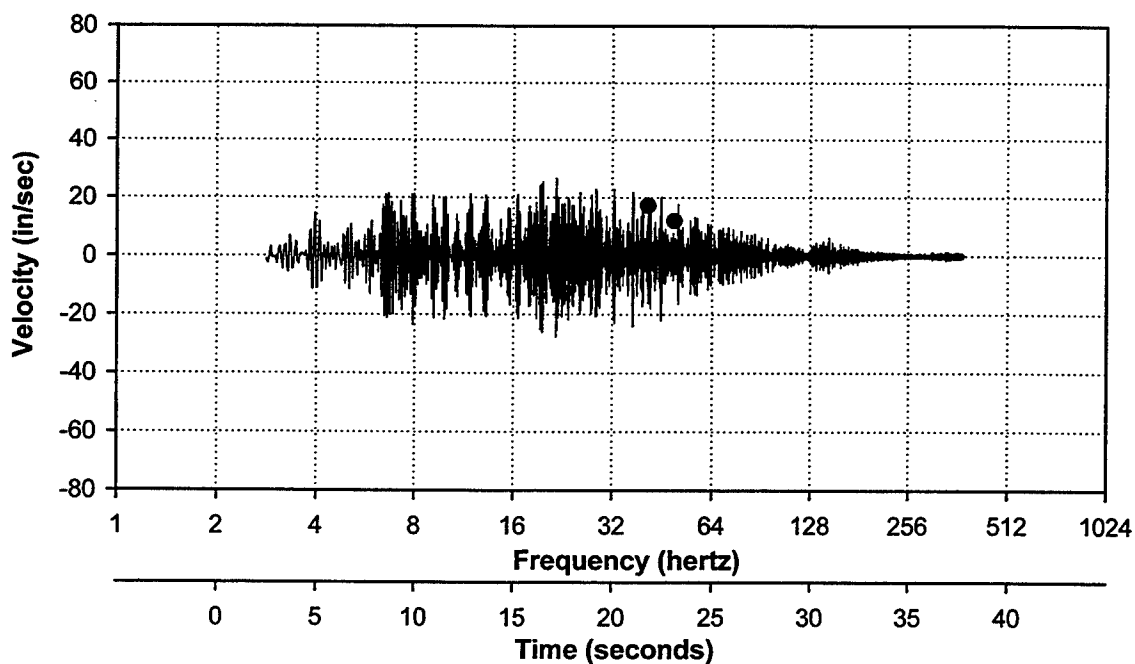
Figure 38b. Fragility Test 72 — support motion.

Appendix A: Matlab Routine RANSWP.M for Digital Generation of Narrow-Band Random Sweep Records

Narrow-band random signals, with a linearly variable sweep rate were generated digitally using the *Matlab* routine RANSWP.M.

Requested input for this routine is:

kern: the current time (entered as *hour.minute*) is used as a kernel for the pseudo-random number generator.   Unless otherwise instructed, the *Matlab* routine "rand" is initiated with the same number each time, thus always generating the same series of normally distributed pseudo-random numbers.   Initiating the routine with the current time is an effort to ensure the creation of unique random series.

aqrate: the sample rate (in hertz) at which the input signal should be created.

swratelow: beginning sweep rate (in octaves per minute).

swratehigh: ending sweep rate (in octaves per minute); the sweep rate varies linearly with time (and logarithmically with frequency) between these two limits.

centerlow: the beginning center frequency (Hz).

centerhigh: the ending center frequency (Hz).

band: the filter bandwidth, in octaves.

error: allowable filter error, in octaves.

outfile: the name of the output file in which to store the generated signal.

The algorithm for generating the test signal is outlined below. The variables used in the equations presented here correspond to the variables used in the *Matlab* routine RANSWP.M.

A series of *npts* random numbers is generated by

$$ran(i) = 2(rand - 0.5), \quad i=1...npts. \qquad \text{[Eq A1]}$$

The *Matlab* function *rand* generates a series of pseudo-random numbers uniformly distributed in the interval (0,1). The *rand* output is adjusted to return a series with 0 mean and unit absolute magnitude. This series is used to represent a time history containing frequencies ranging from 0 Hz (though, with a zero mean, there will be no DC component) to the nyquist frequency (*aqrate÷2*). Eventually sweeping filters will be applied to this raw random series to generate a new narrow band random series with a sweeping center frequency. Before this is done, certain relationships must be developed to determine the time and frequency characteristics of the final record.

The time duration of the final record is determined from the sweep rate and the number of octaves to be generated. The relation between time and sweep rate is shown in Figure A1, and given by

$$swr(t) = swratelow + s*t \qquad \text{[Eq A2]}$$

where

$$s = \frac{swratehigh - swratelow}{dur}, \qquad \text{[Eq A3]}$$

and *dur* is the time length of the record. The number of octaves generated by the record at any time *t*, is then given by

$$numoct(t) = \int swr(t)\, dt. \qquad \text{[Eq A4]}$$

Substituting A2 into A4 and evaluating the integral yields

$$numoct(t) = swratelow*t + \frac{st^2}{2}, \qquad \text{[Eq A5]}$$

where the constant of integration is equal to zero, since at *t*=0, *numoct(t)*=0. Substituting A3 into A5 and evaluating for the limits (0,dur) gives

$$numoct(t) = dur \frac{swratehigh + sratelow}{2},$$ [Eq A6]

which can then be solved to give the total time duration of the record as

$$dur = \frac{2(60)(numoct)}{(swratehigh + swratelow)}.$$ [Eq A7]

The constant of 60 is included to convert *dur* from minutes to seconds.

Knowing the duration of the record in time and the sampling rate, the number of data points in the final record is *limit = dur * aqrate*. Note that there is a difference between the length of the final record (*limit*) and the length of the initial, raw random series (*npts*); the purpose of this is shown schematically in Figure A2. The length of the raw random series is equal to that of the final record augmented by one full bandwidth and a region called a *pad* (i.e., *npts = limit + bandnum + padlength*). The purpose of the addition of an extra bandwidth is that the beginning and ending points of the final record represent center frequencies. To be consistent, and to simplify the structure of the program, the raw random series is extended so that the extreme regions of the final record operate on the exact same length of data as the interior region. There is a difference in the length of the bandwidth at the beginning and the end of the record in terms of data points; for simplicity RANSWP.M always uses the larger of the two. The purpose of the *pad* is to protect the record from magnitude loss as the filters "spool up." The linear, digital finite impulse response (FIR) filters used in this routine (and defined shortly) will not return steady state magnitude until reaching a point in the record equal to one half the filter order. Thus the initial pad region is equal to one half the beginning filter order. The filter order is allowed to vary during a run of RANSWP.M. Each time the filter order is updated the length of the pad is appropriately adjusted.

The operating logic of the main loop of RANSWP.M is to start at the beginning of the raw random series, treating the first point (offset by the pad length and one-half the initial bandwidth) as the beginning center frequency and extracting a region from the raw random series that is equal in length to the bandwidth centered about the center frequency, plus the pad. This region is filtered, and the data point that is associated with the center frequency is stored in a separate vector (*ranfilt*); the rest of the filtered region is discarded. The loop then repeats and advances one data point in the raw random series. The new center frequency associated with this data point is determined and again a region equal in length to the bandwidth (centered about the center frequency) plus the pad is extracted. Once this region is filtered appropriately the data point corresponding to the

present center frequency is stored in the vector *ranfilt* along with the previously filtered point. The loop continues in this manner until the ending center frequency is reached.

To track the center frequency and determine what the filter limits should be at any point in the record, a relationship must be determined between time (and thus data points) and frequency. This is developed by first expressing the number of octaves that have been generated at any particular frequency, *f*, as

$$numoct(f) = \frac{\log(f) - \log(centerlow)}{\log(2)}. \qquad \text{[Eq A8]}$$

Because the distribution of frequency and time must map to the same distinct number of octaves that have been generated at any point in the record, A8 can be equated to A5 to yield

$$\frac{\log(f) - \log(centerlow)}{\log(2)} = swratelow * t + \frac{st^2}{2}. \qquad \text{[Eq A9]}$$

Solving for *f* gives the desired relation:

$$f = 10^{\log(2)[swratelow * t + \frac{st^2}{2}] + \log(centerlow)} \qquad \text{[Eq A10]}$$

At this point, knowing the bandwidth, the center frequency, and the allowable filter error, the necessary design requirements for the band pass filters have been specified. FIR (finite impulse response) filters were selected based on their simplicity, linear phase, and nonrecursive nature (i.e., the filter only operates on the incoming raw, unfiltered data, as opposed to infinite impulse response filters, which operate recursively on previously filtered data). For generation of the FIR filters used by RANSWP.M, first consider the frequency response of the ideal low pass filter shown in Figure A3. To determine the filter coefficients the impulse response of the system are calculated by taking the inverse fourier transform of the frequency response,

$$h(t) = \frac{1}{2\pi} \int_{-\infty}^{\infty} H(\omega) e^{i\omega t} d\omega. \qquad \text{[Eq A11]}$$

Accounting for the step function nature of $H(\omega)$, and using Euler's identity to express the complex sinusoid in terms of elementary trigonometric functions, A11 becomes

$$h(t) = \frac{1}{2\pi} \int_{-\omega_n}^{\omega_0} [\cos\omega t + i\sin(\omega t)] d\omega. \qquad \text{[Eq A12]}$$

Since $H(\omega)$ is an even function in ω, the *sin* term can be discarded, giving

$$h(t) = \frac{1}{2\pi} \int_{-\omega_0}^{\omega_0} \cos\omega t + d\omega = \frac{\sin(\omega_0 t)}{\pi t}, \qquad \text{[Eq A13]}$$

which is a variation of the familiar $\sin(x)/x$, or sinc function. *Matlab* defines its sinc function as

$$sinc(x) = \frac{\sin(\pi x)}{\pi x}. \qquad \text{[Eq A14]}$$

Substituting $x = \omega_0 t/\pi$ into A14 gives

$$sinc(\frac{\omega_0 t}{\pi}) = \frac{\sin(\omega_0 t)}{\omega_0 t}. \qquad \text{[Eq A15]}$$

Therefore, using the *Matlab* sinc function, the impulse response can be expressed as

$$h(t) = \frac{\omega_0}{\pi} sinc(\frac{\omega_0 t}{\pi}). \qquad \text{[Eq A16]}$$

This approach provides the best least squares approximation to the transfer function in Figure A3. For digital implementation, the continuous time variable, t, becomes the discrete integer variable, n, giving

$$h(n) = \frac{\omega_0}{\pi} sinc(\frac{\omega_0 n}{\pi}). \qquad \text{[Eq A17]}$$

The development of a band pass filter from the low pass filter given by A17 is simply achieved by subtracting a low pass filter with a cutoff frequency equal to the lower cutoff frequency of the band pass filter (ω_l), from a low pass filter with a cutoff frequency equal to the higher cutoff frequency of the band pass filter (ω_h). Thus, the impulse response for the band pass filter would be given by

$$h(n) = \frac{\omega_h}{\pi} sinc(\frac{\omega_h n}{\pi}) - \frac{\omega_l}{\pi} sinc(\frac{\omega_l n}{\pi}). \qquad \text{[Eq A18]}$$

The series $h(n)$ must be truncated to a finite number of terms for numerical implementation, the limit of which is the filter order (*order*). The truncation of A18 causes a ripple effect about the cutoff frequencies due to Gibb's phenomenon. To minimize this effect a Hamming window is applied to the filter, smoothing the transfer function (Rabiner and Gold 1975, p92). The final, realizable filter is shown schematically in Figure A4. The effect of the truncation of A18 and windowing is to smooth the discontinuity at the cutoff frequencies into a transition region. The filters designed in this manner will always have a frequency response magnitude, $H(\omega)$, of 0.5 at the cutoff frequencies.

To define the filters, lastly it is necessary to relate the filter order to the error in the transition region. We define filter error as the amount of overshoot allowed by the filter at the cutoff frequencies, as shown in Figure A5. During each increment of the main loop, RANSWP.M updates the allowable filter error based on the present center frequency and the user specified error. This is necessary since the user- specified error is in octaves, and thus the actual filter error, in hertz, is a function of the current center frequency. This filter error, in hertz, is determined from the center frequency and specified error as

$$errhz = 10^{[log(centerfreq) + log(2)error]} - centerfreq. \qquad \text{[Eq A19]}$$

The filter order/error relationship was determined empirically by observing the filter transfer functions over a wide range of filter orders. It was found that the error, normalized to the nyquist frequency, obeys the following relation to filter order *(initorder)*:

$$log(errnorm) = -log(initorder) + 0.531, \qquad \text{[Eq A20]}$$

where

$$errnorm = errhz/nyquist. \qquad \text{[Eq A21]}$$

Or, solving for the filter order *(initorder)*:

$$initorder = 10^{0.531 - log(errnorm)} = \frac{10^{0.531}}{errnorm}. \qquad \text{[Eq A22]}$$

For example, if an allowable filter error *(error)* of 0.1 octave is specified, RANSWP.M first references this to the current center frequency to convert from octaves to hertz. Letting the current center frequency be 100 Hz for illustrative purposes, yields an allowable filter error *(errhz)* of 7.18 Hz. If the sampling rate were 400 Hz the nyquist frequency would be 200 Hz, giving a normalized error *(errnorm)* of 0.0359. From A21, a filter of order *(initorder)* 95 is required to satisfy the error criterion. Since the filter error is specified in terms of octaves, the filter order will vary with the center frequency. At the beginning of RANSWP.M two auxiliary m-files are utilized when the user is asked to specify the allowable filter error. The dialogue box for specifying the error is generated by ERRORBOX.M, and the computations for relating filter order and error within this box are carried out by ORDERR.M; both of these m-files are included at the end of this appendix.

After creating the appropriate bandpass filter, the region of the raw random signal that corresponds to the filter bandwidth (by equating time and frequency) is read into a separate vector *(range)* for filtering. All filtering is conducted using the built-in Matlab function *filter*. Essentially, *filter* operates in the time domain by convolving the filter coefficients *(h)* with the present region of the raw random signal. Since FIR filters are being used there is no phase distortion due to the filtering process, but there is a constant group delay of one-half the filter order

(i.e., the entire filtered region is shifted *order*/2 steps). Because the bandpass filter in RANSWP.M has a variable order, as the filter sweeps through the raw random signal the group delay is not constant, effectively causing a phase distortion in the final filtered record. This problem is avoided by forward and reverse filtering, which negates any group delay in the filtered record. The process of forward and reverse filtering also generates twice the filter order, so that the effective order/error relationship for the total filtering process becomes

$$order = 10^{0.531 - \log(2 \cdot errnorm)} = \frac{10^{0.531}}{2(errnorm)}. \qquad \text{[Eq A23]}$$

So, returning to the previous example, the actual filter order (*order*) that is used by RANSWP.M would be 48. After filtering, the data point corresponding to the current center frequency is stored in *ranfilt* along with all previous center frequencies and the loop is incremented.

After filtering, the midpoint in the filtered region, which corresponds to the center frequency, is extracted and stored in a separate vector that contain all previously filtered midpoints. Each of these points is scaled by a factor of *sf* = *nyquist*/(*highfreq* − *lowfreq*). This was done because it was found that the filtered data points had a relative magnitude that was proportional to the inverse of the filter bandwidth.

At the completion of the main loop, an attenuation function that ramps from zero to unity is applied to one-half of the first period of the filtered data. This was done to address the issue of an initial spike that was often experienced in the record and caused by a lack of rigorous enforcement of a zero initial value.

Finally, the vector *ranfiltm* is written to the output file *(outfile)*.

Transcripts of the code for RANSWP.M, ERRORBOX.M, and ORDERR.M follow.

RANSWP.M

```
% Matlab M-file to calculate narrow band random signal
% based on a sweeping center frequency, with a variable sweep rate.

global loworder highorder lowerrhz higherrhz aqrate centerlow centerhigh error

% Request user input
clear all;
kern = input('To initialize random number generator, enter time as hr.min: ');
aqrate = input('Enter the sample rate (Hz):  ');
swratelow = input('Enter the beginning sweep rate (oct/min):  ');
swratehigh = input('Enter the ending sweep rate (oct/min):  ');
```

```
centerlow = input('Enter the beginning center freq. (Hz):  ');
centerhigh = input('Enter the ending center freq. (Hz):  ');
band = input('Enter the filter bandwidth (oct):  ');

errorbox;

outfile = input ('Select desired error, then enter the name of the signal
output file:  ','s');

% initialize random number generator

seed = (kern^3);
rand('seed',seed);

% calculate system parameters: # octaves, duration, # data points

numoct = round((log10(centerhigh) - log10(centerlow))/.30103);
dur = 2*60*numoct/(swratehigh + swratelow);
time_swr_rel = (swratehigh - swratelow)/dur;
limit = dur*aqrate;
datapt_swr_rel = (swratehigh - swratelow)/limit;

% determine length of initial padding as 1/2 the greatest filter order.
% (the order corresponding to the lowest frequency).
% The purpose of the pad is to protect the beginning and end
% of the record from loss as the filter "spools up".
% Also include 1/2 of the ending bandwidth to account for region of record
% greater than the final center frequency at the end of the record.

padlength = round(loworder/2);
bandtime = 60*band/swratelow;
halfband = round(.5*bandtime*aqrate);
bandnum = 2*halfband;
npts = limit + padlength + bandnum;
padoffset = padlength;
bandoffset = halfband;

% Generate random series with unit absolute amplitude

ran = zeros(1,npts);
for n=1:npts
            ran(n) = 2*(rand - .5);
%sin(.015*pi*n);
end

% MAIN LOOP for sweeping filter through random signal

cntr=1;
order = loworder;
lowpoint = padoffset;
centpoint = padoffset + halfband;
highpoint = padoffset + bandnum;
```

```
swrate = swratelow;

for i=1:limit

t(i) = i;

% echo % finished

            if i/limit > cntr/100
            i/limit
            cntr=cntr+1;
            end

% filter band parameters

bandtime = 60*band/swrate;
halfband = round(.5*bandtime*aqrate);
bandnum = 2*halfband;

% convert from datapoint to time

% NEGATIVE TIME???? CHECK OFFSET

lowtime = (lowpoint - padoffset - bandoffset)/aqrate;
centtime = (centpoint - padoffset - bandoffset)/aqrate;
hightime = (highpoint - padoffset - bandoffset)/aqrate;

% convert from time to frequency

lowfreq = 10^(((lowtime*swratelow/60 + time_swr_rel*lowtime^2/120)*.30103) +
log10(centerlow));
centfreq = 10^(((centtime*swratelow/60 + time_swr_rel*centtime^2/120)*.30103)
+ log10(centerlow));
highfreq = 10^(((hightime*swratelow/60 + time_swr_rel*hightime^2/120)*.30103)
+ log10(centerlow));

% calculate filter order

nyquist = aqrate/2;
errhz = 10^(log10(centfreq) + .30103*error) - centfreq;
errnorm = errhz/nyquist;
order = round(10^(.531)/(2*errnorm));

% generate band pass filter as via sinc functions with
% hamming window.  Filter order (filtlim) is a function
% of the allowable filter error (error) specified in octaves

filtlim = round(order/2);
lowlimit = lowfreq/nyquist;
highlimit = highfreq/nyquist;
highlowpass = highlimit*sinc(highlimit*(-filtlim:filtlim));
lowlowpass = lowlimit*sinc(lowlimit*(-filtlim:filtlim));
```

```
step = highlowpass - lowlowpass;
h = step.*hamming(2*filtlim + 1)';

% read in new piece of raw random series, equal in length to the
% filter band plus pad

padnum = round(order/2);
rangelim = bandnum + padnum;
clear range;
range = zeros(1,rangelim);
            for j= 1:rangelim
              range(j) = ran(j+lowpoint - padnum);
            end

% filter present region of random signal.  Forward and reverse filter
% to return a signal with 0 phase delay and twice the filter order

            rantemp = filter(h,1,range);
            rantemp = rantemp(length(rantemp):-1:1);
            rantemp = filter(h,1,rantemp);
            rantemp = rantemp(length(rantemp):-1:1);

% scale factor to be applied to saved data to maintain reasonable bound
% on magnitude

            sf = (nyquist/(highfreq - lowfreq));

% combine midpoint of the present filtered region to signal containing
% all previously filtered midpoints

            datapoint = halfband;
            ranfilt(i) = sf*rantemp(datapoint);

% increment low, center and high data point markers for next loop iteration

lowpoint = lowpoint + 1;
centpoint = centpoint + 1;
highpoint = highpoint + 1;
swrate = swratelow + datapt_swr_rel * i;

% end main loop

end

%  attenuate 1/2 of beginning period to enforce 0 initial condition

            attentime = 1/(2*centerlow);
        attenpts = round(attentime * aqrate);

            for i = 1:attenpts
            atten(i) = i/attenpts;
        end
```

```
        for i = attenpts + 1: length(ranfilt)
            atten(i) = 1;
    end

    ranfiltm = atten.*ranfilt;
```

```
% write signal to file

fid = fopen(outfile,'w');
    fprintf(fid,'%8.5f\r\n',ranfiltm);
fclose(fid);
```

ERRORBOX.M

```
    clf reset;
%     set(gcf,'Units','normalized','backingstore','off');

echo off
global loworder highorder lowerrhz higherrhz aqrate centerlow
centerhigh error

    % Create intial signal
    min_err = .01;
    max_err = 1;
    err_dummy = num2str(.5);
    freq_text=uicontrol('Style','text','Position',[.18 .02 .38. 07],..
        'Units','normalized','BackgroundColor','black',...
        'ForegroundColor','white','String','Filter Error (Oct):');

    uicontrol('style','text','pos',[.14 .07 .04 .05],...
        'Units','normalized','BackgroundColor','black',...
        'ForegroundColor','white','String',num2str(min_err));

    uicontrol('style','text','pos',[.79 .07 .02 .05 ],...
        'Units','normalized','BackgroundColor','black',...
        'ForegroundColor','white','String',num2str(max_err));

    err_field=uicontrol('Style','edit','Position',[.59 .02 .12. 07],..
        'Units','normalized','String',err_dummy,...

'CallBack',['set(err_slider,''Value'',','str2num(get(err_field,''Strin
g''))),',...
            'orderr(','get(err_slider,''Val'')',');,',...
            'set(order_field1,''String'',','num2str(loworder));,',...
```

```
        'set(order_field2,''String'',','num2str(highorder));,',...
            'set(error_field1,''String'',','num2str(lowerrhz));,',...
        'set(error_field2,''String'',','num2str(higherrhz));,',...
            'error = ','get(err_slider,''Val'');']);


    err_slider=uicontrol('Style','slider','Position',[.15 .12 .65
.04],...

'Units','normalized','Value',str2num(get(err_field,'String')),'Max',ma
x_err,'Min',min_err,...

'CallBack',['set(err_field,''String'',','num2str(get(err_slider,''Val'
'))),',...
            'orderr(','get(err_slider,''Val'')',');,',...
            'set(order_field1,''String'',','num2str(loworder));,',...
        'set(order_field2,''String'',','num2str(highorder));,',...
            'set(error_field1,''String'',','num2str(lowerrhz));,',...
        'set(error_field2,''String'',','num2str(higherrhz));,',...
            'error = ','get(err_slider,''Val'');']);


%

    close_button=uicontrol('Style','Pushbutton','Position',[.85 .02
.12 .07],...
        'Units','normalized','Callback','close(gcf)','String','Done');


% * * * * * * * * * * Filter Order Dialogue * * * * * * * * * * * * * *


% TITLE
    order_text=uicontrol('Style','text','Position',[.15 .8 .22 .07],..
        'Units','normalized','BackgroundColor','black',...
        'ForegroundColor','white','String','Filter Order (# pts):');


% SUBTITLE

    order_sub1=uicontrol('Style','text','Position',[.15 .72 .38.07],...
        'Units','normalized','BackgroundColor','black',...
        'ForegroundColor','white','String','Beginning Frequency ');
    order_sub2=uicontrol('Style','text','Position',[.5 .72 .38 .07],...
        'Units','normalized','BackgroundColor','black',...
        'ForegroundColor','white','String','Ending Frequency');


% Order boxes


    order_field1=uicontrol('Style','edit','Position',[.27 .65 .12
.07],...
        'Units','normalized','String',num2str(loworder));
```

```
        order_field2=uicontrol('Style','edit','Position',[.63 .65 .12
.07],...
            'Units','normalized','String',num2str(highorder));


% * * * * * * * * * Filter Error Dialogue * * * * * * * * * * * * *

% TITLE
   error_text=uicontrol('Style','text','Position',[.15 .45 .22.07],...
            'Units','normalized','BackgroundColor','black',...
            'ForegroundColor','white','String','Filter Error (+/- Hz):');
% SUBTITLE

   error_sub1=uicontrol('Style','text','Position',[.15 .37 .38.07],...
            'Units','normalized','BackgroundColor','black',...
            'ForegroundColor','white','String','Beginning Frequency ');

   error_sub2=uicontrol('Style','text','Position',[.5 .37 .38 .07],...
            'Units','normalized','BackgroundColor','black',...
            'ForegroundColor','white','String','Ending Frequency');

% Error boxes

   error_field1=uicontrol('Style','edit','Position',[.27 .3 .12 .07],
            'Units','normalized','String',num2str(lowerrhz));

   error_field2=uicontrol('Style','edit','Position',[.63 .3 .12 .07],
            'Units','normalized','String',num2str(higherrhz));
```

ORDERR.M

```
function orderr(dummy)

global loworder highorder lowerrhz higherrhz aqrate centerlow
centerhigh error


nyquist = aqrate/2;
lowerrhz = 10^(log10(centerlow) + .30103*dummy) - centerlow;
higherrhz = 10^(log10(centerhigh) + .30103*dummy) - centerhigh;
lowerrnorm = lowerrhz/nyquist;
higherrnorm = higherrhz/nyquist;
loworder = round(10^(.531)/(2*lowerrnorm));
highorder = round(10^(.531)/(2*higherrnorm));
```
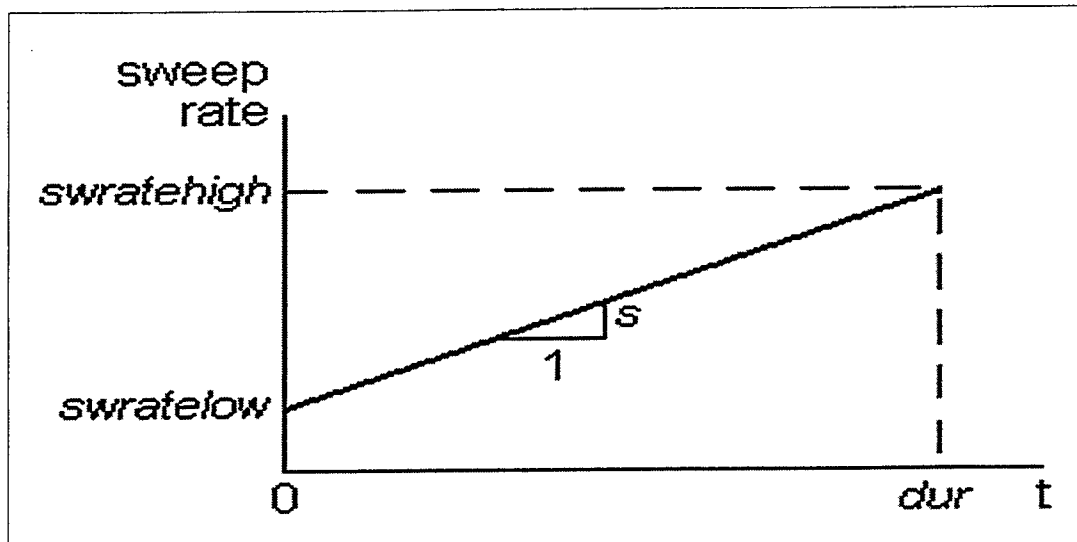
Figure A1. Time sweep rate relationship.
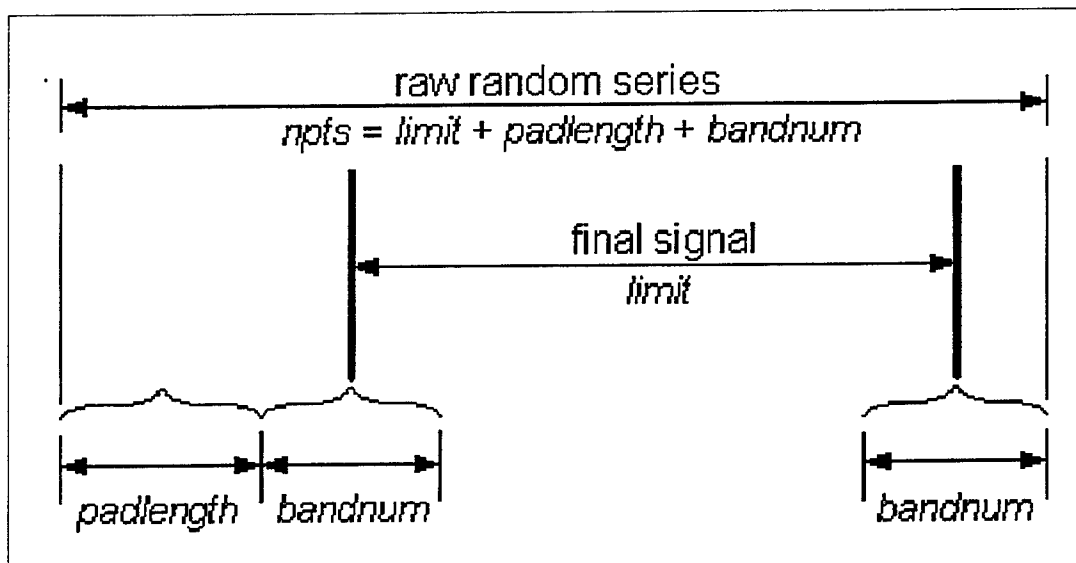
Figure A2. Relationship between the raw random series and final signal length.
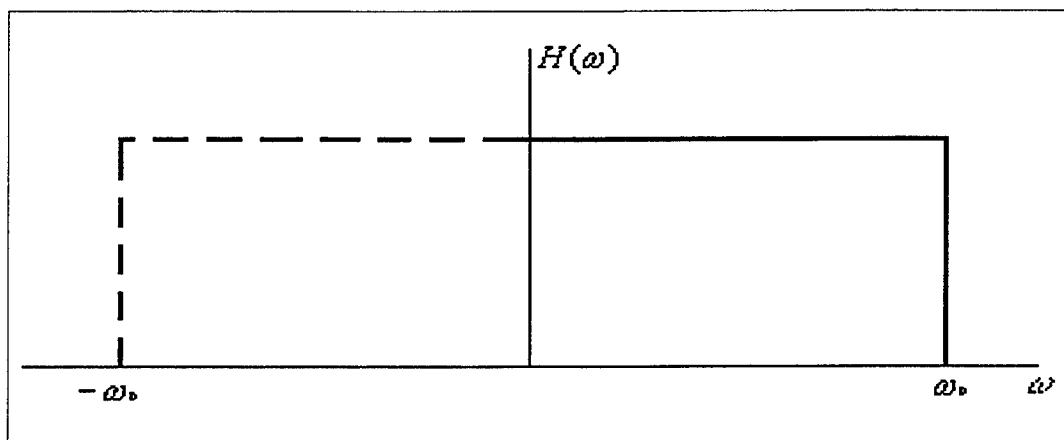
Figure A3. Ideal low-pass filter.
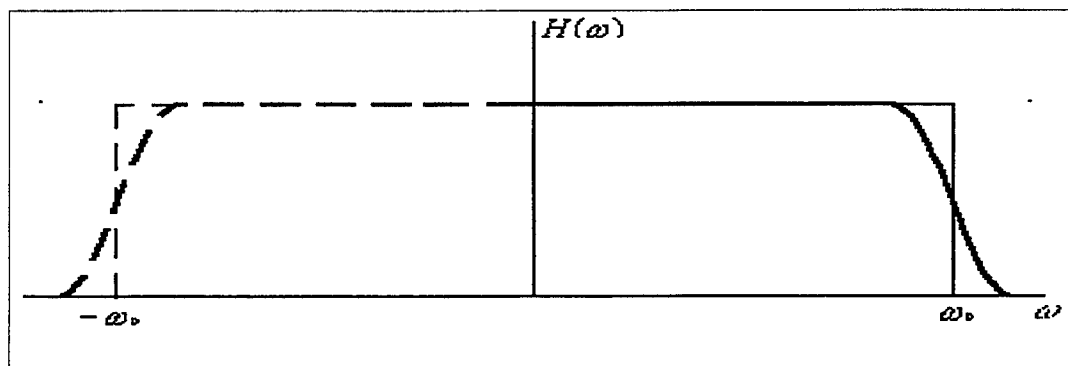
Figure A4. Truncated and windowed low-pass filter.
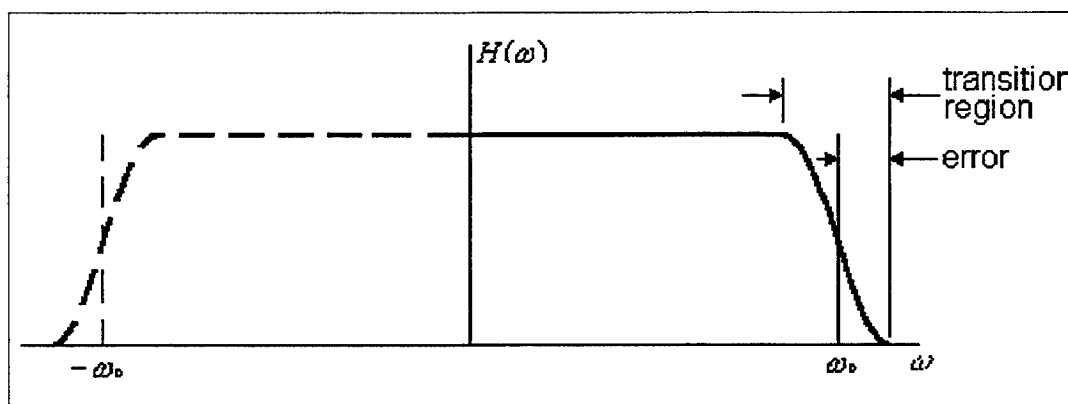
Figure A5. Definition of filter error.

Appendix B: Numerical Analysis of Single Degree of Freedom (SDOF) Oscillators

SDOF Time History Analysis

In determining the appropriate sweep rate, it is necessary to calculate the time history response of single degree of freedom (SDOF) oscillators to base excitation. The nature of the base motion is governed by the type of fragility testing being conducted and is thus arbitrary, ranging from shock to seismic input motions. The method employed for this analysis is to calculate the response of an SDOF oscillator as the convolution of the SDOF impulse response and the base excitation. This method is described below in greater detail.

Arbitrary input motion may be viewed as a sequence of impulses

$$F(t) \cong \sum F(\tau)\, \Delta\tau\, \delta(t-\tau), \qquad\qquad \text{[Eq B1]}$$

where $\delta(t-\tau)$ is the delta function defined at $t=\tau$, and $F(\tau)\,\Delta\tau$ represents the magnitude of the impulse. It can also be shown that the impulse response of an oscillator to base excitation is expressed as

$$I(t) = \frac{1}{\omega_d}\, e^{-\zeta\omega_n t} \sin\omega_d t. \qquad\qquad \text{[Eq B2]}$$

where ω_n and ω_d are the undamped and damped natural frequencies of the system. Applying the series of impulsive forces to the impulse response function yields the system response to general base excitation as

$$x(t) \cong \sum F(\tau)\,\Delta\tau\, I(t-\tau) \qquad\qquad \text{[Eq B3]}$$

or, if we allow $\Delta\tau \to 0$

$$x(t) = \int_0^t F(\tau)\, I(t-\tau)\, d\tau. \qquad\qquad \text{[Eq B4]}$$

Substituting Equation B2 and differentiating yields an expression for the velocity of the system:

$$\dot{x}(t) = \int_0^t F(\tau)\cos\omega_d(t-\tau)e^{-\zeta\omega_n(t-\tau)}d\tau$$

[Eq B5]

$$-\frac{\zeta\omega_n}{\omega_d}\int_0^t F(\tau)\sin\omega_d(t-\tau)e^{-\zeta\omega_n(t-\tau)}d\tau.$$

The total acceleration (input plus response) can be found by substituting (Equations B4 and B5) into the equilibrium expression

$$\ddot{x}(t) = -2\omega_n\zeta\,\dot{x}(t) - \omega_n^2 x(t)$$

[Eq B6]

yielding,

$$\ddot{x}(t) = (2\zeta^2-1)\frac{\omega_n^2}{\omega_d}\int_0^t F(\tau)\sin\omega_d(t-\tau)e^{-\zeta\omega_n(t-\tau)}d\tau$$

[Eq B7]

$$-2\omega_n\zeta\int_0^t F(\tau)\cos\omega_d(t-\tau)e^{-\zeta\omega_n(t-\tau)}d\tau.$$

To apply Equation B7 to sampled data we must return to a discrete formulation expressing B7 as

$$\ddot{x}(i) = (2\zeta^2-1)\frac{\omega_n^2}{\omega_d}\sum_{j=1}^i F(j)\sin\omega_d(i-j)e^{-\zeta\omega_n(i-j)}\Delta\tau$$

[Eq B8]

$$-2\omega_n\zeta\sum_{j=1}^i F(j)\cos\omega_d(i-j)e^{-\zeta\omega_n(i-j)}\Delta\tau,\quad i=1,...,end.$$

This is the expression used to determine system response in the Matlab routine SDOF.M (shown below). Vectors g1 and g2 are used to store the trigonometric and exponential terms of the first and second summation. The Matlab library convolution routine (*conv*) is then used to convolve these system vectors with the forcing vector ($F(\tau)\Delta\tau$).

The code for SDOF.M follows:

```
% Matlab Routine SDOF.M

% Matlab M-file to calculate SDOF response to arbitrary
% base motion.



% request user input
```

```
% open input file and read in excitation

infile = input ('Enter the name of the excitation file:  ','s');
outfile = input ('Enter the name of the SDOF response file:  ','s');
freq = input ('Enter the undamped natural frequency:  ');
etap = input ('Enter the percentage of critical damping:  ');
dt = input('Enter the time step for the input motion:  ');


fid = fopen(infile);
f = fscanf(fid,'%e');
fclose(fid);
numpt = length(f)

% calculate system parameters


eta = etap/100;
wn=2*pi*freq;
wd = ((1 - (eta)^2)^.5)*wn;

% Calculate system vector:  SDOF response to unit pulse, which is
% equivalent to initial velocity response.
% r is the theoretical response to resonant input- used for debugging.

for I = 1:numpt
   t = dt*I;
   g1(I) = exp(-(eta*wn*t))*sin(wd*t);
   g2(I) = exp(-(eta*wn*t))*cos(wd*t);
   r(I) = ((exp(-eta*wn*t)-1)*cos(wn*t) +
eta*exp(-eta*wn*t)*sin(wn*t))/(2*eta);
end


% calculate response as the convolution of the forcing
% vector and the response vector
% The forcing vector does not have a mass term
% to be consistent with ground motion excitation.
% The response has been integrated twice and represents the
% TOTAL acceleration.
%


y = (2*eta^2 - 1)*(wn^2/wd)*conv(dt*f,g1) - 2*wn*eta*conv(dt*f,g2);


% convolution returns 2n data points for a length n record
% vector temp stores only first n values of y


for I = 1:numpt
```

```
temp(I) = y(I);
end

x = temp';

fid = fopen(outfile,'w');
fprintf(fid,'%8.3f\r\n',x);
fclose(fid);
```

SDOF Narrow Band Random Sweep Analysis

SDOF oscillators are excited with narrow band random sweep base motions. A narrow band random base motion provides a Gaussian normal excitation of the SDOF oscillator. The signal generated by low pass and high pass filters on a random signal will have a Rayleigh distribution of the absolute values of its peaks. For a Rayleigh distribution the distribution of peak values is of interest, which can be expressed by:

$$\frac{N_0}{2M} = 1 \qquad \text{[Eq B9]}$$

where N_0 is the number of zero crossings and 2M is the sum of positive and negative peaks.

Figure 1 (immediately following the main body of the report) shows a narrow band random signal of this type. Sweeping the narrow band random record adds another variable to calculating the statistical response of SDOF oscillators in the frequency range of the sweep. Further study of this response is needed.

At this point it is assumed that a SDOF oscillator of frequency, f_n, is excited with the number of strong motion cycles (SMC) that equal the time required for the sweep to move across oscillator frequency (band width / sweep rate) divided by the period, T_n, of the oscillator.

This may be expressed as follows:

$$SMC = \frac{BandWidth}{SR \; T_n} \qquad \text{[Eq B10]}$$

The sweep rate (SR) needed to produce a desired number of SMC for any oscillator at frequency, f_n, subjected to narrow band random sweep base excitation may then be expressed as:

$$SR = \frac{BandWidth}{SMC} \, f_n = \frac{1/3\,octave}{SMC} \, f_n \text{ (60sec/min)}$$ [Eq B11]

Table B1. Calculation of strong motion cycles for 12.2 hz SDOF oscillator at 2% damping subjected to the El Centro earthquake record.

Figure 3b Cycle (#)	Time (sec)	Positive Peak (g)	Negative Peak (g)	Difference (g)	Percentage of Max Diff (%)
1	2.12	0.369	-0.472	0.841	69%
2	2.42	0.393	-0.771	1.164	95%
3	2.46	0.448	-0.771	1.219	100%
4	2.54	0.355	-0.496	0.851	70%
5	2.62	0.322	-0.588	0.91	75%
6	2.7	0.339	-0.452	0.791	65%
7	2.82	0.276	-0.382	0.658	54%
8	3.34	0.282	-0.483	0.765	63%
9	3.42	0.383	-0.265	0.648	53%
10	4.68	0.301	-0.318	0.619	51%
11	4.8	0.514	-0.139	0.653	54%
12	4.88	0.47	-0.692	1.162	95%
13	4.96	0.126	-0.499	0.625	51%
14	9.54	0.317	-0.299	0.616	51%

Appendix C: Fragility Test Support Motion Filtering and Integration

Accelerometer data recorded at the equipment attachment locations and on the equipment were processed to obtain plots of velocity versus time. This required that the raw data be filtered and integrated as defined below. (Note that these steps were not needed for the bushing test data presented in Chapter 4.)

Data Filtering

The measured signal from accelerometers is expressed in terms of voltage. These data are converted to engineering units by multiplying it by the accelerometer's calibration factor (in g's/volt) and dividing it by the amplifier's gain factor set in the data acquisition system for that particular channel at the time the data was recorded. The voltage data will include certain levels of noise from various sources (e.g., line current at 60hz, 120 hz etc.). Normally this noise is fairly small relative to the measured response if the gains have been set properly. The gain for each channel is normally set as high as possible to achieve maximum resolution in the recorded data while ensuring that the recording limits are not exceeded. For the fragility tests conducted at USACERL, a very wide frequency range was used, which means that the gains had to be set to measure the relatively large accelerations at higher frequencies while minimizing the relative magnitude of noise at the lower accelerations at lower frequencies. Understanding the nature of the recorded data is important to guiding the use of appropriate filtering procedures.

One advantage of narrow band sine-sweep fragility testing is the knowledge of the frequency content at any point in the time history. Filtering is facilitated by this in that response outside of the 1/3 octave band (+/- 1/6 octave about the center frequency) is known a *priori* to be noise. Ideally a 1/3 octave band pass filter (+/- correction factor for singularity at the cutoff frequency) would be applied to the time history of the response, matching the center frequency. Since the capability of a continuously varying filter was not available at the time, the record was divided into four discrete frequency ranges to isolate regions of consistent noise. Appropriate band pass filters were then applied to each region. Table C1 and

Table C1. Filters used for narrow-band random data presented in Chapter 2.

Data Time Range (sec)	Data Frequency Range (Hz)	Filter / Band (Hz)
0 - 12.5	2.245 - 12.7	15 / Low Pass
12.5005 - 27.5	12.7 - 101.6	100 / Low Pass 12 / High Pass
27.5005 - 35.5	101.6 - 310	305 / Low Pass 98 / High Pass
35.5005 - 40.0	310 - 574.7	295 / High Pass
0 - 40.0	2.245 - 574.7	562 / Low Pass 1.5 / High Pass
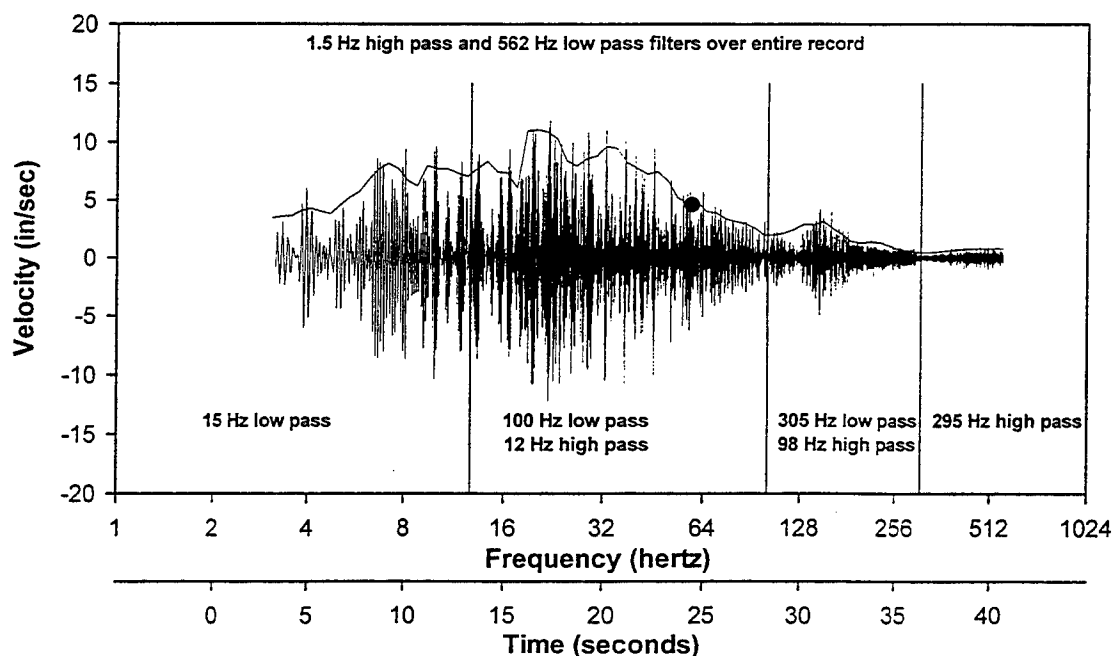
Figure C1. Filters used for narrow-band random data presented in Chapter 2.

Figure C1 illustrate these filter ranges used for all the narrow-band random data presented in Chapter 2.

The four frequency ranges were determined via power spectrum analysis at various regions of the time history. Noise that was consistently found to occur at certain frequencies was blocked into a range for filtering. (i.e., noise was observed just over 100 Hz and just below 300 Hz; the 98 to 305 Hz filtering range isolates that part of the record so that the remaining record may be filtered). Obviously, compromises were made between the numerical rigor and computational practicality in deciding the number of filtering ranges.

A problem arises when there is suspected error of the same frequency content as known to exist in the time history because there is no way to filter out the noise without destroying the valid signal. Knowing the magnitude of the noise at other frequency ranges it could be assumed that the noise maintains that level in unfilterable region of the record. One could attempt to apply a suitable attenuation to the fourier coefficients in that frequency range of the time history, but such a method was not employed in this analysis. For the present work, the simplifying assumption was made that in regions where noise and valid signal overlap, the true signal would be of significantly greater magnitude than the noise so as to self-limit the induced error. For example, low-frequency noise (2 Hz) was found in higher frequency regions at an amplitude in physical units of 0.25g, while the true signal was at an amplitude of similar magnitude. Clearly, in this range, filtering was necessary to avoid significant error. However, in the low-frequency region of the record where the application of a 2 Hz filter would not be possible, magnitudes were of the order of 5g.

Thus, if the 2 Hz noise is still 0.25g in this range, its impact on the overall error is relatively small.

Appendix D: Development of Single Degree of Freedom (SDOF) Oscillator Envelopes

The purpose of the CEFAPP is to define the levels of motion at which equipment fails across a broad frequency range. These levels can be defined in terms of support motion spectral amplitude or response spectral amplitude (the example in Chapter 4 uses response spectral amplitude). The CEFAPP support motion is a narrow-band random signal with a center frequency that shifts across the desired range. An envelope representing spectral support motion, related to the peaks of this signal is developed by calculating the response of damped SDOF oscillators that cover the frequency range of the test signal (Appendix B). The magnitude of this envelope at the frequency of equipment failure is then used as the definition of support motion magnitude (spectral support motion) that caused failure at that frequency. The purpose and method of defining support motion in this way is described below.

Methodology and Assumptions

It is assumed that the equipment being analyzed is responding to the input motion as an SDOF system. Sustaining the appropriateness of this assumption may require more complex equipment assemblies to be reduced to simpler components suitable to a SDOF model.

For the fragility data to be useful in a general sense, a basis for comparison is needed to extrapolate fragility test results to records of expected site support motion (i.e., seismic or shock). However, these site records will generally be in the form of a time history, with the frequency content not being known *apriori* at discreet times in the record as it is for the fragility test records. The site record is thus subjected to the response spectrum analysis for a determination of its frequency content.

The basis for comparison now becomes the response spectrum analysis of the fragility record and the site record. Two modifications were required of the response spectrum analysis, as discussed below.

Octave Marching

Given the narrow-band nature of the random sweep input ($^1/_3$ octave) it would not be consistent to apply the entire fragility record as input to each of the SDOF systems of the response spectra. Ideally, each SDOF system would only receive as input that part of fragility record within ± 1/6 octave of its frequency. As a model less demanding in terms of computerization, the fragility record was marched through one octave at a time, applying each octave as input only to those SDOF systems that would have been subjected to that frequency range during the test procedure. The rationale for this is that lower-frequency input early in the record could not have excited a high-frequency failure later in the fragility testing, so any high-frequency failures that occurred were caused only by the high-frequency input at the end of the record. However, in a traditional response spectrum analysis the maximum response of the high-frequency SDOF systems may be controlled by the low-frequency input. Octave marching mitigates this problem. Octave marching is only applied to the fragility input record; there is no need for it to be applied to the site records.

Damping

For compatibility between the amplitude of equipment capacity defined by the failure data and the demand defined by design or analysis procedures it was desired to have magnitudes from the response spectrum analysis of the same order as the magnitudes of the fragility test signal. In other words, it was desired to have the ratio of response (X) to input (Y) as close as possible to unity. This was accomplished by using a damping ratio of 50% in the response spectrum analysis. The purpose of this is understood easiest by considering transmissibility. Transmissibility (T) of a damped SDOF oscillator is illustrated in Figure D1 and expressed as

$$T = \left|\frac{X}{Y}\right| = \sqrt{\frac{k^2 + (\omega c)^2}{(k-m\omega^2)^2 + (c\omega)^2}} = \sqrt{\frac{k^2 + (2\pi f c)^2}{(k-(2\pi f)^2 m)^2 + (2\pi f c)^2}}.$$ [Eq D1]

The transmissibility when the excitation frequency equals the SDOF undamped natural frequency with 50% damping is $\sqrt{2}$. Transmissibility is determined from the ideal steady-state response of an SDOF oscillator to harmonic support motion. A smaller response is achieved in the narrow band tests conducted here because the sweep rate does not allow a steady-state response and the excitation is not

harmonic. For the narrow band random sweep tests it was found that 50% damping returned magnitudes of comparable values to the recorded signal, effectively enveloping the support motion across the frequency range of the test (see Figures 6a through 6n). If later work determines that a different sweep rate is to be used, an investigation would be needed to determine what level of steady-state response is being excited and thus the appropriate artificial damping for calculating the envelopes. Care must be taken if the damping is too high to account for the resulting offset between natural and damped frequency. Critical damping of 50 percent was applied to the response spectrum analyses for both the fragility and validation (seismic and shock) records.

These modified response spectra are generated for all fragility records that produced unique failures. The frequency and spectral magnitude of all failure points are then assembled into a failure envelope. Finally, this failure envelope is used for comparison with the response spectrum (with appropriate damping) of the site records to determine if they contain any failure critical frequency content.

For the seismic validation tests, the Lucerne seismic record was subjected to the response spectrum analysis to determine its frequency content. The strongest peaks of the spectrum were located at 2 Hz and 12.5 Hz. A power spectrum analysis was also run on the portion of the Lucerne record running from 9.2 to 10.2 seconds (failure was documented at 10.2 seconds). The power spectra also had a strong peak at 12.5 Hz, but showed little frequency content at 2 Hz. It was thus assumed that the 12.5 Hz peak in the response spectra corresponded to the failure. A similar procedure was used with the shock verification test. However, in using the power spectrum analysis to determine which peak of the shock response spectra was appropriate for defining failure, the entire record was used (as opposed to a particular time interval of the record). This was required by the short duration of the shock test, and the resulting inability to define a discrete time in the record at which failure occurred. The power spectra of the shock record had a very strong peak near 11 Hz, reinforcing the selection of the maximum peak of the response spectra (11.1 Hz) to define the frequency at which failure occurred. There is thus an important difference in the selection of the response spectra peaks for the seismic and shock tests. For the seismic test we were able to validate the selection of the failure point from the response spectrum that was run over the entire test with a power spectrum that was run over only a limited range of the record (and thus an independent and distinct spectrum from the response spectrum). The shock record loses that distinction between the two spectra by calculating them both over the entire record.

Response spectra developed based on time history analyses of a building should be generated by subjecting SDOF oscillators with 50% damping to the entire

equipment support location time history predicted motions. These response spectra may then be compared with equipment fragility in the same manner as described for the NEHRP-based response spectra.
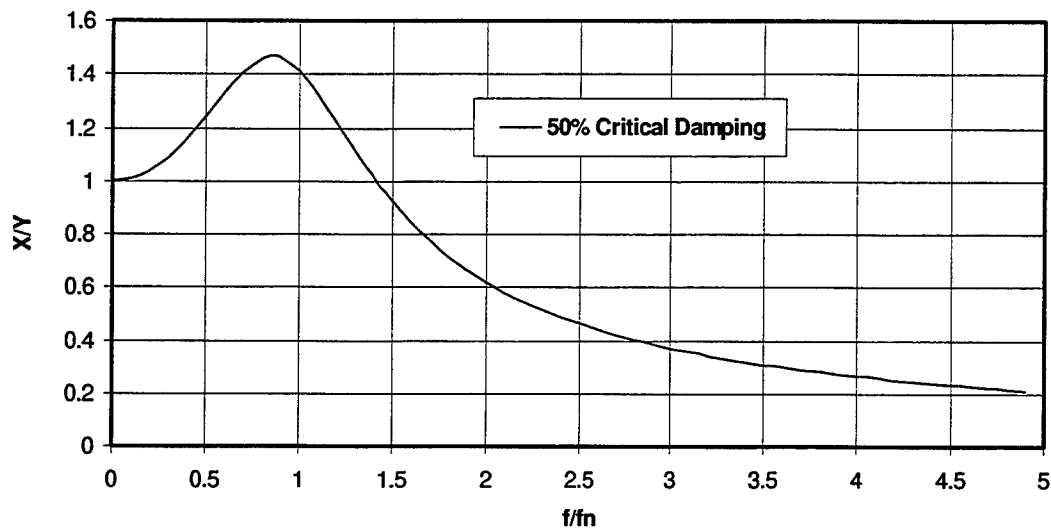

Figure D1. SDOF response (X) over harmonic support motion (Y).

Abbreviations and Acronyms

APSD	acceleration power spectral density
CEFAPP	CERL Equipment Fragility and Protection Procedure
CERL	(U.S. Army) Construction Engineering Research Laboratories
FEMA	Federal Emergency Management Agency
FIR	finite impulse response
HP	high pass
LVDT	linear variable differential transformer
NEHRP	National Earthquake Hazards Reduction Program
PE	probability of exceedence
PL	performance level
SDOF	single degree of freedom
SMC	strong-motion cycle
SR	sweep rate
TESS	Triaxial Earthquake and Shock Simulator
TRS	test response spectra
TVA	Tennessee Valley Authority
USGS	U.S. Geological Survey
USACERL	U.S. Army Construction Engineering Research Laboratories

USACERL DISTRIBUTION

Chief of Engineers
  ATTN: CEHEC-IM-LH (2)
  ATTN: CEHEC-IM-LP (2)
  ATTN: CECG
  ATTN: CECC-P
  ATTN: CECC-R
  ATTN: CECW
  ATTN: CECW-O
  ATTN: CECW-P
  ATTN: CECW-PR
  ATTN: CEMP
  ATTN: CEMP-E
  ATTN: CEMP-C
  ATTN: CEMP-M
  ATTN: CEMP-R
  ATTN: CERD-C
  ATTN: CERD-ZA
  ATTN: CERD-L
  ATTN: CERD-M (2)

ACS(IM) 22060
  ATTN: DAIM-FDP

CECPW 22310-3862
  ATTN: CECPW-E
  ATTN: CECPW-FT
  ATTN: CECPW-ZC

US Army Engr District
  ATTN: Library (42)

US Army Engr Division
  ATTN: Library (8)

US Army Engineering and Support Center
  ATTN: CEHND 35807-4301

US Army Europe
  ATTN: AEAEN-EH 09014
  ATTN: AEAEN-ODCS 09014

US Army Materiel Command (AMC)
  Alexandria, VA 22333-0001
  ATTN: AMCEN-F

FORSCOM
  Forts Gillem & McPherson 30330
    ATTN: FCEN

TRADOC
  Fort Monroe 23651
  ATTN: ATBO-G

Fort Belvoir 22060
  ATTN: CETEC-IM-T
  ATTN: CETEC-ES 22315-3803
  ATTN: Water Resources Support Ctr
  USA Natick RD&E Center 01760
  ATTN: STRNC-DT

  ATTN: AMSSC-S-IMI

CEWES 39180
  ATTN: Library

CECRL 03755
  ATTN: Library

Defense Nuclear Agency
  ATTN: NADS 20305

Defense Logistics Agency
  ATTN: MMBIR 22060-6221

National Guard Bureau 20310
  ATTN: NGB-ARI

Naval Facilities Engr Command
  ATTN: Facilities Engr Command (8)
  ATTN: Engrg Field Divisions (11)
  ATTN: Public Works Center (8)
  ATTN: Naval Constr Battalion Ctr 93043
  ATTN: Naval Facil. Engr. Service Ctr 93043-4328

8th US Army Korea
  ATTN: DPW (11)

US Army MEDCOM
  ATTN: MCFA 78234-6000

American Public Works Assoc. 64104-1806

US Army CHPPM
  ATTN: MCHB-DE 21010

US Gov't Printing Office 20401
  ATTN: Rec Sec/Deposit Sec (2)

Nat'l Institute of Standards & Tech
  ATTN: Library 20899

Defense General Supply Center
  ATTN: DGSC-WI 23297-5000

Defense Construction Supply Center
  ATTN: DCSC-WI 43216-5000

Defense Tech Info Center 22060-6218
  ATTN: DTIC-O (2)

                        141
                      (+60)
                      11/97